Characterisation and development of antifouling coatings for metal surfaces in aquatic environments

by

Mercia Volschenk

Thesis presented in partial of the requirements for the degree of Master of Science
at Stellenbosch University
Faculty of Science
Department of Chemistry and Polymer Science

Supervisor: Prof TE Cloete
Co-supervisors: Dr M Botes; Dr. N Gule

March 2015

DECLARATION

By submitting this thesis electronically, I declare the entirety of the work contained therein is my own, original work, that I am the owner of the copyright thereof (unless to the extent explicitly otherwise stated) and that I have not previously in its entirety or in part submitted it for obtaining any qualification.

Mercia Volschenk March 2015

Summary

Biofouling in cooling water systems lead to several problems resulting in reduced efficiency and financial losses. Antifouling coatings present an environmental friendly solution to prevent biofouling alternatively to the current use of toxic chemicals in cooling water systems.

In this study biofilm growth in a cooling water system was simulated in a modified flow cell system to evaluate industrial antifouling coatings and biocide-enriched coatings as potential antifouling coatings for metal surfaces. The design of a novel antifouling coating was also attempted. Firstly, analytical methods for biofilm monitoring to evaluate selected antifouling coatings and biocides were optimised. Pseudomonas sp. strain CT07 was selected to grow biofilms in the biofilm studies. A metal alloy of stainless steel and mild steel (3CR12) showed no corrosion after a 24 h biofilm growth and was selected as metal surface for the biofilm growth discs. Sonification for 5 min was determined as the optimum biofilm removal method from the growth discs. After biofilm removal the metal growth discs were stained with the LIVE/DEAD® BaclightTM Bacterial Viability kit. Visualisation by confocal laser scanning microscopy and flow cytometry revealed auto fluorescence signals from metal discs that hindered quantitative and qualitative analysis of the metal substrate. The use of Pseudomonas sp. strain CT07::gfp to grow biofilms on the metal growth discs and the exclusion of the stain SYTO9 from the LIVE/DEAD® BaclightTM Bacterial Viability kit reduced auto fluorescence signals from the metal discs. The industrial coatings containing quaternary ammonium salt (QAC), triclosan (TC) and copper oxide (CUO) respectively, showed the highest antimicrobial activity in the disc diffusion test. The minimum inhibition concentrations for silver nitrate (SN) and copper sulphate (CS) were 432 ppm and 160 ppm respectively. A minimum of 6.25 % of furanone solution (FR) was biocidal in the dilution susceptibility test.

Secondly, the metal growth discs were coated respectively with the three selected industrial coatings QAC, TC and CUO and the epoxy biocide-enriched coatings SN, CS and FR and chemically characterised before and after exposure to biofilm formation. The antifouling activity of these coatings was also characterized. Growth media inoculated with Pseudomonas sp strain CT07::gfp was circulated through the modified flow cell system via a multichannel peristaltic pump for 48 h before the coated metal discs were removed and washed to perform chemical or antifouling analysis. All the industrial coatings and biocide enriched epoxy coatings complied with the thermal stability requirements of a cooling water system. Scanning electron microscopy (SEM) imaging and Energy dispersive X-ray spectroscopy (EDX) analysis confirmed that the adhesion properties of industrial coatings TC and QAC in aqueous environments were insufficient and that the copper and silver ions leached out of the biocide-enriched epoxy coatings.

The qualitative analyses of the attachment of bacteria on the surfaces of both the industrial and biocide enriched epoxy coatings was confirmed by SEM, CLSM. The attached bacteria were

removed and analysed quantitatively through plate counts and flow cytometry. None of the industrial coatings or the biocide incorporated epoxy coatings that were used in this study would therefore be efficient for the use on metal surfaces in cooling water systems.

Thirdly, several approaches were followed to synthesise a poly(styrene-alt-maleic anhydride) (SMA) coating, chemically bind a furanone derivative, 2,5-dimethyl-4-hydroxy-3-(2H)-furanone, to the polymer back bone of the SMA coating for the application as an antifouling coating for cooling water systems. The synthesis of SMA was confirmed through 1H NMR and SEC and the synthesis of tert-butyl 2-(2-hydroxyethoxy) ethylcarbamate and 4-(2-(2-(tert-butoxycarbonyl)ethoxy)ethoxy)-4-oxobutanoic acid was confirmed through 1H NMR and ES-MS+. The synthesis of the end furanone derivative product could however not be achieved.

Opsomming

Bio-aanpaksels in waterverkoelingsisteme veroorsaak talle probleme wat lei tot verminderde doeltreffendheid en finansiële verliese. Antimikrobiese oppervlakbedekkings verskaf ‘n omgewingsvriendelike oplossing om bio-aanpaksels te voorkom en ‘n alternatief vir die huidige gebruik van giftige chemikalieë in waterverkoelingsisteme.

Biofilm groei in waterverkoelingsisteme was nageboots in ‘n gewysigde vloeiselsisteem om industriële aanpakwerende en biopsied bevattende antimikrobiese oppervlakbedekkings as potensiële aanpakwerende beskermingslae vir metaaloppervlaktes te evalueer. Die ontwerp van ‘n nuwe aanpakwerende beskermingslaag is ook ondersoek. Eerstens is analitiese moniteringsmetodes vir bio-aanpaksels op geselekteerde aanpakwerende antimikrobiese oppervlakbedekkings en biosiedes geoptimiseer. *Pseudomonas* sp. stam CT07 was verkies om bio-aanpaksels te simuleer gedurende hierdie studie. ‘n Metaalalooi van vlekvrye staal en sagte staal (3R12) het geen korrosie getoon na 24 uur se groei van bio-aanpaksels nie en is vir hierdie rede gebruik as metaal vir die bio-aanpaksel groeiplate. Dit was vasgestel dat sonifisering die optimale verwyderingsmetode vir groeiplate was. Na verwydering van bio-aanpaksels was die metaal groeiplate bedek met die LIVE/DEAD® BaclightTM bakteriële lewensvatbaarheid-toestel. Visualisering deur middel van konfokale mikroskopie en vloeisitrometrie het outofluoreserende seine vanaf die metaal groeiplate onthul wat kwantitatiewe en kwalitatiewe analise van die metaal substraat verhinder het.

Die gebruik van *Pseudomonas* sp. stam CT07:gfp om bio-aanpaksels te kweek op metal plate en die uitsluiting van SYT09 van die LIVE/DEAD® BaclightTM bakteriële lewensvatbaarheid-toestel, het die outofluoreserende seine van die metaalskywe verminder. Industriële beskerminglae, wat onderskeidelik Kwaternêre ammonium sout (QAC), triclosan (TC) en koperoksied (CUO) bevat, het die hoogste antimikrobiese aktiwiteit in die skyf-diffusie toets getoon. Die minimum inhibisie-konsentrasies vir silwernitraat (SN) en kopersulfaat (CS) was onderskeidelik 432 dpm en 160 dpm. ‘n Minimum konsentrasie van 6.25% van die furanoonoplossing (FO) is geklassifiseer as ‘n biosied in die oplossingstoets.Tweedens was die metaal groei-skywe bedek met drie industriële beskermingslae QAC, TC en CUO en die epoksie-biosied-verrykte lae SN, CS en FR en chemies-gekarakteriseerd voor en na die vorming van bio-aanpaksel. Die karaktereienskappe van die aktiwiteit van die beskermingslae was ook vasgestel. Opgeloste triptiese soja sop vermeng met *Pseudomonas* sp strain CT07: gfp was gesirkuleer in die gemodifiseerde vloeisel deur ‘n multikanaal peristaltiese pomp vir 48 uur voordat die beskermde metaalskywe verwyder en gewas is om chemiese en aanpakwerende analise uit te voer. Al die industriële beskermingslae en biosied-verrykte epoksie-beskermingslae het aan die vereistes van termiese stabiliteit van ‘n waterverkoelingsisteem voldoen. Skandeer elektronmikroskopie (SEM) en X-straal spektroskopie (EDX) analise het aangetoon dat die aantrekkingseienskappe van industriële beskermingslae TC

en QAC in waterige oplossings onvoldoende was en dat die koper- en silwerione uit die biosied-verrykte epoksie-resin beskermingslae diffundeer. Die kwalitatiewe analise van die aanpaksel van bakterieë op die oppervlaktes van beide industriële en biosied -verrykte epoksie-beskermingslae was bevestig deur SEM en CLSM. Die aangepakte bakterieë was verwyder en kwantitatief geanaliseer deur middel van plaattellings en vloeisitrometrie. Nie een van die industriële beskermingslae of die biosied-bevattende epoksie beskermingslae wat in hierdie studie gebruik is, is dus gepas vir gebruik op metaaloppervlaktes in waterverkoelingsisteme nie.

Derdens was verskeie pogings aangewend om ‘n poli(stireen-alt-maleic anhidried) (SMA) beskermingslaag chemies te bind tot ‘n furanoon afgeleide 2.5-demitiel-4-hidroksie-3-(2H)-furanoon, tot die polimeer-ruggraat van die SMA beskermingslaag vir aanwending as ‘n aanpakwerende beskermingslaag vir waterverkoelingsisteme. Die sintese van SMA was bevestig deur 1H NMR en SEC en die sintese van tert-butyl 2-(2-hirdoksie-etoksie) etielkarbamaat en 4-(2-(2-(tert-butoksiekarboniel)etoksie)etoksie)-4-oksobutanoiesesuur was bevestig deur 1H NMR en ES-MS+. Die sintese van die uiteindelike afgeleide furanoon kon egter nie behaal word nie.

Acknowledgements

I sincerely wish to thank the following people who contributed towards the completion of this study

- My supervisor Prof Cloete for the opportunity to conduct this study under his leadership and for funding.
- My co-supervisor Dr Marelize Botes, for being there with me every step of the way.
- ESKOM and NRF for funding this study.
- The free radical group for all their help.
- The central analytical facility staff for all the analysis.
- The water research group, ladies you made this journey a pleasure.
- My parents and sister for all their support and love.
- My housemate Anneke, thank you for all the lunches, editing and emotional support.
- John – thank you for all the support, gangnam charts, and calming hugs.

Table of contents

List of figures

List of tables

List of Schemes

List of equation

CHAPTER 1

Introduction and objectives

1.1 Introduction

Water is utilised as a cooling medium in cooling water systems for the purpose of excess heat removal from the system.[1–4] Water in industrial cooling systems contains micro-organisms, organic matter and minerals. The organic matter and minerals serve as nutrients for micro-organisms.[4,5] These micro-organisms, specifically the free floating planktonic bacterial cells, prefer to adhere to supporting abiotic or biotic surfaces in aqueous environments such as metal surfaces used throughout cooling water systems as heat transfer material and water transport pipelines.[6–8] The attachment of these multi species bacteria or consortiums on surfaces is defined as biofilms. These consortiums are enclosed in glycocalyx that predominantly consist of water and extracellular polymeric substances (EPS).[9–12] EPS produced by bacteria present in the biofilm consist mainly of polysaccharides, lipids, nucleic acids and proteins[13,14] and protects biofilm bacteria against the environment, hydration, aids in structural support and accumulates nutrients from the environment.[14] The growth of biofilms can either be beneficial or detrimental. It is favourable in natural settings as well as for bio-filtration and biodegradation of waste products.[15] Biofouling, on the other hand, has negative effects in many industrial settings such as in recirculating cooling water systems where surfaces are constantly exposed to water, bacteria and nutrients.[9,16–18]

Currently there are a number of different approaches used to remove biofilms from cooling water systems.[19] Chemical dosing treatment is however the most common. The term biocides refers to chemicals that are toxic towards microbes.[5,15] Biocides can be divided into two groups: oxidising and non-oxidising biocides. The mode of action toward microbes differs between biocides depending on the type of microbe, concentration of biocide, as well as contact time between the biocide and the microbe.[20] Most of the biocides that are currently used have toxic effects on the surrounding environment which is a reason for the development of resistant microbes.[1,5,21,22] The harmful impact of these chemicals can however be reduced by using environmentally friendly biocides or alternative methods in combatting biofouling in cooling water systems.[17]

One such a method would be covering metal surfaces of cooling water systems with an antifouling coating.[23,24] Antifouling coatings that kill microorganisms have been implemented in the maritime industry since 1500 BC.[25] Metal coatings contain different components which would be determined by the end use of the coating.[26] Bacteriostatic antifouling coatings have one component in common which is the incorporation of a biocide in the coating. There are three different coatings which releases biocides from the matrix, namely contact leaching coatings, controlled depletion polymer coatings and self-polishing copolymer coatings.[25]

To date the most successful antifouling coating is a protective coating containing tributyltin (TBT). TBT leached out of the polymer matrix which prevented the adhesion of organisms.[23] During the

1980's coatings containing TBT were banned from use due to its toxic effects on the surrounding environment.[27] The coating industry shifted from only focussing on technical, quality and economical aspects to placing more emphasis on environmentally friendly properties, toxicology, recyclable products and the conservation of energy and raw materials when developing new antifouling coatings.[28]

Alternative strategies for antifouling coatings have ever since been investigated and a few of these are;

1) covalently bonding biocides to polymer matrixes which would prevent leaching of the biocide into the environment,[29,30]
2) incorporation of natural environmentally friendly biocides such as furanones into polymer matrixes,[31]
3) to develop a foul release coating which would reduce the attachment of organisms to surfaces but has no bacteriostatic effect.[25]

Development of an ideal coating containing a biocide for application as an antifouling agent should comply with the following properties; the synthesis process should be inexpensive and uncomplicated, the coating should be stable over a long period of time, it should be environmentally friendly and insoluble in water.[32]

The aim of this study was to develop and characterise antifouling coatings, specifically for application in cooling water system environments. Different approaches were followed. Firstly, commercially available coatings were sourced as well as an epoxy coating that could be enriched with selected biocides. Coatings were characterised according to their chemical, physical and antifouling properties. Secondly the synthesis of a novel antifouling coating with an environmentally friendly biocide was attempted. A poly (styrene-alt-maleic anhydride) (SMA) coating was synthesised through conventional radical polymerization and it was attempted to synthesise a furanone derivative that could be chemically bound to a SMA coating through nucleophilic substitution.

1.2 Objectives

1) Sourcing of commercially available antifouling coatings for metal surfaces that can be utilized in aqueous environments.
2) Sourcing of an epoxy anticorrosive coating, selection of different biocides and incorporation of these biocides into the epoxy coating.
3) Optimisation and selection of analytical methods, industrial antifouling coatings and biocides.
4) Synthesis of a high molecular mass alternating SMA co-polymer that can be utilised as a coating.

5) Synthesis a furanone derivative that can be chemically attached to a SMA coating through nucleophilic substitution reaction.
6) Application of all coatings to metal surfaces and characterisation according to their chemical, physical and antifouling properties before and after biofilm growth.

1.3 Thesis layout

Chapter 1
A brief introduction regarding the background and objectives of this study.

Chapter 2
In this Chapter a literature review is given on the broad overview of the workings of cooling water systems, biofilm growth, biofouling in cooling water systems, biocides and the specific biocides used in this study. A historical background on antifouling coatings and a summary of relevant research that has been done on specific biocides incorporated into coatings is presented.

Chapter 3
To conduct chemical and antifouling studies on respective coatings for recirculating cooling water systems, the selected coatings were coated onto metal surfaces, subjected to a modified flow cell system. In Chapter 3 the optimisation of chemical and microbial analytical methods and selection of different techniques, coatings and biocides were conducted.

Chapter 4
In Chapter 4 commercial antifouling coatings for metal surfaces in aqueous environments were sourced from manufacturers globally. An anticorrosive epoxy coating was also sourced and enriched with biocides. All coatings were characterised before and after biofilm growth through thermogravimetric analysis (TGA), differential scanning calorimetry (DSC), energy dispersive X-ray spectroscopy (EDX), scanning electron microscopy (SEM) and transmission electron microscopy (TEM). Coatings were also characterised according to fouling ability: qualitatively through SEM and confocal laser scanning microscopy (CLSM) and quantitatively through plate counts (pour plate method) and flow cytometry.

Chapter 5
In Chapter 5 a SMA coating was synthesised and it was attempted to synthesise a furanone derivative that could be chemically bound to the SMA coating through nucleophilic substitution.

Chapter 6
Concluding remarks and recommendations for future research are discussed in this chapter.

1.4 References

1. Choi, D.-J., You, S.-J. & Kim, J.-G. Development of an environmentally safe corrosion, scale, and microorganism inhibitor for open recirculating cooling systems. *Mater. Sci. Eng. A* **335,** 228–235 (2002).

2. Panjeshahi, M. H. & Ataei, a. Application of an environmentally optimum cooling water system design in water and energy conservation. *Int. J. Environ. Sci. Technol.* **5,** 251–262 (2008).

3. Castro, M. M., Song, T. W. & Pinto, J. M. Minimization of Operational Costs in Cooling Water Systems. *Chem. Eng. Res. Des.* **78,** 192–201 (2000).

4. Meesters, K. P. H., Van Groenestijn, J. W. & Gerritse, J. Biofouling reduction in recirculating cooling systems through biofiltration of process water. *Water Res.* **37,** 525–32 (2003).

5. Cloete, T. E., Jacobs, L. & Brözel, V. S. The chemical control of biofouling in industrial water systems. *Biodegradation* **9,** 23–37 (1998).

6. Dunne, W. M. Bacterial Adhesion: Seen Any Good Biofilms Lately? *Clin. Microbiol. Rev.* **15 ,** 155–166 (2002).

7. Costerton, J. Microbial biofilms. *Annu. Rev. Microbiol.* **49,** 711–745 (1995).

8. Melo, L. F. & Bott, T. R. Biofouling in water systems. *Exp. Therm. Fluid Sci.* **14,** 375–381 (1997).

9. Flemming, H.-C. Biofouling in water systems--cases, causes and countermeasures. *Appl. Microbiol. Biotechnol.* **59,** 629–40 (2002).

10. Mah, T. F. & O'Toole, G. a. Mechanisms of biofilm resistance to antimicrobial agents. *Trends Microbiol.* **9,** 34–9 (2001).

11. Korber, D. R., Wolfaardt, G. M., Brözel, V., MacDonald, R. & Niepel, T. Reporter Systems for Microscopic Analysis of Microbial Biofilms. *Methods Enzymol.* **310,** 3–20 (1999).

12. Bester, E., Wolfaardt, G., Joubert, L., Garny, K. & Saftic, S. Planktonic-Cell Yield of a Pseudomonad Biofilm. *Appl. Environ. Microbiol.* **71 ,** 7792–7798 (2005).

13. Dror-Ehre, A., Adin, A., Markovich, G. & Mamane, H. Control of biofilm formation in water using molecularly capped silver nanoparticles. *Water Res.* **44,** 2601–2609 (2010).

14. Stoodley, P., Sauer, K., Davies, D. G. & Costerton, J. W. Biofilms as complex differentiated communities. *Annu. Rev. Microbiol.* **56,** 187 (2002).

15. Bott TR, *Industrial biofouling. Elsevier:* The boulevard, Langford Lane, Kidlington, Oxford, UK (2011)

16. Poulton, W. I. J., Cloete, T. E. & Von Holy, A. Microbiological survey of open recirculating cooling water systems and their raw water supplies at twelve fossil-fired power stations. *Water SA* **21,** 357-364 (1995).

17. Bott, T. R. Techniques for reducing the amount of biocide necessary to counteract the effects of biofilm growth in cooling water systems. *Appl. Therm. Eng.* **18,** 1059–1066 (1998).

18. Bott, T. R. Potential Physical Methods for the Control of Biofouling in Water Systems. *Chem. Eng. Res. Des.* **79,** 484–490 (2001).

19. Flynn, D. *Nalco Water Handbook*. McGraw-Hill: Global education Holdings, LCC: Penn Plaza, 10th Floor, New York

20. Maillard, J. Y. Bacterial target sites for biocide action. *Symp. Ser. Soc. Appl. Microbiol.* 16S–27S (2002).

21. Touir, R. *et al.* Corrosion and scale processes and their inhibition in simulated cooling water systems by monosaccharides derivatives. *Desalination* **249,** 922–928 (2009).

22. White, D. G. & McDermott, P. F. Biocides, drug resistance and microbial evolution. *Curr. Opin. Microbiol.* **4,** 313–7 (2001).

23. Fay, F., Linossier, I., Langlois, V., Haras, D. & Vallee-Rehel, K. SEM and EDX analysis: Two powerful techniques for the study of antifouling paints. *Prog. Org. Coatings* **54,** 216–223 (2005).

24. Le, Y., Hou, P., Wang, J. & Chen, J.-F. Controlled release active antimicrobial corrosion coatings with Ag/SiO2 core–shell nanoparticles. *Mater. Chem. Phys.* **120,** 351–355 (2010).

25. Dafforn, K. a, Lewis, J. a & Johnston, E. L. Antifouling strategies: history and regulation, ecological impacts and mitigation. *Mar. Pollut. Bull.* **62,** 453–65 (2011).

26. R Lambourne. *Paint and surface coatings - Theory and practice*. Woodhead Publishing Limited, Teddington, Middlesex, UK Consultant (1999).

27. Valkirs, A. O., Seligman, P. F., Haslbeck, E. & Caso, J. S. Measurement of copper release rates from antifouling paint under laboratory and in situ conditions: implications for loading estimation to marine water bodies. *Mar. Pollut. Bull.* **46,** 763–79 (2003).

28. Stoye, D. *Paints, Coatings and Solvents*.WILEY-VCH : Weinheim, Germany (1998)

29. Lee, S. B. *et al.* Permanent, nonleaching antibacterial surfaces. 1. Synthesis by atom transfer radical polymerization. *Biomacromolecules* **5,** 877–82 (2004).

30. Charnley, M., Textor, M. & Acikgoz, C. Designed polymer structures with antifouling–antimicrobial properties. *React. Funct. Polym.* **71,** 329–334 (2011).

31. Baveja, J. K. *et al.* Biological performance of a novel synthetic furanone-based antimicrobial. *Biomaterials* **25,** 5013–21 (2004).

32. Kenawy, E.-R., Worley, S. D. & Broughton, R. The chemistry and applications of antimicrobial polymers: a state-of-the-art review. *Biomacromolecules* **8,** 1359–84 (2007).

CHAPTER 2

Literature Review

2.1 Cooling water systems

The process of electricity generation at coal fired power stations is based on heat energy transfer principles. Raw coal stores chemical energy which is transferred to heat energy when ignited. The heat energy boils purified water to generate steam which retains mechanical energy (Figure 2.1 (a)).[1] The steam passes through the turbine and produces larger amounts of mechanical energy (Figure 2.1(b)).[1] Mechanical energy transferred from the turbine to the generator produces energy in the form of electricity (Figure 2.1(c)) which is transported to power lines (Figure 2.1(d)).[1] Steam formed during this process is recovered to liquid through condensers, with the steam on the outside of the condenser. Condensation from steam to liquid is achieved due to the temperature difference. Heat transferred from gas to water is then removed by a cooling water system (Figure 2.1(e)).[1]

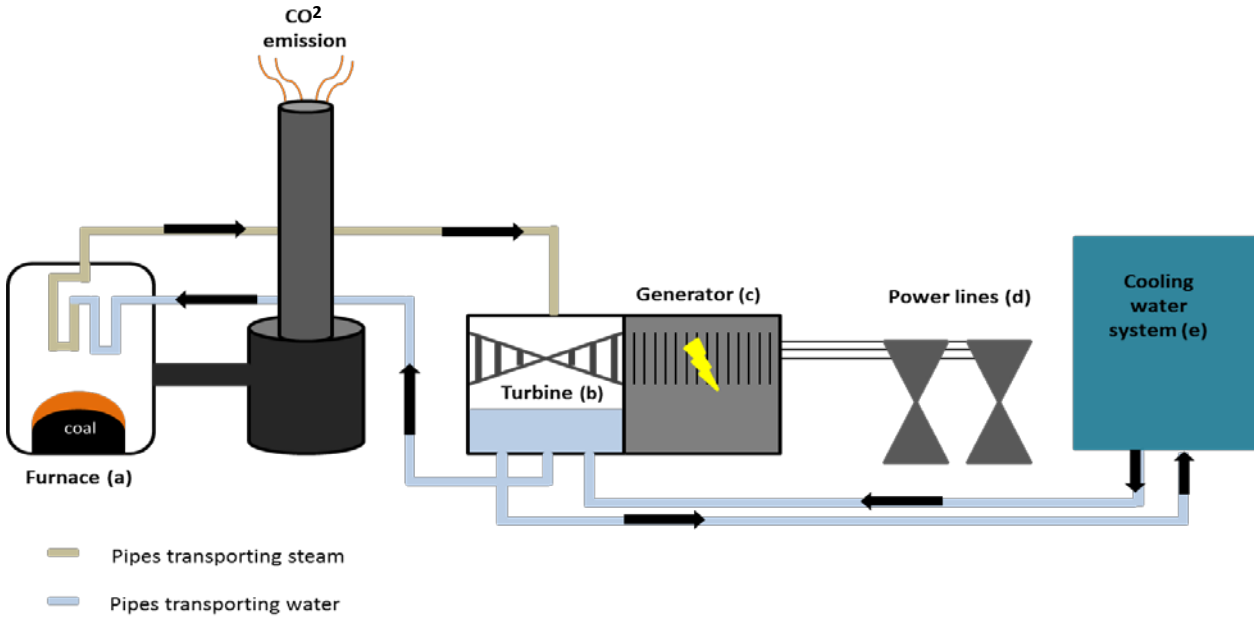

Figure 2.1: Electricity generation throug a coal fired power plant

Cooling water systems remove excess heat generated through industrial processes by utilizing water as cooling medium.[2–5] Water is used for this purpose since it is available in high volumes in industrial areas, easy to work with, and has a high heat capacity.[6]

Cooling water systems vary according to different specifics in terms of source water, size of the system, system design, distance the water needs to travel and the temperature at which the operation runs.[7] The composition of the raw water that is used in recirculating cooling water systems contributes to the microbial and chemical quality of the water in the system. However, environmental and operating system conditions play a greater role.[8]

There are two types of cooling water systems, classified on the way water is utilized as cooling medium:

1. Once-through systems

In these systems water is utilized only once through out the cooling process. Cold water from an environmental source is pumped into the system to remove unwanted heat through nonevaporative cooling and is then directly deposited back into the source. This is a simplistic method since no cooling tower is required. However, the water volumes used are extremely high.[6,7]

2. Recirculating systems

a) Closed recirculating systems

In a closed recirculating system water is not exposed to environmental elements, thus the chemical and biological properties are minimally altered. Hot water is cooled down through air-blown heat exchangers after which it is collected in water basins and reintroduced into the system. Small amounts of make-up and blowdown water are neccesary. The disadvantages of this method are the high equipment costs involved for heat exchangers and extra filtering steps.[6,7]

b) Open recirculating systems

In an open recirculating system, excess heat is removed from the system through evaporative cooling by a cooling tower, evaporative condenser or an evaporation pond. Cooled water is collected in a water basin and reintroduced into the system. Water lost through evaporation and blowdown during the cooling process is replaced with make-up water to maintain the water level and to control water chemistry.[6,7]

Responsible water usage is a priority as it is becoming one of our most scarce resources.[5,8] Therefore the use of recirculating cooling water systems has gained large popularity over the past few years due to its concervative nature regarding water usage.[2,5,8] This study was focused on an open recirculating cooling water system with a cooling tower (Figure 2.2).

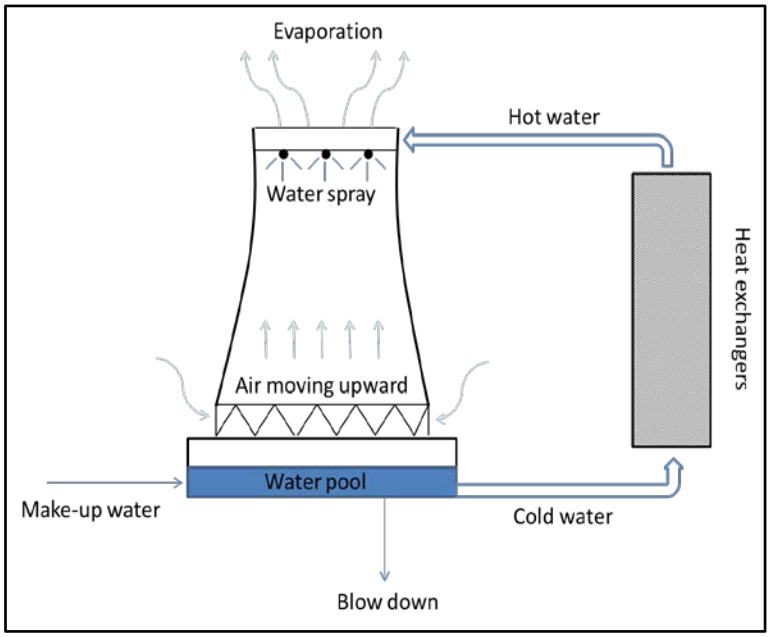

Figure 2.2: Cooling water system utilizing a cooling tower

In a cooling tower the hot water is transferred from the heat exchangers and sprayed over fill material inside the tower whilst air move upwards into the tower. The water is then partially cooled as latent heat through evaporation.[7] The concentration of dissolved salts in the water builds-up as water is lost through evaporation. Precipitation of these salts is prevented by excreting a certain percentage of the water out of the system into the environment.[9] This excreted water is referred to as blow down. Some water is lost in the system through water vapour, blow down and leakages.[7] To maintain the correct water volume and chemistry in the system, make-up water is added.[3,4,9] Cooled water is collected in a water pool from where it is re-introduced into the system.

2.2 Biofilm growth

Water in industrial systems contain micro-organisms, organic matter and minerals. The organic matter and minerals serve as nutrients for the bacteria resulting in biofilm growth.[4,10]

Biofilm growth dates back 3.5 billion years ago, recognizing it as the first verified form of life on earth.[11] In simple terms biofilms can be described as a consortium of micro-organisms, single or multiple species that are adhered to a surface, enclosed by a substance named glycocalyx and interspersed with water channels.[11–15] Almost all micro-organisms have the ability to form biofilms which can be detected in a wide variety of ecosystems, including extreme natural and man-made milieus.[11,16] It is estimated that the majority of all micro-organisms found on earth can be found in these consortiums.[11] A biofilm will develop in the presence of water, a supporting abiotic or biotic surface where nutrients are available.[12–14,17,18] In aqueous environments bacteria prefer to adhere to a surface rather than being in planktonic cell suspension.[18–20] This phenomenon is advantageous for bacteria looking from an ecological point of view as biofilm formation encourages symbiotic relationships between microorganisms that are bound in one biofilm.[18]

Biofilms are enclosed in a substance termed glycocalyx which consist mostly of water and extracellular polymeric substances (EPS). EPS predominantly contains polysaccharides, lipids, nucleic acids and proteins [21,22] that are produced by the bacteria themselves. Substances such as proteins, minerals, DNA, nutrients etc. are also absorbed from the environment into the glycocalyx and utilized by the biofilms.[18,22]These substances protect the biofilm from outside environment, bind the cells together, keep the biofilm hydrated, accumulate nutrients from environment and provide structural support.[21]

The gene expression of bacteria from the same species in a biofilm consortium differ from their planktonic counterparts in terms of cellular physiology and their increased antibiotic resistance.[19,21,23,24]

When surfaces are submerged into aqueous environments, macro-molecules that are present in the water adhere to the surface creating a preconditioning film which is a favourable environment for microbial attachment which happens in a series of steps (Figure 2.3).

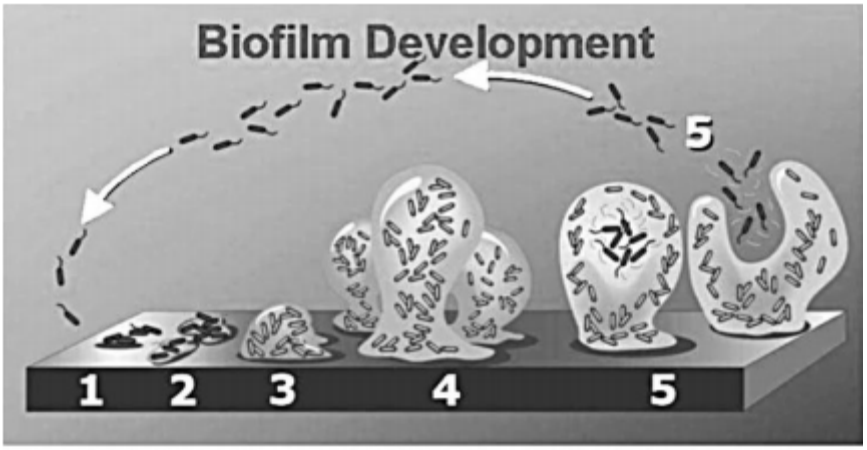

Figure 2.3: Biofilm development outlined in 5 steps (Adapted from Stoodley et al (2002)[21]

Step 1: The transportation of the bacteria through van der Waals forces, electrostatic forces or hydrophobic interactions to a surface where primary attachment of the cells takes place. After the first step the removal of the cells can still easily be done through liquid motions.[21]

Step 2: The production of EPS is initiated which ensures that the bacteria are irreversibly attached to the surface. Much stronger chemical or physical forces will be needed for removal.[21,25]

Step 3: Initial development of the biofilm design.[21]

Step 4: Maturation of biofilm design which will be dependent on the bacterial strain and the environmental conditions.[21]

Step 5: Dispersal of planktonic cells from biofilm which is favourable for new biofilm development.[21]

2.3 Biofouling in cooling water systems

The aqueous environment inside a recirculating cooling water system is ideal for micro-organism growth.[6] Bacteria are the largest group of micro-organisms responsible for micro-fouling in cooling water system.[6] The amount of nutrients and bacteria in the system varies daily, the two main sources being the make-up water and from the air blown into the system.[4,6,10]

Parameters in an industrial cooling system that would influence biofilm growth include the following:[26]

- Temperature

Bacterial growth is extremely temperature sensitive. For example an 80 % increase in biofilm thickness was observed for *Escherichia coli* by elevating the temperature from 30 °C to 35 °C .[20] The average temperature of water in cooling water systems is mainly 40 °C which promotes the growth of bacteria that have 40 °C as optimum growth temperature.[20]

- Flow rate

Flow rate influences the biofilm structure. The biofilm is thicker at a slow water flow rate and thinner but firmer in faster flow rates. [20,27]

- Nutrient concentration and availability

In an open recirculating cooling water system nutrient availability is much higher than in a closed system as the system is in direct contact with the environment. Biofilm growth will continue when nutrients are available even if no new bacteria are introduced in the system.[20] Nutrients present in the cooling water depend on the composition of the make-up water as well as the environmental and operating system conditions. [6,7,10,26]

- Surface texture

Biofilm growth on textured surfaces differs tremendously to biofilm growth on smooth surfaces. Smooth surfaces have 35 % fewer bacteria adhered to it.[20]

- Water pH

Bacterial adhesion and movement are influenced by the pH of their surrounding water. Bacteria grow predominantly at neutral pH or slightly alkaline pH.[28]

- Biofouling control measurements

Addition of biocides to water utilized in cooling water systems.[29]

In industrial settings such as cooling water systems bacterial adhesion to metal surfaces results in bio corrosion (also known as microbial induced corrosion) which has detrimental financial implications.[30] Metals are used in cooling water systems as part of the heat transfer material and the pipelines along which the water is transported in the system.[9] Metal is defined by the Oxford dictionary as: “solid material which is typically hard, shiny, malleable, fusible, and ductile, with good electrical and thermal conductivity”. Metal can be classified into two main groups namely ferrous

metals which are metals containing iron and non-ferrous metals which do not contain any iron. A metal alloy is a combination of two different types of metals.

When metal is in contact with water, corrosion starts taking place.[26] The rate of corrosion depends on the composition of the water that can differ in properties of microorganisms, metallurgy, electrochemistry and chemical properties.[26] Different types of corrosion take place depending on the environment, water composition and type of metal. In cooling water systems the most common type of corrosion is bio corrosion. [31]

Factors influencing the rate of bio corrosion are:[31]

- Presence of oxygen concentration cells
- Presence of ion concentration cells
- Influence of iron and manganese oxidising bacteria
- Production of acid
- Anaerobic niche creation

The long term problems that may occur due to biofouling of metal surfaces and bio corrosion include:[4,6,32]

- Reduced heat transfer – Biofouling and bio corrosion insulate heat transfer material inhibiting it from removing heat efficiently.
- Increased upkeep – By products produced through biofouling and bio corrosion should be removed from the system which leads to increased time spent on up keeping equipment.
- Equipment deterioration – Hardware in cooling water systems deteriorates as a result of bio corrosion and biofouling which leads to the replacement of the equipment more frequently.
- Unscheduled shutdowns – Biofouling and bio corrosion can lead to equipment failure which can stop processes in industrial plants.

Currently, five different methods physical or chemical are used for the removal biofilms in cooling water systems.[11,33]

1) Chemical treatment through oxidising and non-oxidising biocides
2) Physical removal of biofilms through a process called “pigging”
3) Heat exchangers can be cleaned through ice-nucleation
4) The dispersion of biofilms with dispersants
5) The degradation of biofilms through the use of enzymes

Physical management is the more attractive option because it is environmental friendly. Unfortunately these methods are rarely feasible and extremely expensive.[7] Several studies have been done in the field of biofouling inhibition in cooling water systems but currently the addition of

toxic chemicals is still the main practice.[33] Biocides used in industrial water systems always ends up being discharged into the environment through blow down water.[4,33]

2.4 Biocides

Biofilm growth in industrial cooling water systems can be controlled by physical and/or chemical treatment.[31] Chemicals that are toxic towards microbes are named biocides.[10,32] Biocides are commonly used to control adhering microorganisms from the surfaces they attach to.[10,32] Biocides can either have a bacteriostatic or bacteriocidal effect on microbes depending on the type of biocide and their concentration.[27,31]

The mode of action toward microbes differs between biocides according to the type of microbe, concentration of biocide as well as contact time between the biocide and the microbe. Although literature available on the different modes of actions is limited, it is accepted that biocides attack the functional components of living cells placing the cells under extreme stress.[29]

Biocides that control microbial growth are classified into two groups namely oxidising and non-oxidising biocides. The primary mode of action of oxidising biocides is the oxidization of composites inside microbes. These biocides include chlorine, chlorine dioxide, bromine, iodine, hydrogen peroxide and stabilized halogens.[6,27]

Non-oxidising biocides include toxic metal compounds, quaternary ammonium compounds (QAC), aldehydes, isothiazoline etc. [6,32]

The five modes of action towards micro-organisms include of non-oxidising biocides are:[31]

1) Obstruction of a metabolic pathway of the micro-organism
2) Disruption of the cell wall of the microorganism
3) Deactivation of the enzymes that are produced by the micro-organisms
4) Interference with the binding of proteins.

Biocide efficiency depends on using the appropriate biocide at the correct concentration and dosing frequency. If biocides are not used correctly poor results with expensive consequences are to be expected.[10,31]

The following aspects should be considered when selecting a biocide treatment regime:

1) Chemical parameters of the water to be treated, including pH, water hardness, organic compounds present and other additives such as anti-scaling agents. These parameters will influence the effectivity of the biocide to different degrees. [10]
2) The type of microbial species and their number will determine the biocide selection, dosage concentration and contact time needed for the required bactericidal effect.[10,29]

3) The system parameters such as flow rate and retention time will be used to determine the dosage frequency whether it be continuous, intermittently or through shock dosing the system.[10]
4) The environmental impact of the biocides when discharged into the environment.[32]
5) Evaluating the hazardous effect of the biocides on the specific system as well as to humans dosing the biocides.[32]
6) The cost effectivity of the biocide program. [32]
7) The monitoring technique used to determine the biocide efficiency is a critical parameter. [32]

The main disadvantage of the use of biocides is the development of resistance in microbes.[34] There are three types of resistance, namely intrinsic resistance, modified resistance and resistance that develops due to transformation.[32,35] The resistance of sessile microorganisms in biofilms towards biocides are much higher than planktonic cells. The structure of the biofilm would also directly influence the effectiveness of the biofilm against biocides.[10] Specific bacteria in a biofilm consortium also react differently towards biocides than if encountered in planktonic form.[18]
This is mainly due to:[27]

1) Biofilms covered with an EPS layer that form a barrier to entry for the biocide and protect the bacteria in the biofilm against the biocide.
2) Microorganisms in a biofilm that produce enzymes and in turn destroy the biocides.
3) The microbe alters its cytoplasmic membrane to prevent the biocide from entering the cell.
4) There is a possibility for a spontaneous mutation inside the cell.

The use of most commercially available biocides especially those containing heavy metals have toxic effects on plant and animal life in the environment.[5,10,30] For future application, the use of environmentally benign biocides should be utilised. These biocides are not stable for long periods and break down into environmentally friendly compounds such as water and oxygen or serve as additional source of nutrients for organisms outside the system. The effectiveness, resistance, biodegradability, cost and environmental impact of these biocides however must be investigated for it to be cost effective and industrially acceptable.[5,10,33] The impact of the harmful chemicals to the environment can be reduced by using benign biocides or to follow a treatment programme that would reduce the amount of biocide needed in the system.[7]

During this study the five biocides were selected and incorporated into various coatings and characterized. Copper, Silver, Triclosan, quaternary ammonium salt and furanone were used as biocides during this study and will therefore be discussed. All of these biocides are non-oxidising biocides.

2.4.1 Copper

Since 2000 BC, the biocidal properties of copper have been utilized by civilizations around the globe [36–39] Ancient Egyptians used copper to disinfect wounds, while Greek physicians treated pulmonary diseases with it. Phoenicians nailed copper strips to ship hulls to prevent fouling and American pioneers added copper coins to their drinking water casks to ensure safe drinking.[36–39] Over time a number of scientific studies showed that copper have antifungal, antiviral, molluscicidal, nematocidal, algaecidal, antifouling and antibacterial properties which render it as a powerful antimicrobial agent.[40] Over 300 surfaces containing copper ions were recognized by the United States Environmental Protection Agency (EPA) for its antimicrobial properties in 2008.[38] Since its recognition, the commercial interest in copper as antimicrobial compound has significantly increased. [38]

Copper ions that are released from copper compounds have more than one mode of action when in contact with microorganisms. A few of these are illustrated and discussed below (Figure 2.4).

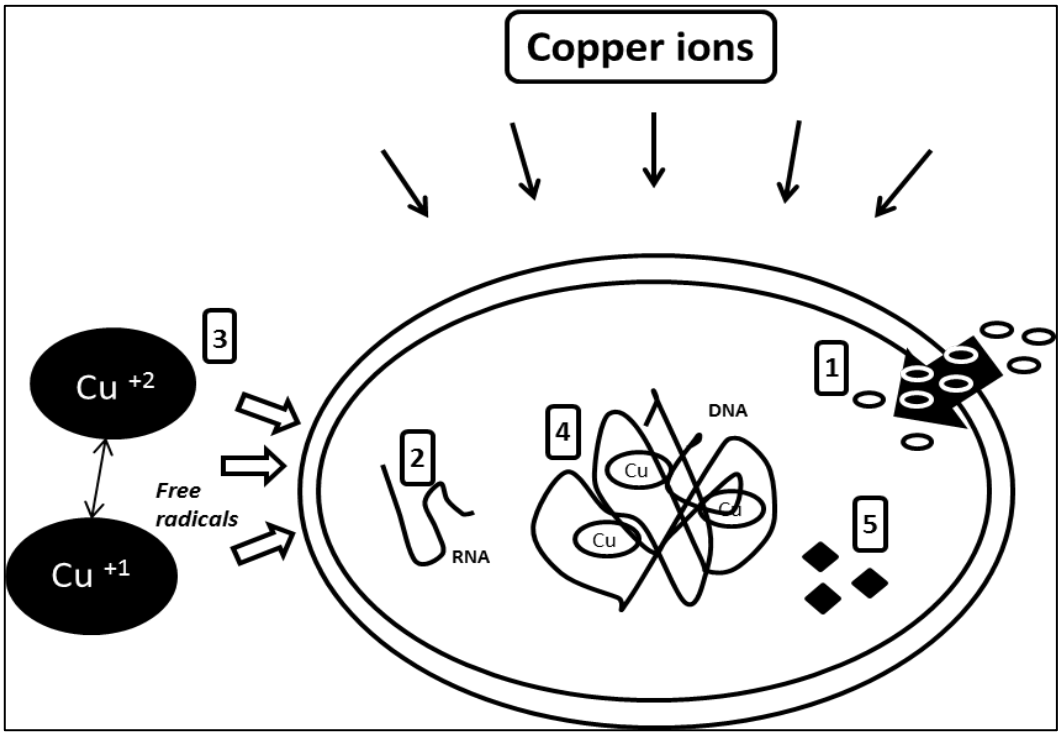

Figure 2.4: Mode of actions of copper ions (adapted from Gadi Baorkow and Jefferey Gabbay (2005)

1. Depolarization of the plasma membrane leads to leakage of cellular solutes.[37–39] The redox reaction between Cu^{2+} and Cu^{1+} initiates the production of reactive oxygen species (ROS) such as hydroxyl radicals. Lipids, proteins, DNA and other biomolecules can be damaged through these ROS.[37–39]
2. Copper ions are prone to crosslink in between a DNA helix which interferes with the hydrogen bonds leading to DNA degradation.[37–39]
3. Copper ions can outcompete and exclude other metal ions and bind to a protein binding site, inhibiting the biological activities of the protein.[38,39]

Copper is a vital trace element in over 30 proteins rendering it essential for living organisms.[41] When copper is applied externally in low concentrations, it is non-toxic to humans. Examples include the continuous use of intrauterine devices by women and the clearly visible skin reactions caused by dermal contact with copper, without harming the individual.[37,38] However, when consumed in excess or accumulated in sediment and water, copper could be hazardous for humans, animals, organisms and the environment.[38,42,43] The likelihood of bacterial strains developing resistance against copper is low, which can be attributed to rapid killing upon contact as well as degradation of the bacterial DNA.[38]

2.4.2 Silver

Similar to copper, the antimicrobial properties of silver have been known since ancient times.[42,44,45] Silver vessels kept water fresh during sea voyages and milk was preserved by silver coins. In the medical field the ancient Egyptians, Greeks and Romans used silver salts to clean wounds and silver threads for wound closures. The use of silver decreased after the discovery of antibiotics in the 20th century, but remained useful in the treatment of eye infections and various skin injuries, especially burn wounds.[46,47] Silver in pure metal form, silver acetate, silver nitrate, silver protein and silver sulfadiazine have been listed in *Martindale: the Extra Pharmacopoeia* and is currently widely used in the medical field.[44,48] Silver has also been successfully applied at low concentrations to disinfect waste water.[42,45,47]

Recently, it was also discovered that the antimicrobial activity of silver can be attributed to the silver cation (Ag^+).[47] Silver cations are spontaneously released from metallic silver, silver nitrate, silver sulfadiaze, especially when in contact with water.[46,47] The positive silver cation (Ag^+) will be strongly attracted to electron donating groups which are present at the surface of bacterial cell walls.[49] Silver has more than one antibacterial mode of action which include:

1. Binding to DNA inhibiting essential processes. [45,48–50]
2. Inhibiting enzymes that mediate bacterial respiration. [45,48–50]
3. Reacting with protein and enzyme thiol groups, destroying the normal functioning of the protein.[45,48–50]
4. Displacing other essential metal ions.[45,48–50]

Silver is a natural component of the crust of the earth and is found in salt and fresh water, air and soil. Humans readily absorb silver at low concentrations, which is nontoxic towards mammalian cells. It is not a cumulative poison and is easily excreted by the body.[45,47,51,52] The continuous efficacy of silver as an antimicrobial agent suggests that resistance to silver is uncommon.[46,53] This can be attributed to the broad range of antimicrobial processes that are affected through the mode

of action of silver.[46] Only a few bacterial strains are intrinsically resistant to silver through a plasmid derived resistance mechanism.[51]

The increasing number of multi-drug resistant pathogens against conventional prophylactic agents led to the reverting to older known antimicrobial agents including silver.[46,50] The use of silver as an antimicrobial agent in coatings received significant attention during the last few decades. A sol-gel, silver ion releasing coating and biocidal against *S. aureus* and *E. coli* was developed by Jeon et al., 2003 for medical devices.[50] Stobie et al., 2009 characterized an ambient processed perfluoropolyehter-urethane silver doped coating with the release of silver ions over a period of 6 days. The coating was proposed to be used on biomedical and environmental surfaces.[50]

2.4.3 Quaternary ammonium salt

Quaternary ammonium salt (QAS) is the product of reactions between a quaternary ammonium cation and an anion, schematically shown below (Figure 2.5).

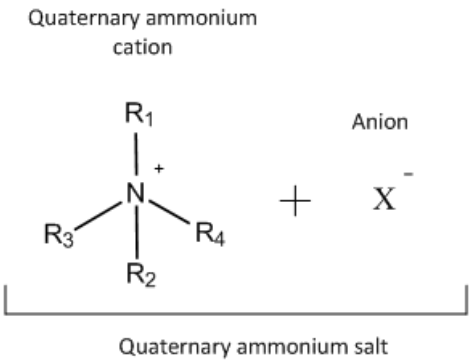

Figure 2.5: Schematic illustration of the reaction between a quaternary ammonium cation and an anion

Although QAS has been used as a preservative, detergent, surfactant, antistatic, and antiseptic agent,[54] this review will focus on the disinfecting properties of QAS.

The antimicrobial property of certain quaternary ammonium cations was first observed in 1916, but it was not until 1935 when Domagk investigated the antimicrobial properties of long-chain QAS that the great potential of this chemical group/group of chemicals came to light.[55] Ever since, it has been known as one of the most popular low molecular weight antimicrobial agents.[56,57] QAS is widely used by a variety of industries as biocide.[58–62]

A QAS with one alkyl substituent containing a minimum of eight carbons has shown antimicrobial properties against Gram-positive and Gram-negative bacteria, fungi and protozoa.[55,59,63,64] It was even more effective with an alkyl chain containing 16-18 carbon atoms.[56] Gram-positive bacteria are more susceptible towards QAS's than Gram-negative bacteria depending on the type of QAS and organism.[58] The negative charge of bacterial cell walls and the positive charge of QAS lead to an electrostatic interaction between them.[56,60,65] Charge density, molecular size and molecular mobility of the QAS determines the degree to which the QAS will be attracted to the bacterial cell

wall.[60] The effectiveness of QAS bound to the cell wall is dependent on the microorganism species.[60]

The mode of action proposed by Salton in 1968 is still accepted today. It follows a sequence of six steps:[66,67]

1. Attraction, adsorption and penetration of the QAS into the bacterial cell wall.
2. QAS reaction with the lipid or protein cytoplasmic membrane.
3. Leakage of intracellular cytoplasm.
4. Degradation of nucleic acids and proteins.
5. Cell wall lysis caused by autolytic enzymes.
6. Cell death.

2.4.4 Triclosan

Triclosan (5-chloro-2-(2,4-dichlorophenoxy)phenol), commercially known as Irgasan DP300 or Irgacare MP, is a broad spectrum organic antimicrobial agent. Triclosan has been used over the past 30 years and has been incorporated into a wide variety of products including personal care, household, textiles and polymers. The molecular structure of Triclosan consists of a trichloro derivative of 2-hydroxydiphenyl ether as seen in Figure 2.6.[68]

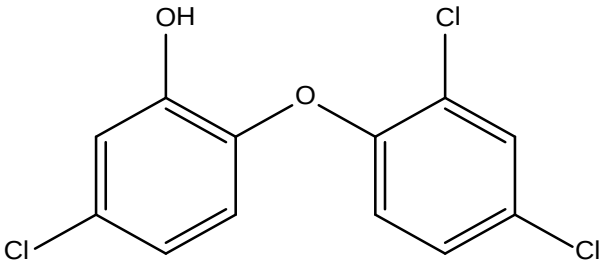

Figure 2.6: Triclosan (5-chloro-2-(2,4-dichlorophenoxy)phenol)

Triclosan is bacteriostatic at low concentrations and bactericidal at higher concentrations.[68,69] The proposed mode of action of Triclosan against Gram-positive and Gram-negative bacteria is prevention of bacterial fatty acid biosynthesis through inhibiting of the enoyl-acyl carrier enzyme (ENR) protein reaction. The absence of lipids inhibits the synthesis of lipopolysaccharides, lipoproteins and phospholipids, leading to the disruption of the cell membrane integrity and functionality, aerobic respiration and membrane proteins which leads to cell death.[68,70–74]

Large quantities of Triclosan are present in the environment, due to its' incorporation in a wide range of everyday products. It is one of the most common organic compounds present in waste water and surface water worldwide.[70,75,76] To date, no evidence exists that Triclosan is toxic to mammals, however, it has shown toxicity towards aquatic organisms including fish and algae. The prolonged accumulation of Triclosan in the environment could nevertheless have a significant negative impact.[70] The continuous use of Triclosan in household products is currently being

investigated by the FDA. Bacterial resistance towards Triclosan has been well documented and is of great concern.[68]

The development of novel, benign antimicrobial coatings is of high importance against the fight of fouling on surfaces in the medical, maritime and food industries.[77] In order to develop a benign antimicrobial coating containing Triclosan it is necessary to covalently bond the triclosan to the polymer matrix to prevent it from leaching into the environment.[77]

2.4.5 Furanones

The majority of natural and artificial surfaces submerged in marine environments would over a short period of time show signs of fouling caused by bacteria, plants and animals, leading to detrimental consequences over time.[78] However, certain marine species do not show any signs of fouling on the outer surface. These species differ from others in that they have physical and chemical defence mechanisms that prevent biofouling.[78] One of these species is the Australian marine algae, *Delisea pulchra*,[78–83] that has the ability to produce antifouling compounds classified as halogenated furanones.[78,79,81,84] *Delisea pulchra* produces more than 30 different furanone derivatives[85] which can be found in gland cells captured in vesicles under the surface of the algae.[78,81,86] The furanones are released onto the surface of the algae in concentrations of 10 ng cm^{-2} to more than 100 ng cm^{-2}, depending on the type of furanone, where it inhibits fouling.[78]

A wide variety of analogues of synthetic and natural furanones are known.[87] For example, 3(2H)-furanones are widely present in nature and has anti-allergenic, -bacterial, -fungal and –diabetic properties.[82] In this study 4-hydroxy-2, 5-dimethyl-3(2H)-furanone (HDF) was used. This group of furanones are not only known for its unique aroma due to its exceptional flavour, and low odour threshold, but also its antifouling properties as mentioned above.[88,89]When used in high concentrations they have a burnt caramel flavour and in low concentrations, a strawberry-like aroma.[88,89] HDF was initially extracted from pineapples but later also from strawberries, raspberries, insects, yeasts, bacteria and soy sauce.[89] HDF can also be synthesized produced through a reaction called the Maillard reaction which has been up scaled. Therefore HDF is widely used in different industries. [89] The structure of any furanone derivative is based on the five-membered ring structure of furan, the active antifouling part of the furanone being centred on the furan ring.[90] Schematic illustration of furan and HDF is shown below in Figure 2.7.

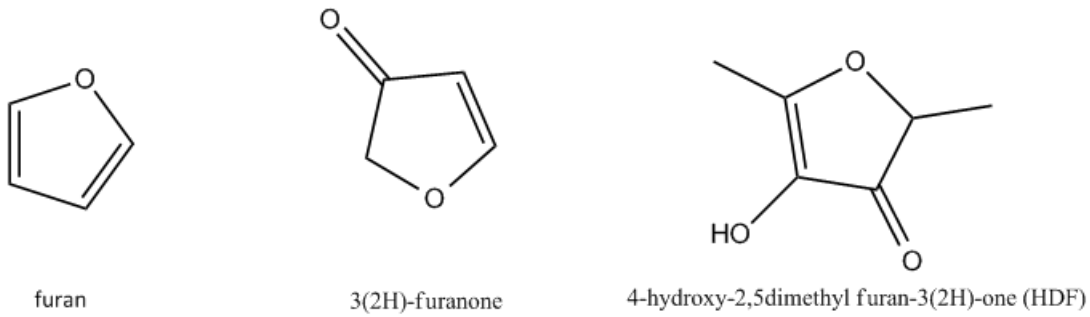

Figure 2.7: Chemical structures of furan, 3(2H)-furanone and 4-hydroxy-2,5dimethyl furan-3(2H)-one

Microorganisms prefer living in populations attached to surfaces rather than in planktonic form.[90] These sessile populations are termed biofilms and it was reported by Tomasz in 1965 that they can behave cooperatively towards each other through a cell-cell communication system.[32,87] Nealson and co-researchers discovered that bacterial populations monitor their own population densities through this communication system[32], termed quorum sensing (QS).[32,87] QS is as essential for biofilm formation as is nutrient availability.[90] QS in biofilms are accomplished through acyl homoserine lactones (AHL), synthesized by a LuxI-type synthases in bacteria that diffuse into target cells. As the bacterial population increases the AHL levels will increase. Once AHL reaches a critical level they bind to similar LuxR-type receptor proteins, which trigger the expression of quorum-dependent genes. These genes indicates that the biofilm population has grown to an acute density, parts of the population in the biofilm will then break off and establish themselves in a different area.[32,83] Gram-negative and Gram-positive bacteria are capable of QS (x). The mode of action that furanone compounds follow is through inhibiting QS between bacteria, and are therefore termed quorum sensing inhibitors.[79,90,91] They achieve this through displacing the AHL from the LuxR-type receptor proteins as they are very similar in chemical structure to AHL.[81,85,91] Furanones can influence both species-specific and non-specific receptor proteins. Hentzer et al (2002) demonstrated that the presence of furanones will reduce the production of QS signal molecules without effecting bacterial protein synthesis or growth.[83]

Analogues of natural furanones have been synthesized and characterized for their antifouling properties.[82] It was shown by Kjelleberg et al (1999 and 2001) that Gram-positive and Gram-negative bacterial growth was inhibited through furanones at a concentration non-toxic to mammalian cells.[79,82] In 1983 furanones were registered in the United States as a pesticide used in a cat repellent.[92]

2.5 Historical background of antifouling coatings

Dating back to the 16th millennium, B.C historic paintings are found on cave walls in Spain, Southern France and South-Africa. These primitive paintings are the earliest historical evidence that confirms the use of coatings. These coatings were made from animal fat, water, bone marrow

or egg whites which were mixed with a variety of natural pigments to achieve three different colours; black, red and yellow. [93,94] Furniture and utensils were painted from 200 BC with milky juices which were extracted from the bark of the *Rhus vernicifera* tree in China. A monk, Rogerus Von Helmershausen, developed the first known recipe for a lacquer in 1100 A.D which was prepared from linseed oil and sandarac and used as a protective coating for wood.

During the industrial revolution the use of iron and steel increased which led to the development of lead and zinc based coatings to prevent or prolong corrosion.[94] Until the early 1900's coatings could only be manufactured on small scale using only natural products such as vegetable oils and resins from wood. After Wold War I, binders for coatings could be manufactured on large scale. Synthetic resin and phenolic resin were manufactured during the 1920's and alkyd resins were introduced in the 1930's. Today there are a large variety of synthetic binders available for the use of coatings development which can be tailored for specific end uses.[93] Two of the main reasons for the use of coatings are to extend surfaces durability or to add functionality to a surface for a variety of applications.[95] Coatings do not consist of only one compound but of numerous components. The composition of the coating will be determined by the properties, surface to be coated, coating method, economic and ecological constraints. The different components in a coating can be classified into two groups depending on their evaporation ability, namely volatile and non-volatile components.[93] The functionality of every component in the liquid and final solid product differs and not every coating consists of all the compounds mentioned (Table 2.1).

Table 2.1: The main functions of Volatile and Non-volatile components in coatings [93,94]

Volatile	**Main function**	**Non-volatile**	**Main function**
Organic solvents	Dissolves solid and viscous binders, enables application	Binders	Macromolecular polymers which forms the basis of coatings
Water	Carrier liquid for latex coatings, partial solvent for water reducible coatings	Plasticizers	Decreases the hardening temperature of binders, and improves the flow, flexibility and adhesion properties.
Coalescing agents	Used to optimize the film formation process during application	Paint additives	Added as auxiliary component in small quantities to improve specific properties of a coating
		Pigments and extenders	Provides colour and increases covering ability

The most important component is the binder which also makes up the better part of the coating.[93] Coatings can be divided into a few groups based on their binders e.g. oil based, cellulose, chlorinated rubber, vinyl, acrylic, alkyd, saturated polyester, unsaturated polyester, polyurethane,

epoxy silicone, asphalt, bitumen, pitch and silicate coatings.[94] Different additives are incorporated into these coatings to manufacture coatings with specific properties.

Surfaces which are in constant contact with water are prone to biofouling and bio corrosion. The life span of these surfaces could be extended through the application of antifouling coatings.[96] Antifouling coatings can be applied in the medical, food and water industry as biofilm formation in these industries are common.[97,98] The development of such coatings has therefore been the goal of numerous researchers for decades. [97] The timeline of the development of antifouling coatings are outlined in Table 2.2.

Table 2.2: Historical development of antifouling strategies (Adapted from Daffron et al (2011)[99]

Time line	Major events
1500-300 BC	Use of lead and copper sheets on wooden vessels
1800-1900s	Heavy metals (copper, arsenic, mercury) incorporated into coatings
1800s-present	Continued use of copper in antifouling coatings
1960's	Development of TBT conventional coatings
1977	First foul release antifouling patent
1980s	Development of TBT self-polishing copolymer coatings allowed control for biocide release rates
1987-1990	TBT coatings prohibited on vessels
1990s-present	Copper release rate restrictions introduced in Denmark and considered elsewhere
2000s	Research into environmentally friendly antifouling alternatives increases
2003	Prohibition of further application of TBT
2008	Prohibition of active TBT presence

2.6 Utilization of biocides in antifouling coatings

The majority of the developed antifouling coatings are based on the incorporation and release of biocides.[97] (Joerg C Tiller) The use of antifouling coatings was first used for the protection of ship vessels against the accumulation of micro and macro organisms developing fouling.[100] Heavy metals or tributyltin (TBT) was traditionally incorporated into the matrixes of the coatings that leached out and prevented the adhesion of the organisms. [100] The use of these biocides contaminated the ocean which led to the banning of the use of these compounds. [100,101] The

prevention of biofouling for steel surfaces could also be achieved through the application of an antifouling coating.[102]

The release rate of the biocides from the polymer matrixes is one of the most important aspects. If the release rate is too fast the durability of the antifouling property of the coating would be very short lived and the concentration biocide in the environment too high. If the release rate is too slow it will not be able to exert antifouling properties and fouling would take place. [102] Three different processes are used to prepare biocide containing coatings with different leaching properties as discussed below. (Figure 2.8: a) Contact leaching coatings b) Controlled depletion polymer coatings c) Self-polishing copolymer coating)

Contact leaching coatings are manufactured from high molecular weight insoluble binders such as epoxy, vinyls, acrylics etc. Large amounts of biocides can be incorporated into these polymer matrixes. The polymer matrix is insoluble in water and the biocides are water-soluble. The biocides are gradually released from the matrix and leave a honey comb structure behind. The water penetrates the structure to release the biocides deeper in the matrix. After a certain period of time the biocide ions cannot diffuse through the thick layer of the honeycomb structure therefore the antifouling properties of the coating decrease (Figure 2.8(a)).[103,104]

Controlled depletion polymer coatings consist of a water-soluble binder through hydration. As the coating and the biocide are water-soluble they are dissolved simultaneously. The depletion of the coating takes place over a few months (Figure 2.8(b). [103]

Self-polishing copolymer coatings are made from co-polymers that are easily hydrolysed when in contact with water. As hydrolysis of the polymer matrix takes place the biocide are gradually released, leaving an unstable polymer matrix which would gradually wear away. These coatings can exert antifouling properties for up to 5 years.[93,100,103] However the coatings from which the biocides are released as mentioned above are not durable and are toxic to the environment (Figure 2.8 (c)). [97]

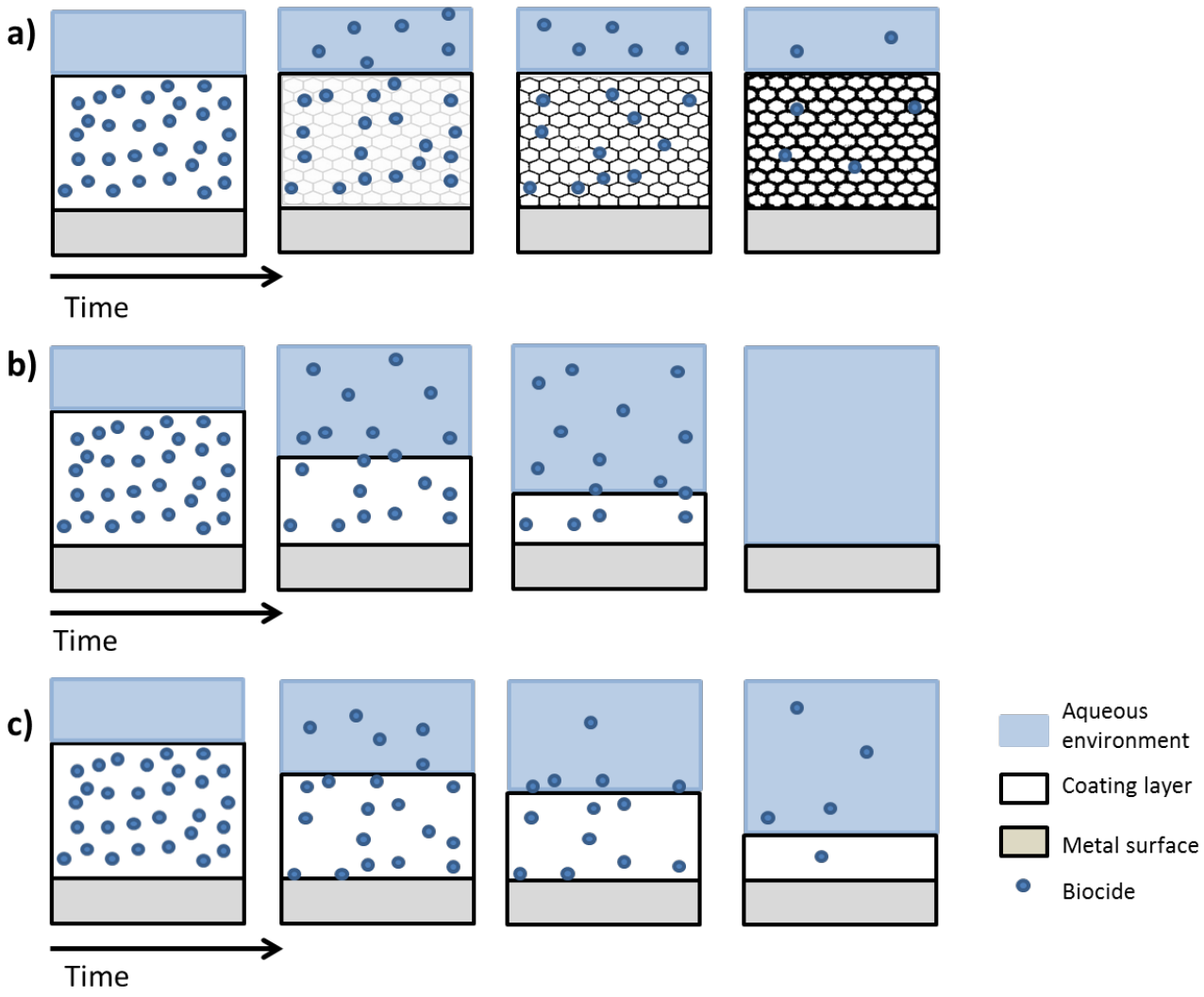

Figure 2.8: a) Contact leaching coatings b) Controlled depletion polymer coatings c) Self-polishing copolymer coating

Alternative strategies to leaching coatings include to covalently attach antifouling compounds to the polymer matrix which would prevent leaching of the biocides [97,105]; to develop foul release coatings which reduces the attachment of micro and macro organisms but is not biocidal to the organisms[99]; or to incorporate natural antifouling compounds such as furanones which is produced by the red algae, although such coatings are to date not commercially available.[99]

Three aspects should be considered in the manufacturing of environmentally friendly biocide containing coatings namely the functionality of the biocides being incorporated, the contact between the coating and the micro and macro organisms and the degradation of the polymer matrixes.[96] In the past the coating development industry mainly focused on the technical, quality and economical aspects when developing new coating products. Currently environmental friendly properties, toxicology, recycling of products at the end of their use and the conservation of energy and raw materials take preference in the development of new coatings.[93,94]

The ideal polymer with incorporated biocide for the application as an antifouling coating should consist of the following properties;[98]

1. The synthesis process should be inexpensive and not complicated
2. Should be stable over a long period of time
3. Should be environmentally friendly towards the environment and humans
4. Not soluble in water
5. When antifouling activity is depleted should be able to be regenerated with ease
6. Should exert antifouling properties to a variety of micro-organisms

2.7 Usage of selected biocides in antifouling coatings

Biofilm formation on various substrates is a major concern in many industries.[62] Currently one of the leading solutions for substrates to exert antimicrobial property is to coat the substrates with antifouling coatings.[57]

Incorporation of copper particles into polymer matrixes may extend the use of copper as antimicrobial agent in a variety of industries. The efficiency of an antifouling coating is directly linked to the leaching rate of the biocide.[106,107] Nadagouda and Varma (2007) followed an environmentally friendly approach by incorporating copper salt into carboxymethyl cellulose which could be applied as antimicrobial coatings or food packaging.[108] Copper oxide and copper metal embedded in a polypropylene matrix with an ion-copper-delivery plastic material was developed in 2011 by Delgado *et al.*[41] Cioffi et al (2004, 2005) developed and characterized biostatic coatings with controlled copper ion release for application in biomedical devices and antimicrobial packaging.[109,110] Copper is known to be one of the most toxic biocides against microorganisms in aquatic environments. Copper in coatings have been used by the maritime sector for centuries, and after the banning of Tributyltin (TBT) in 2003, copper usage increased.[111]

An environmentally friendly coating was synthesized by Ruparelia et al (2007)[42] through a green chemistry process in which silver nanoparticles were embedded into already developed paint. The coating showed antibacterial properties against *S. aureus* and *E. coli* and can be applied to wide variety of surfaces including wood, steel, glass, steel etc.[42]

QAS's are low molecular weight molecules which cause it to leach out of coatings easily, creating antimicrobial surfaces.[63] Coatings containing non-covalently bonded QAS have decreased antimicrobial activity. These leached molecules can potentially be toxic towards the environment and mammalian cells and promote bacterial resistance.[63,64,112] Consequently, research on covalently binding the molecules to the backbone of the polymer has received more attention lately.[56,57,62,63,112] QAS has successfully been incorporated as a biocide into a number of coatings. Gottenbos et al (2001) [56]and Oosterhof et al (2006)[113] developed coatings for silicone rubber to which the QAS was covalently bonded for the coating of biomedical implants.[56,113] Self-assembled monolayers (SAM) with a thiol group on one side and a QAS on the other was successfully grafted

onto gold by Thebault et al (2008)[57]. These SAMs showed contact active antimicrobial properties against several bacterial strains.[57] Majumdar et al (2009)[60] synthesized polyhedral aligomeric silsesquioxane (POSS) and functionalized it with a QAS. The synthesized product showed antimicrobial activity against Gram-positive and Gram-negative bacteria (8).[60] An antimicrobial active polymer was synthesized by Kenaway et al (1998)[63] through modifying poly(glycidyl methacrylate) with QAS molecules.[63]

Thomas et al., 2010 incorporated Triclosan into the backbone of siloxanes through covalent bonds. The characterization of the different coatings showed that the glass transition temperature (Tg) and the modules of the coatings influenced the anti-fouling property of the coating. Coatings with moduli between 0.1 and 10 Mpa exerted antifouling properties (7).[75] A coating developed for packaging material was synthesized by adding 10 % (w/w) Triclosan into a styrene-arcylate copolymer by Cung et al., 2002.[114] The coating inhibited the growth of *E. faecalis* and showed excellent releasing kinetics of the Triclosan when n-heptane was used as solvent.[114] Kugel et al (2008)[115] modified the triclosan molecule in order to copolymerized it with hydroxyethyl acrylate and butyl acrylate through free radical polymerization. It was showed that the coating does not leach triclosan and it inhibited *Staphylococcus epidermidis* biofilms.[115]

Studies have shown that when furanones are associated with surfaces they are non-cytotoxic.[84]Properties that enable furanones as good biocide candidates for incorporation into coatings are its low toxicity, broad spectrum of activity, and being amenable to the development of structural analogues with even greater efficacy. A patent by Christie et al (1998) showed that the incorporation of furanones into polymer matrixes inhibits fouling.[78,88] The development of novel commercial antifouling coatings with the use of furanones as antifouling agent has shown great potential since then.[78] Hume et al (2004)[82] and Baveja et al (2004)[86] bonded 3-(1'-bromohexyl)-5-dibromomethylene-2(5H)-furanone to polystyrene and then covalently bonded it to a variety of polymeric materials successfully used as medical devices with reduced biofilm formation and slime production of *Staphylococcus epidermidis*.[82,86]

2.8 References

1. Pather Vasanie. *Eskom and water*. (2004). http://www.ewisa.co.za/literature/files/260.pdf

2. Panjeshahi, M. H. & Ataei, a. Application of an environmentally optimum cooling water system design in water and energy conservation. *Int. J. Environ. Sci. Technol.* **5,** 251–262 (2008).

3. Castro, M. M., Song, T. W. & Pinto, J. M. Minimization of operational costs in cooling water systems. *Chem. Eng. Res. Des.* **78,** 192-201 (2000).

4. Meesters, K. P. H., Van Groenestijn, J. W. & Gerritse, J. Biofouling reduction in recirculating cooling systems through biofiltration of process water. *Water Res.* **37,** 525–32 (2003).

5. Choi, D.-J., You, S.-J. & Kim, J.-G. Development of an environmentally safe corrosion, scale, and microorganism inhibitor for open recirculating cooling systems. *Mater. Sci. Eng. A* **335,** 228–235 (2002).

6. Flynn, D. *Nalco Water Handbook*. McGraw-Hill: Global education Holdings, LCC: Penn Plaza, 10th Floor, New York

7. Bott, T. R. Techniques for reducing the amount of biocide necessary to counteract the effects of biofilm growth in cooling water systems. *Appl. Therm. Eng.* **18,** 1059–1066 (1998).

8. Poulton, W. I. J., Cloete, T. E. & Von Holy, A. Microbiological survey of open recirculating cooling water systems and their raw water supplies at twelve fossil-fired power stations. *Water SA* **21,** 357-364 (1995).

9. Kim, J.-K. & Smith, R. Cooling water system design. *Chem. Eng. Sci.* **56,** 3641–3658 (2001).

10. Cloete, T. E., Jacobs, L. & Brözel, V. S. The chemical control of biofouling in industrial water systems. *Biodegradation* **9,** 23–37 (1998).

11. Flemming, H.-C. Biofouling in water systems--cases, causes and countermeasures. *Appl. Microbiol. Biotechnol.* **59,** 629–40 (2002).

12. Mah, T. F. & O'Toole, G. a. Mechanisms of biofilm resistance to antimicrobial agents. *Trends Microbiol.* **9,** 34–9 (2001).

13. Watnick, P. & Kolter, R. Biofilm, City of Microbes. *J. Bacteriol.* **182 ,** 2675–2679 (2000).

14. Macdonald, R. Reporter Systems for Microscopic Analysis of Microbial Biofilms. *Methods Enzymol.* **310,** 3-20 (1999).

15. Bester, E., Wolfaardt, G., Joubert, L., Garny, K. & Saftic, S. Planktonic-Cell Yield of a Pseudomonad Biofilm. *Appl. Environ. Microbiol.* **71 ,** 7792–7798 (2005).

16. Costerton, J. W. *et al.* Bacterial biofilms in nature and disease. *Annu. Rev. Microbiol.* **41,** 435–464 (1987).

17. Bishop, P. The role of biofilms in water reclamation and reuse. *Water Sci. Technol.* **55,** 19–26 (2007).

18. Dunne, W. M. Bacterial Adhesion: Seen Any Good Biofilms Lately? *Clin. Microbiol. Rev.* **15 ,** 155–166 (2002).

19. Costerton, J. Microbial biofilms. *Annu. Rev. Microbiol.* **49,** 711-745 (1995).

20. Melo, L. F. & Bott, T. R. Biofouling in water systems. *Exp. Therm. Fluid Sci.* **14,** 375–381 (1997).

21. Stoodley, P., Sauer, K., Davies, D. G. & Costerton, J. W. Biofilms as complex differentiated communities. *Annu. Rev. Microbiol.* **56,** 187-209 (2002).

22. Dror-Ehre, A., Adin, A., Markovich, G. & Mamane, H. Control of biofilm formation in water using molecularly capped silver nanoparticles. *Water Res.* **44,** 2601–2609 (2010).

23. Toole, G. O., Kaplan, H. B. & Kolter, R. Biofilm formation as microbial development. *Rev. Microbiol* **54,** 49–79 (2000).

24. Purevdorj, B., Costerton, J. W. & Stoodley, P. Influence of Hydrodynamics and Cell Signaling on the Structure and Behavior of Pseudomonas aeruginosa Biofilms. *Appl. Environ. Microbiol.* **68 ,** 4457–4464 (2002).

25. Palmer, J., Flint, S. & Brooks, J. Bacterial cell attachment, the beginning of a biofilm. *J. Ind. Microbiol. Biotechnol.* **34,** 577–588 (2007).

26. Coetser, S. E. & Cloete, T. E. Biofouling and biocorrosion in industrial water systems. *Crit. Rev. Microbiol.* **31,** 213–32 (2005).

27. Cloete, T. E. Biofouling control in industrial water systems: What we know and what we need to know. *Mater. Corros.* **54,** 520–526 (2003).

28. Chen, M. J., Zhang, Z. & Bott, T. R. Effects of operating conditions on the adhesive strength of Pseudomonas fluorescens biofilms in tubes. *Colloids Surf. B. Biointerfaces* **43,** 61–71 (2005).

29. Maillard, J. Y. Bacterial target sites for biocide action. *Symp. Ser. Soc. Appl. Microbiol.**31*** **,** 16S-27S (2002)

30. Touir, R. *et al.* Corrosion and scale processes and their inhibition in simulated cooling water systems by monosaccharides derivatives. *Desalination* **249,** 922–928 (2009).

31. Cloete, T. E., Brözel, V. S. & Von Holy, A. Practical aspects of biofouling control in industrial water systems. *Int. Biodeterior. Biodegradation* **29,** 299–341 (1992).

32. Bott TR, *Industrial biofouling. Elsevier:* The boulevard, Langford Lane, Kidlington, Oxford, UK (2011)

33. Bott, T. R. Potential Physical Methods for the Control of Biofouling in Water Systems. *Chem. Eng. Res. Des.* **79,** 484–490 (2001).

34. White, D. G. & McDermott, P. F. Biocides, drug resistance and microbial evolution. *Curr. Opin. Microbiol.* **4,** 313–7 (2001).

35. Simões, M. Use of biocides and surfactants to control Pseudomonas fluorescens biofilms: role of the hydrodynamic conditions. (2005).

36. Gabbay, J. Copper Oxide Impregnated Textiles with Potent Biocidal Activities. *J. Ind. Text.* **35,** 323–335 (2006).

37. Borkow, G. & Gabbay, J. Putting copper into action: copper-impregnated products with potent biocidal activities. *FASEB J.* **18,** 1728–30 (2004).

38. O'Gorman, J. & Humphreys, H. Application of copper to prevent and control infection. Where are we now? *J. Hosp. Infect.* **81,** 217–23 (2012).

39. Borkow, G. & Gabbay, J. Copper as a biocidal tool. *Curr. Med. Chem.* **12,** 2163–75 (2005).

40. Grace, M., Sc, M., Chand, N., Ph, D. & Bajpai, S. K. Copper Alginate-Cotton Cellulose (CACC) Fibers with Excellent Antibacterial Properties. **4,** 24–35 (2009).

41. Delgado, K., Quijada, R., Palma, R. & Palza, H. Polypropylene with embedded copper metal or copper oxide nanoparticles as a novel plastic antimicrobial agent. *Lett. Appl. Microbiol.* **53,** 50–4 (2011).

42. Ruparelia, J. P., Chatterjee, A. K., Duttagupta, S. P. & Mukherji, S. Strain specificity in antimicrobial activity of silver and copper nanoparticles. *Acta Biomater.* **4,** 707–16 (2008).

43. Cík, G., Bujdáková, H. & Sersen, F. Study of fungicidal and antibacterial effect of the Cu(II)-complexes of thiophene oligomers synthesized in ZSM-5 zeolite channels. *Chemosphere* **44,** 313–9 (2001).

44. Jung, W. K. *et al.* Antibacterial activity and mechanism of action of the silver ion in Staphylococcus aureus and Escherichia coli. *Appl. Environ. Microbiol.* **74,** 2171–8 (2008).

45. Yuranova, T. *et al.* Antibacterial textiles prepared by RF-plasma and vacuum-UV mediated deposition of silver. *J. Photochem. Photobiol. A Chem.* **161,** 27–34 (2003).

46. Knetsch, M. L. W. & Koole, L. H. New Strategies in the Development of Antimicrobial Coatings: The Example of Increasing Usage of Silver and Silver Nanoparticles. *Polymers (Basel).* **3,** 340–366 (2011).

47. Lansdown, a B. G. Critical observations on the neurotoxicity of silver. *Crit. Rev. Toxicol.* **37,** 237–50 (2007).

48. McDonnell, G. & Russell, a D. Antiseptics and disinfectants: activity, action, and resistance. *Clin. Microbiol. Rev.* **12,** 147–79 (1999).

49. Schierholz, J. M. Medical Devices Efficacy. *J. Hosp. Infect.* 257–262 (1998).

50. Stobie, N., Duffy, B., Hinder, S. J., McHale, P. & McCormack, D. E. Silver doped perfluoropolyether-urethane coatings: antibacterial activity and surface analysis. *Colloids Surf. B. Biointerfaces* **72,** 62–7 (2009).

51. Ewald, A., Glückermann, S. K., Thull, R. & Gbureck, U. Antimicrobial titanium/silver PVD coatings on titanium. *Biomed. Eng. Online* **5,** 22 (2006).

52. Balogh, L., Swanson, D. R., Tomalia, D. a., Hagnauer, G. L. & McManus, A. T. Dendrimer−Silver Complexes and Nanocomposites as Antimicrobial Agents. *Nano Lett.* **1,** 18–21 (2001).

53. Spacciapoli, P., Buxton, D., Rothstein, D. & Friden, P. Antimicrobial activity of silver nitrate against periodontal pathogens. *J. Periodontal Res.* **36,** 108–13 (2001).

54. Purohit, a *et al.* Quaternary ammonium compounds and occupational asthma. *Int. Arch. Occup. Environ. Health* **73,** 423–7 (2000).

55. Cook, E. W. & Moss, P. H. Quaternary ammonium compounds. (1949).

56. Gottenbos, B., van der Mei, H. C., Klatter, F., Nieuwenhuis, P. & Busscher, H. J. In vitro and in vivo antimicrobial activity of covalently coupled quaternary ammonium silane coatings on silicone rubber. *Biomaterials* **23,** 1417–1423 (2002).

57. Thebault, P. *et al.* Preparation and antimicrobial behaviour of quaternary ammonium thiol derivatives able to be grafted on metal surfaces. *Eur. J. Med. Chem.* **44,** 717–24 (2009).

58. To, M. S., Favrin, S., Romanova, N. & Griffiths, M. W. Postadaptational Resistance to Benzalkonium Chloride and Subsequent Physicochemical Modifications of Listeria monocytogenes. **68,** 5258–5264 (2002).

59. Chen, C. Z. *et al.* Quaternary ammonium functionalized poly(propylene imine) dendrimers as effective antimicrobials: structure-activity studies. *Biomacromolecules* **1,** 473–80 (2000).

60. Majumdar, P. *et al.* Synthesis and antimicrobial activity of quaternary ammonium-functionalized POSS (Q-POSS) and polysiloxane coatings containing Q-POSS. *Polymer (Guildf).* **50,** 1124–1133 (2009).

61. Sundheim, G., Langsrud, S., Heir, E. & Holck, a. L. Bacterial resistance to disinfectants containing quaternary ammonium compounds. *Int. Biodeterior. Biodegradation* **41,** 235–239 (1998).

62. Murata, H., Koepsel, R. R., Matyjaszewski, K. & Russell, A. J. Permanent, non-leaching antibacterial surface--2: how high density cationic surfaces kill bacterial cells. *Biomaterials* **28,** 4870–9 (2007).

63. Kenawy el-R, Abdel-Hay, F. I., el-Raheem, a, el-Shanshoury, R. & el-Newehy, M. H. Biologically active polymers: synthesis and antimicrobial activity of modified glycidyl methacrylate polymers having a quaternary ammonium and phosphonium groups. *J. Control. Release* **50,** 145–52 (1998).

64. Thorsteinsson, T., Kristinsson, K. G., Hja, M. A., Hilmarsson, H. & Loftsson, T. Soft Antimicrobial Agents: Synthesis and Activity of Labile Environmentally Friendly Long Chain Quaternary Ammonium Compounds. *Med. Chem.* **46**, 4173–4181 (2003).

65. Tashiro, T. Antibacterial and Bacterium Adsorbing Macromolecules. *Macromol. Mater. Eng.* **286,** 63–87 (2001).

66. Boothe, H. W. Antiseptics and disinfectants. *Vet. Clin. North Am. Small Anim. Pract.* **28,** 233–248 (1998).

67. Salton, M. R. Lytic agents, cell permeability, and monolayer penetrability. *J. Gen. Physiol.* **52,** 227–52 (1968).

68. Saleh, S., Haddadin, R. N. S., Baillie, S. & Collier, P. J. Triclosan - an update. *Lett. Appl. Microbiol.* **52,** 87–95 (2011).

69. Tabak, M. *et al.* Effect of triclosan on Salmonella typhimurium at different growth stages and in biofilms. *FEMS Microbiol. Lett.* **267,** 200–206 (2007).

70. Adolfsson-Erici, M., Pettersson, M., Parkkonen, J. & Sturve, J. Triclosan, a commonly used bactericide found in human milk and in the aquatic environment in Sweden. *Chemosphere* **46,** 1485–9 (2002).

71. Levy, C. W. *et al.* Molecular basis of triclosan activity. *Nature* **398,** 383–4 (1999).

72. McMurry, L. M., Oethinger, M. & Levy, S. B. Triclosan targets lipid synthesis. *Nature* **394,** 531–2 (1998).

73. Singer, H., Müller, S., Tixier, C. & Pillonel, L. Triclosan: occurrence and fate of a widely used biocide in the aquatic environment: field measurements in wastewater treatment plants, surface waters, and lake sediments. *Environ. Sci. Technol.* **36,** 4998–5004 (2002).

74. Heath, R. J. *et al.* Mechanism of triclosan inhibition of bacterial fatty acid synthesis. *J. Biol. Chem.* **274,** 11110–4 (1999).

75. Thomas, J., Choi, S.-B., Fjeldheim, R. & Boudjouk, P. Silicones containing pendant biocides for antifouling coatings. *Biofouling* **20,** 227–36 (2010).

76. Brausch, J. M. & Rand, G. M. A review of personal care products in the aquatic environment: environmental concentrations and toxicity. *Chemosphere* **82,** 1518–32 (2011).

77. Majumdar, P. *et al.* Combinatorial materials research applied to the development of new surface coatings IX: an investigation of novel antifouling/fouling-release coatings containing quaternary ammonium salt groups. *Biofouling* **24,** 185–200 (2008).

78. De Nys, R. & Steinberg, P. D. Linking marine biology and biotechnology. *Curr. Opin. Biotechnol.* **13,** 244–248 (2002).

79. Ren, D. & Wood, T. K. (5Z)-4-bromo-5-(bromomethylene)-3-butyl-2(5H)-furanone reduces corrosion from Desulfotomaculum orientis. *Environ. Microbiol.* **6,** 535–40 (2004).

80. Mahajan, V. a., Borate, H. B. & Wakharkar, R. D. Efficient synthesis of 1,4-dihydronaphthalenelignans from 5-methylene-4-substituted-2(5H)-furanones and a concise synthesis of solafuranone. *Tetrahedron* **62,** 1258–1272 (2006).

81. Manefield, M. *et al.* Evidence that halogenated furanones from Delisea pulchra inhibit acylated homoserine lactone (AHL)-mediated gene expression by displacing the AHL signal from its receptor protein. *Microbiology* **145 ,** 283–91 (1999).

82. Baveja, J. K. *et al.* Furanones as potential anti-bacterial coatings on biomaterials. *Biomaterials* **25,** 5003–12 (2004).

83. Hentzer, M. *et al.* Inhibition of quorum sensing in Pseudomonas aeruginosa biofilm bacteria by a halogenated furanone compound. *Microbiology* **148,** 87–102 (2002).

84. Baveja, J. K. *et al.* Biological performance of a novel synthetic furanone-based antimicrobial. *Biomaterials* **25,** 5013–21 (2004).

85. Kuehl, R. *et al.* Furanone enhances biofilm of staphylococci at subinhibitory concentrations by luxS repression. *Antimicrob. Agents Chemother.* **53**, 4159-4166 (2009).

86. Hume, E. B. H. *et al.* The control of Staphylococcus epidermidis biofilm formation and in vivo infection rates by covalently bound furanones. *Biomaterials* **25,** 5023–30 (2004).

87. Steenackers, H. P. *et al.* Structure-activity relationship of brominated 3-alkyl-5-methylene-2(5H)-furanones and alkylmaleic anhydrides as inhibitors of Salmonella biofilm formation and quorum sensing regulated bioluminescence in Vibrio harveyi. *Bioorg. Med. Chem.* **18,** 5224–33 (2010).

88. Hauck, T., Brühlmann, F. & Schwab, W. Formation of 4-hydroxy-2, 5-dimethyl-3 [2H]-furanone by Zygosaccharomyces rouxii: Identification of an intermediate. *Appl. Environ. Microbiol.* **69,** 3911–3918 (2003).

89. Hauck, T., Landmann, C., Raab, T. & Bru, F. Chemical formation of 4-hydroxy-2 , 5-dimethyl-3 [2 H] -furanone. **337,** 1185–1191 (2002).

90. Al-Bataineh, S. a., Britcher, L. G. & Griesser, H. J. XPS characterization of the surface immobilization of antibacterial furanones. *Surf. Sci.* **600,** 952–962 (2006).

91. Martinelli, D., Grossmann, G., Séquin, U., Brandl, H. & Bachofen, R. Effects of natural and chemically synthesized furanones on quorum sensing in Chromobacterium violaceum. *BMC Microbiol.* **4,** 25 (2004).

92. Cook, E. Furanone R . E . D . FACTS. *United States Environ. Prot. Aggency* (1996).

93. Stoye, D. *Paints, Coatings and Solvents*.WILEY-VCH : Weinheim, Germany (1998)

94. R Lambourne. *Paint and surface coatings - Theory and practice*. Woodhead Publishing Limited, Teddington, Middlesex, UK Consultant (1999).

95. Muñoz-Bonilla, A. & Fernández-García, M. Polymeric materials with antimicrobial activity. *Prog. Polym. Sci.* **37,** 281–339 (2012).

96. Fay, F., Linossier, I., Langlois, V., Haras, D. & Vallee-Rehel, K. SEM and EDX analysis: Two powerful techniques for the study of antifouling paints. *Prog. Org. Coatings* **54,** 216–223 (2005).

97. Lee, S. B. *et al.* Permanent, nonleaching antibacterial surfaces. 1. Synthesis by atom transfer radical polymerization. *Biomacromolecules* **5,** 877–82 (2004).

98. Kenawy, E.-R., Worley, S. D. & Broughton, R. The chemistry and applications of antimicrobial polymers: a state-of-the-art review. *Biomacromolecules* **8,** 1359–84 (2007).

99. Dafforn, K. a, Lewis, J. a & Johnston, E. L. Antifouling strategies: history and regulation, ecological impacts and mitigation. *Mar. Pollut. Bull.* **62,** 453–65 (2011).

100. Dafforn, K. a, Glasby, T. M. & Johnston, E. L. Differential effects of tributyltin and copper antifoulants on recruitment of non-indigenous species. *Biofouling* **24,** 23–33 (2008).

101. Konstantinou, I. K. & Albanis, T. A. Worldwide occurrence and effects of antifouling paint booster biocides in the aquatic environment: a review. *Environ. Int.* **30,** 235–48 (2004).

102. Le, Y., Hou, P., Wang, J. & Chen, J.-F. Controlled release active antimicrobial corrosion coatings with Ag/SiO2 core–shell nanoparticles. *Mater. Chem. Phys.* **120,** 351–355 (2010).

103. Lejars, M., Margaillan, A. & Bressy, C. Fouling release coatings: a nontoxic alternative to biocidal antifouling coatings. *Chem. Rev.* **112,** 4347–90 (2012).

104. Yebra, D. M., Kiil, S. & Dam-Johansen, K. Antifouling technology—past, present and future steps towards efficient and environmentally friendly antifouling coatings. *Prog. Org. Coatings* **50,** 75–104 (2004).

105. Charnley, M., Textor, M. & Acikgoz, C. Designed polymer structures with antifouling–antimicrobial properties. *React. Funct. Polym.* **71,** 329–334 (2011).

106. Chambers, L. D., Stokes, K. R., Walsh, F. C. & Wood, R. J. K. Modern approaches to marine antifouling coatings. *Surf. Coatings Technol.* **201,** 3642–3652 (2006).

107. Lindner, E. Failure mechanism of copper antifouling coatings. *Int. Biodeterior.* **24,** 247–253 (1988).

108. Nadagouda, M. N. & Varma, R. S. Synthesis of thermally stable carboxymethyl cellulose/metal biodegradable nanocomposites for potential biological applications. *Biomacromolecules* **8,** 2762–7 (2007).

109. Cioffi, N. *et al.* Antifungal activity of polymer-based copper nanocomposite coatings. **2417,** 10–13 (2004).

110. Cioffi, N. *et al.* Copper Nanoparticle/Polymer Composites with Antifungal and Bacteriostatic Properties. *Chem. Mater.* **17,** 5255–5262 (2005).

111. Valkirs, A. O., Seligman, P. F., Haslbeck, E. & Caso, J. S. Measurement of copper release rates from antifouling paint under laboratory and in situ conditions: implications for loading estimation to marine water bodies. *Mar. Pollut. Bull.* **46,** 763–79 (2003).

112. Moriarty, T. F., Zaat, S. A. J. & Busscher, H. J. Staphylococcus epidermidis in Biomaterial-Associated Infections. *Biomater. Infect.* Chapter 2, 25–56 (2013).

113. Oosterhof, J. J. H. *et al.* Effects of Quaternary Ammonium Silane Coatings on Mixed Fungal and Bacterial Biofilms on Tracheoesophageal Shunt Prostheses. Appl. Environ. Microbiol. **72,** 3673-3677 (2006)

114. Chung, D., Papadakis, S. E. & Yam, K. L. Evaluation of a polymer coating containing triclosan as the antimicrobial layer for packaging materials. *Int. J. Food Sci. Technol.* **38,** 165–169 (2003).

115. Kugel, A. J. *et al.* Combinatorial materials research applied to the development of new surface coatings XII: Novel, environmentally friendly antimicrobial coatings derived from biocide-functional acrylic polyols and isocyanates. *J. Coatings Technol. Res.* **6,** 107–121 (2009).

CHAPTER 3

Optimisation of analytical methods for biofilm monitoring and selection of potential antifouling coatings for metal surfaces

3.1. Introduction

In an open recirculating cooling water system, water is recirculated and topped up with make-up water from a variety of different sources.[1,2] Depending on the make-up water source, organic material, nutrients and a variety of micro-organisms are regularly introduced into the system creating an ideal environment for bacterial growth leading to biofouling.[2,3] Biofouling in cooling water systems causes several problems resulting in reduced system efficiency and financial losses.[4,5]

Generally the treatment of biofouling in cooling water systems entails chemical processes.[3,6] Unfortunately chemical treatments have a negative environmental impact[5,6], lead to the development of microbial resistance[3] and cost increases.[2] Alternative methods include physical cleaning methods[5] and the use of antifouling surfaces.[7] Most successful methods for fabricating antifouling surfaces involves either applying antimicrobial compounds to surfaces or combining biocides with coating materials.[7,8] Coatings with antifouling properties for use on metal substrates are commercially available, however a durable coating containing environmentally friendly biocides is currently not available.[9] Therefore this study aimed to evaluate the antifouling activity of environmentally friendly biocides that could potentially be incorporated into a durable coating for metal surfaces. The antifouling properties of potential coatings were determined by conducting biofilm studies.

Chemical and biological analysis of biofilms in the environment is extremely complicated as there are many variables in these settings. To analyse different properties of biofilms in a specific area, biofilm growth is often simulated in a laboratory environment in a system with controlled growth conditions.[10–12] For this study it was necessary to simulate biofilm growth as in a cooling water system. There are different devices available for biofilm growth simulations. A few of these devices include the deposit development probe, side stream deposit developing monitoring device, tubular geometry monitoring device, the Pedersen device, the Robbins device, flow cells, rotating annular reactors and the capillary reactor.[3,13–15] Each device has its own advantages and disadvantages.[4]

In their natural habitat, biofilms rarely consist of pure culture organisms[16] Biofilms occurring specifically in industrial cooling water systems mainly consist of a diversity of micro-organisms, primarily bacteria.[2,5] In order to conduct controlled laboratory experiments it is extremely difficult to replicate experiments when using mixed cultures, especially when performing quantitative analysis.[5]

To conduct quantitative enumeration studies on a biofilm it is necessary to completely remove the biofilm from the growth disc and to limit damage to bacterial cells. Several methods such as

swabbing, scraping, sonification, stomaching, ozone and vortexing have been reported to remove biofilms.[17]

Furthermore, quantitative characterization of sessile biofilm bacteria requires more than one analytical method and is much more complex than studying their planktonic counter parts.[18] Fast and direct enumeration methods for viable and non-viable bacterial cells are gaining importance. The need for such techniques is pressing in the microbiological health, biotechnology, food, water and pharmaceutical industries.[18,19] Current methods include bacterial plate counts and flow cytometry.

The purpose of this study was to select and optimise analytical methods for biofilm monitoring to evaluate antifouling coatings in a simulated cooling water system. Visualisation of biofilms has been done through a selection of microscopic techniques, including light microscopy, transmission electron microscopy (TEM) and scanning electron microscopy (SEM).[20–22] The use of confocal laser scanning electron microscopy (CLSM) has also been introduced as it provides a high resolution image in three dimensions without disrupting the biofilm.[20]

3.2. Materials and methods

3.2.1 Materials

Media

Brain Heart Infusion Broth (BHI, BioLab, BioLab Diagnostics, Midrand SA), Tryptic Soy Broth (TSB) (Sigma-Aldrich South-Africa) and Bacterial Agar (BioLab, BioLab Diagnostics, Midrand, SA) were used for culturing of micro-organisms.

Bacterial strains

For every experiment fresh cultures were grown from freezer cultures that were stored in 40 % glycerol at -80 °C. *Escherichia coli* ATCC 25922 and *Staphylococcus aureus* ATCC 25923 were grown in BHI broth for 18 h at 37 °C. *Pseudomonas* sp. strain CT07 (GenBank Accession No.DQ 777633) and *Pseudomonas* sp. strain CT07::*gfp* were kindly provided by the Biofilm Ecology Group (Ryerson University, Canada) and grown in 3 g/L Tryptone Soy Broth (TSB) at 26 °C for 48 h on a rotating wheel.

Metal growth discs

Mild steel, alloy of mild steel and stainless steel (3CR12), 1.2 mm discs were used, both laser cut into 2x5 cm.

Coatings

Five commercially available antifouling coatings were sourced from different manufactures. All information regarding the coating is propriety information except for the active biocide. The active biocides in the coatings and their abbreviations are listed below (Table 3.1).

Table 3.1: Commercially available industrial antifouling coatings evaluated in this study

Coating	Coating description	Abbreviation
Metal control	No coating	CC
Quaternary ammonium salt 1	Coating for metal surfaces containing quaternary ammonium salt as biocide	QAC1
Quaternary ammonium salt 2	Broad spectrum antifouling coating for metal surfaces containing an ammonium salt and ethanol biocide	QAC2
Silver nano particle	Coating with silver nanoparticles	SNP
Triclosan	Coating for metal surfaces with triclosan biocide	TC
Copper oxide	Coating for metal surfaces with copper oxide biocide	CUO

Four commercially available biocides were sourced and microbially evaluated (Table 3.2)

Table 3.2: Commercially available biocides for inclusion in coatings evaluated in this study

Biocides	Abbreviation
Silver nitrate (Sigma Aldrich, SA)	SN
Copper (II) sulphate pentahydrate (Sigma Aldrich, SA)	CS
Copper (II) chloride dehydrate (Sigma Aldrich, SA)	CC
2,5-dimethyl-4-hydroxy-3(2H)-furanone 15% in propylene glycol (Sigma Aldrich, SA)	FR

3.2.2 Methods

3.2.2.1 Selection of metal growth discs and determination of optimal biofilm growth time for biofilm analysis

Bacterial strain selection

To eliminate variables in this study, it was decided that biofilms will be grown from a pure culture. *Pseudomonas* species are known to be primary settlers and slime forming bacteria in natural environments.[5,23] They are also the predominant bacterial species in cooling water systems and as

aerobic bacteria flourishes in the aerated environment of a cooling water system. They are also metabolically diverse and can adapt their pathways under different conditions.[2] An isolate from industrial cooling tower water was identified as closely related to a known *Pseudomonas* species by 16S rDNA sequencing .[24] This isolate was later designated as *Pseudomonas* sp. strain CT07 (GenBank Accession No.DQ 777633). Biofilm experiments were conducted by using *Pseudomonas* sp. strain CT07.

Selection of metal growth disc

Mild steel growth discs (2x5 cm) were submerged in a container containing sterile TSB broth representing the biofilm growth device (Figure 1). *Pseudomonas* sp. strain CT07 was inoculated into sterile TSB broth and the container was closed with a lid. The broth was magnetically stirred for 24 h after which the discs were individually removed. Bacterial cells attached to the growth discs were fixated with 1 ml 2.5 % gluteraldehyde (kept in dark for 2 h) and dehydrated with an ethanol dilution series of 50 %, 70 %, 90 % and 100 %. Scanning electron microscopy (SEM) analyses of the growth discs were done at the Stellenbosch University Microscopy Unit on a LEO® 1430VP and a Cambridge S200 scanning electron microscope after gold sputter coating was applied. The conditions for image acquisition were an accelerating voltage of 7 kV and a probe current of 150 pico amperes (pA). Images were taken at 2000X enlargement. The experiment was repeated with 3CR12 stainless steel discs consisting of alloy stainless steel combined with mild steel.

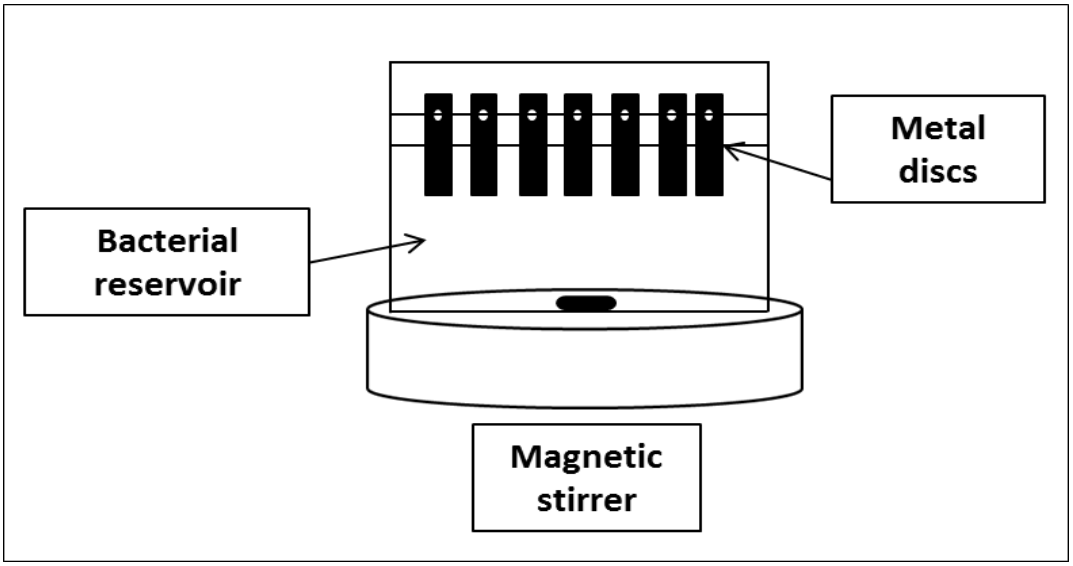

Figure 3.1: Diagram of biofilm growth device

Biofilm growth optimisation time

The experiment described above was repeated by using 3CR12 metal discs as growth discs in the biofilm growth device. The growth discs were removed after 12, 24, 36, 48, 60 and 72 h after which it was visualised through SEM as described before.

3.2.2.2 Microbial analysis of the biofilm

Modified flow cell system

The modified flow cell system was designed to simulate properties of an open recirculating cooling water system, although it was kept closed to exclude contamination and to ensure biofilm growth from a pure culture. It was also designed to accommodate different analysis techniques by incorporating ten growth discs (2x5 cm) in serial to ensure exposure of all the discs to the same elements. Nine growth discs were used for the experimental analysis and one served as a control. Optimal growth conditions of the selected bacteria, *Pseudomonas* sp. strain CT07, are aerobic and at 26 °C as determined by Bester et al. (2005). The temperature of the flow cell system was therefore kept between 20 and 26 °C and a magnetic stirrer was used to create aerobic conditions throughout the 48 h biofilm growth time. Flow speed was maintained at 13 mL h^{-1} using a multichannel peristaltic pump and more than one flow cell could be set up simultaneously (Figure 3.2).

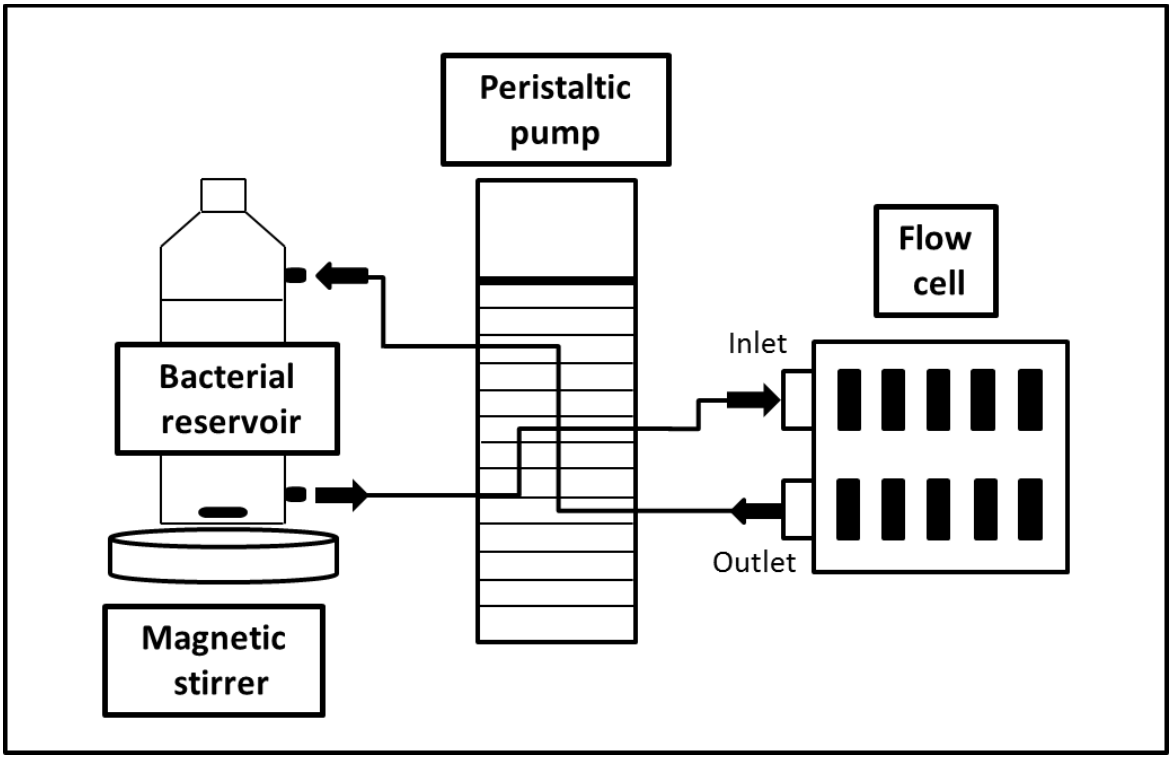

Figure 3.2: Diagram of the modified flow cell system

Biofilm removal method

After discs were exposed to *Pseudomonas* sp. strain CT07 for 48 h in the modified flow cell system, different methods including scraping, swabbing and sonificating [17,25] were used to remove biofilms from the metal growth discs. Serial dilutions of the removed biofilm samples were prepared in sterile saline solution (SSS) and the pour plate technique was used for the enumeration of bacteria. One mL of each dilution and each sample was added to 3 g/L TSB soft agar (1 %) plates and incubated at 26 °C for 72 h. After biofilm removal by either scraping, swabbing or sonification,

discs were visualised by SEM to determine which method most successfully removed biofilms from the discs.

Scraping

A surgical blade (Invitrogen™) was flame sterilized with 70 % ethanol. After metal discs were rinsed with SSS, the exposed surface was scraped with the surgical blade five times with consecutive movements. Between each scrape the material scraped off was deposited in 10 ml SSS. The surgical blade was also dipped into 10 ml SSS after each scrape. After scraping the bacterial suspension was vortexed for 10 s, and enumerated as described above.

Swabbing

Swabs (Invitrogen™) were autoclaved at 121 °C for 15 min. Sterile swabs were pre-moistened in SSS. Swabs were firmly pressed against metal discs at the top of each disc. The swab was then rolled down the surface of the exposed area of the disc five times. Between each swabbing action the swab was rinsed in 10 mL SSS. After swabbing the bacterial suspension was vortexed for 10 s for dislodging purposes and enumerated as described above.

Sonificating

Discs removed from the flow cells were rinsed in 25 mL SSS and submerged into an enclosed 250 mL glass beaker containing 10 mL SSS. Beakers were sonicated with a Branson 5510 sonificator for 3 min. After sonification the bacterial suspension was vortexed for 10 s and enumerated as described above.

3.2.2.3 Optimisation of fluorescence analytical methods

Confocal laser scanning microscopy of biofilms on growth discs

Confocal laser scanning microscopy (CLSM) provides high resolution, three dimensional images without disrupting the biofilm though dehydration, fixing, or embedding .[20,26] Through this method biofilms can be studied in a hydrated form as they exist in the environment.[26] Biofilms are not flat entities but have a three dimensional structure. Information regarding the biofilm structure can be collected with CLSM by acquiring images at different depths throughout the biofilm. These images can then be re-assembled to give a three dimensional image. CLSM was used in combination with the LIVE/DEAD® Baclight™ Bacterial Viability kit (Invitrogen™). The LIVE/DEAD® stain consists of SYTO 9 and propidium iodide (PI) that discriminates between live and dead cells through staining of nucleic acids. SYTO 9 is a green fluorescing stain which enters all cells and is used to determine total cell count. Propidium iodide is a red fluorescing stain which only enters cells with damaged cytoplasmic membranes and is used to identify dead cells. The degree of viability of bacterial cells in the biofilms grown from *Pseudomonas* sp. CT07 on growth discs was determined in this way.

Biofilms of *Pseudomonas* sp. CT07 samples were stained with PI and SYTO 9 and those of *Pseudomonas* sp. CTO7*::gfp* with PI only. Stock solutions of SYTO9 and PI stains were diluted to

concentrations of 0.3 % (v/v) in sterile saline. The SYTO 9 and PI solution (100 µL) was pipetted onto each metal plate, covered with a 2.2 x 5 cm coverslip and kept in dark conditions for 15 min. Three images were taken of every sample and analysed on a Carl Zeiss LSM780 confocal microscope (Carl Zeiss, Germany). Using an Argon multiline laser as light source, images were excited at 488 nm or 514 nm. Emission was collected using a Spectral detection LSM780 GaAsP detector at 490-560 nm (eGFP) and 646-709 nm (PI). For image frame acquisition, a Plan-Apochromat 63x/1.40 Oil DIC M27 objective was used. The ZEN 2011 imaging software (Carl Zeiss, Germany) was used to acquire Z-stacks at 1 µm step width and images were processed by applying maximum intensity projection. After staining, images of the growth discs coated with respective coatings were acquired before biofilm growth (0 h) and after biofilm growth (48 h).

Flow cytometry of biofilms removed from growth discs

Through the use of flow cytometry large quantities of individual cells of homogeneous or heterogeneous populations in solution pass through the measuring apparatus in single file enumerating them in seconds.[27,28] The first use of flow cytometry was in the medical sciences field, and still accounts for the predominant use. The value of flow cytometry has however been recognized in the biology, toxicology, virology, pharmacology, environmental science, bioprocess monitoring and bacteriology fields.[28] The reason for the recent wider use of flow cytometry can be attributed to the fact that the equipment, that is commercially available, is robust, versatile and works in line with modern data interpretation software. The use of flow cytometry combined with a variety of staining assays to determine bacterial viability is emerging as a leading technology.[28,29] Flow cytometry shows to be a promising technique in the enumeration of cells in a biofilm after removal .[30]

Flow cytometry and the LIVE/DEAD® Baclight™ Bacterial Viability and Counting Kit (Invitrogen™) were used to obtain the ratios of Live/Dead planktonic cells. By distinguishing between two fluorescence colours (either red or green), two distinctive populations of live and dead cells could be observed. Total cell counts, total viable cells and total dead cells were calculated from the data obtained from flow cytometric analysis and statistically verified using ANOVA.

The staining procedure developed by Paulse et al. (2009)[31] was followed. Equal volumes (4 µL) of PI and SYTO 9 were added to 1 mL of sterile saline. This solution (200 µL) of dyes was then added to 1 mL of the biofilm sample of *Pseudomonas* sp. CT07 and kept in dark conditions for 15 min. Next, 50 µL of liquid counting beads (BD™ Liquid Counting Beads) was added and samples were subjected to flow cytometry at the Central Analytical Facility (CAF), Stellenbosch University. The procedure was repeated with biofilms of *Pseudomonas* sp. CTO7*::gfp* by using the PI stain only, with added liquid counting beads.

Each sample was analysed by a Becton Dickinson FACS Aria flow cytometer with a 13 mW, 488 nm Coherent® Sapphire™ Solid State laser. For this study, the bacterial population was identified

and gated on a forward scatter (FSC) vs. a side scatter (SSC) dotplot and a SSC vs. PerCP at 695/40 nm dotplot. The bead count was identified and gated on SSC vs. PerCP dotplot. The parameters were all measured using a logarithmic amplification scale. The threshold was set to 1000 FSC channels to remove debris from the sample.

To calculate fluorescence overlap between the two fluorochromes, compensation was measured in the following manner. The SYTO 9 and *gfp* green fluorescent emission and PI red fluorescent emission were individually measured in the PE-Texas Red channel (610/20 nm) and the FITC channel (530/30 nm). For this purpose the following controls of *Pseudomonas* sp. CT07 and *Pseudomonas* sp. CT07*::gfp* bacterial samples were included: *Pseudomonas* sp. CT07 i) non-stained ii) viable bacteria stained with SYTO9 iii) non-viable bacteria stained with PI, as well as *Pseudomonas* sp. CT07 *::gfp* i) non-stained bacteria ii) non-viable bacteria stained with PI. Compensation values were calculated by using the software BD FACSDiva (version 6.1.3).

3.2.2.4 Selection of coatings and biocides

Five different antifouling coating samples for metal surfaces were obtained from a local distributor that imports coatings from different manufacturers from around the globe (Table 3.1). Five potential biocides for incorporation into a base coating were identified (Table 3.2). A modified Kirby Bauer diffusion test was used to select the coatings and biocides with the highest antifouling activity against both Gram-negative and Gram-positive microorganisms, namely *E. coli* ATCC 25922 and *S. aureus* ATCC 25923 respectively.

Modified Kirby Bauer disc diffusion test

The biocides, copper sulphate (0.32 g/mL), copper chloride (0.75 g/mL) and silver nitrate (2.16 g/mL) were diluted in sterile water to prepare saturated solutions of each. Furanone in propylene glycol solution is in liquid form and used as is. Filter paper discs (10 mm^{-3}, Invitrogen^{TM}) were autoclaved and dried at 30 ˚C for 24 h. After drying, each disc was coated with 10 µL of each respective coating or concentrated biocide solution. Coated discs were left overnight to cure. *E. coli* and *S. aureus* were inoculated into 5 mL BHI broth incubated at 37 °C for 18 h. Nutrient agar plates were then spread-plated with 100 µL of a 2-times dilution of each culture. Coated paper discs were then placed face down in the centre of plates and incubated at 37 °C for 48 h and evaluated for inhibition zones.

After selecting the biocides to be used, the minimum inhibitory concentration (MIC) of each biocide was determined with a dilution susceptibility test.

Dilution susceptibility test

The MIC can be defined as the lowest concentration of a biocide which will result in the inhibition of micro-organism growth after overnight incubation of a 5 x 10^5 CFU/mL culture.[32,33] This was done through the dilution susceptibility test. Saturated solutions of each biocide were prepared as discussed in the previous section. One millilitre of sterile 3 g/L TSB broth was added to sterile

glass test tubes. A saturated biocide solution (1 mL) was added to the first tube and a dilution series was prepared up to 0.005 % of the saturated biocide solution as described in paragraph above. To each tube, 1 % (v/v) of *Pseudomonas* sp. strain CT07 culture was added aseptically, vortexing after each addition. Tubes were incubated on a rotating wheel at 26 °C for 48 h where after each tube was visually inspected for bacterial growth. The MIC was calculated by using the lowest biocide dilution in the dilution series where no bacterial growth could be visualised and converting the percentage dilution to milligrams per litre and express it as parts per million (ppm).

3.3. Results and discussion

3.3.1 Selection of metal growth discs and determination of optimal biofilm growth time for biofilm analysis

Selection of metal growth discs

The mild steel growth discs corroded after 24 h exposure in the biofilm growth device (Figure 3.3).

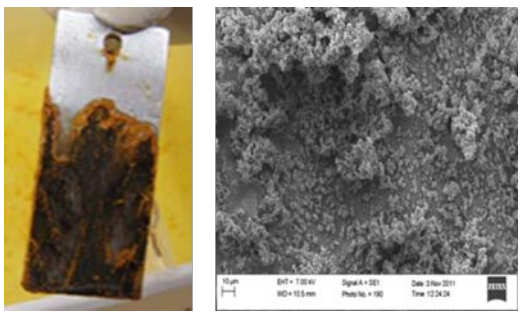

Figure 3.3: Digital and SEM image of mild steel growth disc after 24 h exposure to biofilm growth device

Severe corrosion was observed on the discs and SEM analysis also indicated a few bacterial colonies intertwined within the corroded metal (Figure 3.3). Qualitative or quantitative analysis of the biofilms could therefore not be conducted as a clear distinction between the bacterial cells and corrosion could not be observed. With the plate count method, the corrosion also inhibited bacterial growth. Corrosion after 24 h on mild steel is normal as the initial corrosion rate of mild steel is high and only decreases after a few days. [2]

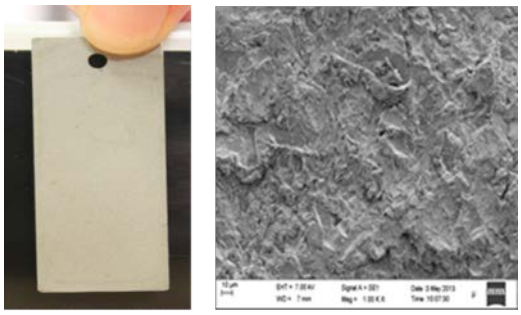

Figure 3.4: Digital and SEM image of 3CR12 growth disc after 24 h exposure to biofilm growth device

No corrosion was observed on 3CR12 growth discs after 24 h (Figure 3.4). It was therefore possible to conduct qualitative as well as quantitative analysis using SEM and plate counts without

the interference of corrosion residue. Stainless steel was therefore used instead of mild steel 3CR12 throughout the study.

Biofilm growth optimisation time

The biofilm was at its optimum density after 48 h and became less dense after 60 h (Figure 3.5). This is in agreement with Costerton et al. (1995)[34] who proposed that micro-organisms need nutrients to multiply and upon depletion of the nutrient source the micro-organisms will stop growing and start dying off. It was therefore decided that the discs would be exposed for 48 h and then subjected to the different analytical methods.

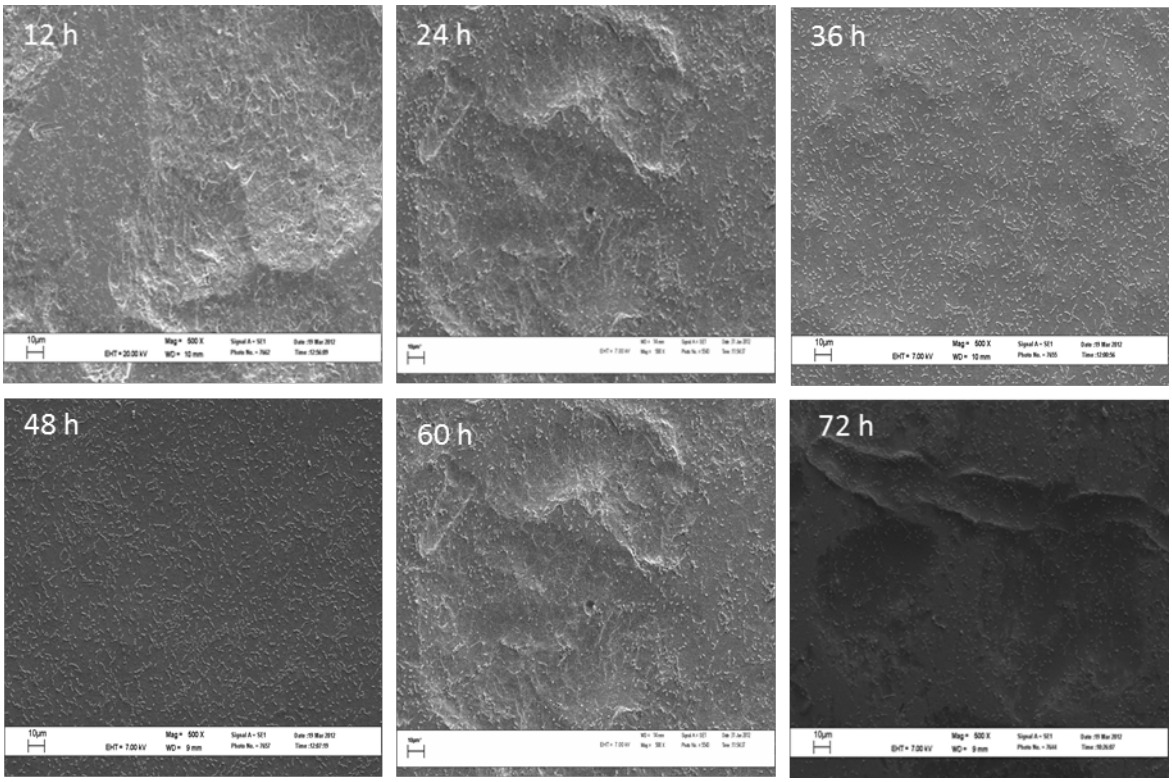

Figure 3.5: SEM images of biofilm growth rate

3.3.2 Microbial analysis of the biofilm

Biofilm removal method

Enumeration of cells recovered from biofilm removal

The average viable cell numbers obtained through the pour plate method for the three biofilm removal techniques were 5.19 log CFU/mL for sonification, 5.17 log CFU/mL for scraping and 5.17 log CFU/mL for swabbing. There is a significant difference between the plate counts of the sonification method and the methods of scraping and swabbing, but no significant difference between the plate counts after scraping and swabbing (Figure 3.6).

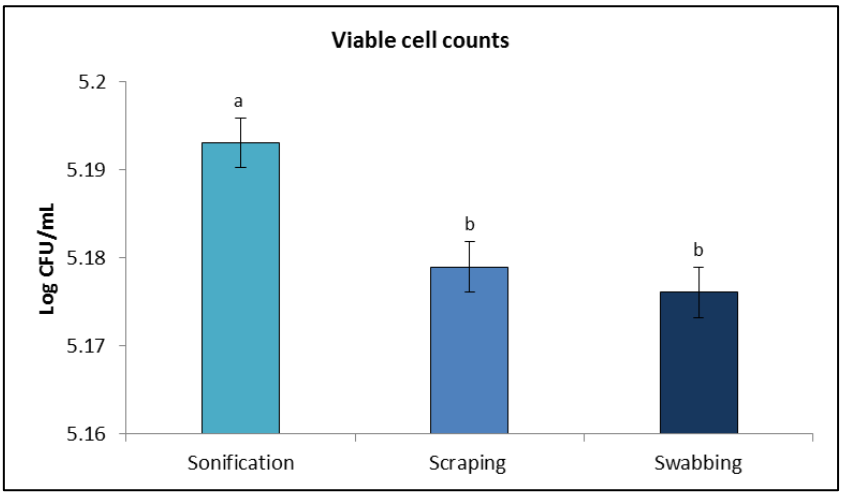

Figure 3.6: Enumeration of total viable and culturable bacteria (CFU/mL) using the pour plate technique for different biofilm removal techniques (a,b indicating a significant difference (P<0.05) as compared to Sonification).

SEM images showed a few single cells on the surfaces of the growth discs after swabbing and scraping, but none could be observed after sonification (Figure 3.7). This correlates with the enumeration results in Figure 3.6.

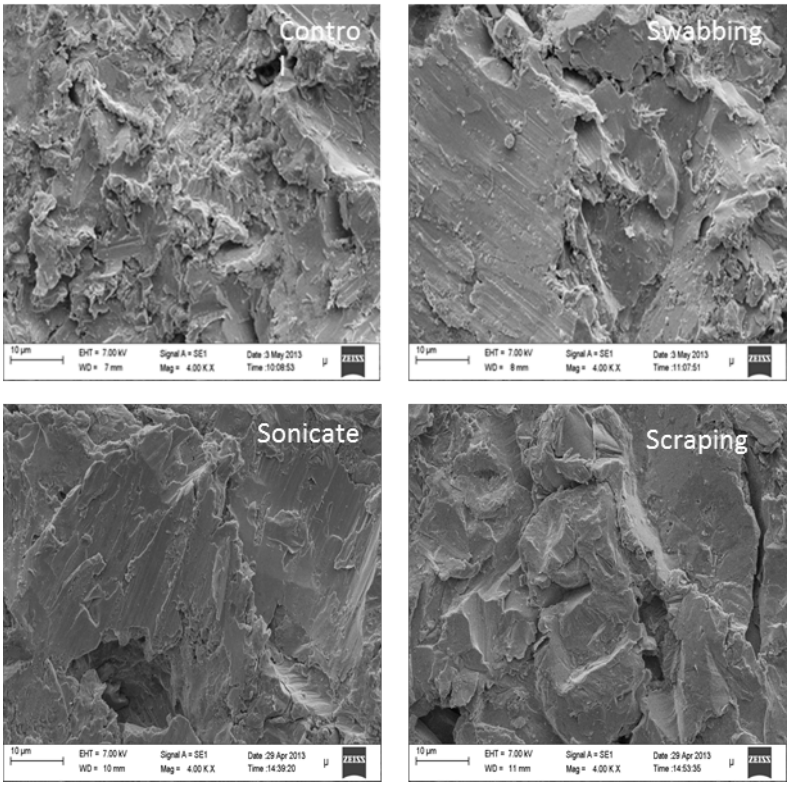

Figure 3.7: SEM images of control growth disc and growth discs after swabbing, scraping and sonification biofilm removal methods have been utilised. The scale bar in the images corresponds to length of 10 µm.

Results from Figures 3.6 and 3.7 were confirmed by previous studies on biofilm removal methods.[17] Gagnon et al. (1999)[17] found that stomaching, followed by scraping and swabbing was the most successful method to remove biofilms from coupons. The authors also observed contamination on agar plates after scraping and questioned the accuracy of this technique. Lindsay

and von Holy (1997)[25] found no significant difference in the CFU counts after sonification, vortexing or shaking with beads to remove *P. fluorescence* biofilms from stainless steel coupons. Percival et al. (1998)[35] determined that sonification, scraping and swabbing removed 80 – 85 % of the biofilm from stainless steel.

It was concluded that sonification was the optimum method for removal of the biofilm from the metal substrate. Cell membranes of bacterial cells are however damaged if sonicated for too long.[36] Therefore a further investigation was done to determine the optimum sonification time. Fifteen metal discs which were subjected to 48 h biofilm growth, sonicated and one disc was removed every minute. It was determined that 5 min sonication was the optimum time period for these specific experimental procedures.

3.3.3 Optimisation of fluorescence analytical methods

Confocal laser scanning electron microscopy

Images taken at 0 h for CC, TC, CUO and QAC1 (Figure 3.8) displayed green fluorescent particles as well as a hazy green background. Images for TC and QAC1 also had a hazy red background. Thus it is evident that the metal control as well as all the coatings interacted chemically with SYTO 9 stain and TC and QAC1 slightly with PI stain. Images taken at 48 h of CC, TC, CUO and QAC1 displayed similar fluorescent green particles and hazy green and red backgrounds as in images taken at 0 h. Additional fluorescence signals from the attached bacteria on the metal growth discs were also observed. It was therefore not possible to make clear distinctions between the fluorescence signals from the micro-organisms and that of the metal disc and coatings on metal growth discs.

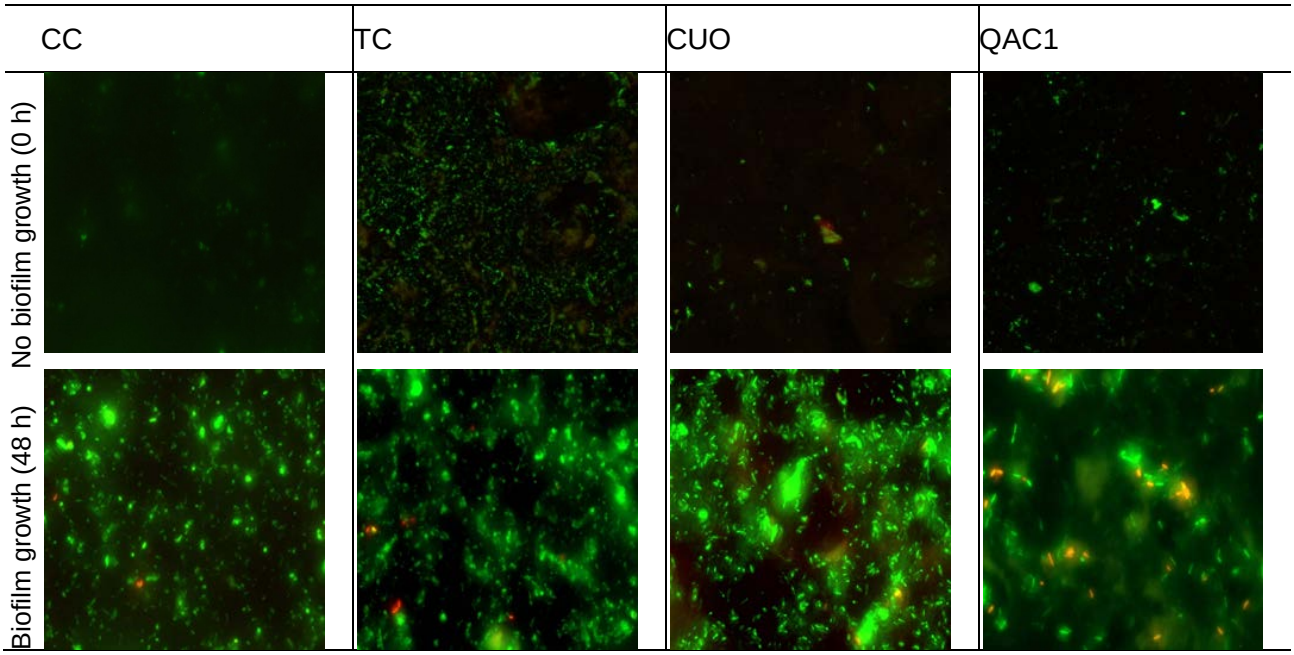

Figure 3.8: CLSM images of growth discs with respective coatings before and after biofilm growth with *Pseudomonas* sp. CT07 stained with SYTO 9 and PI stain

In order to eliminate the chemical interaction between the SYTO 9 stain and the metal and coatings it was decided to use the same micro-organism into which green-fluorescent protein gene (*gfp*) was inserted into the chromosome.[23] The *gfp* gene encodes the green fluorescent protein (GFP) in bacteria and GFP fluoresces without a substrate or additional cofactors.[37] The efficient integration of the *gfp* gene into the chromosome of a micro-organism enables it to be visualised by fluorescence principal analytical methods.[37]

GFP fluorescence phenotype does not indicate metabolic status of bacterial cells and was therefore used in combination with PI stain.

CLSM images taken at 0 h of TC and CUO showed a hazy red background indicating that the PI stain interacted chemically with the coatings while CC and QAC1 had no signs of PI stain interacting with the metal or coating. The hazy red background did not involve bright red particles so clear distinctions could be made between the nonviable bacteria (bright red particles) and the background as confirmed through the images taken after 48 h biofilm growth of CC, TC, CUO and QAC1 (Figure 3.9).

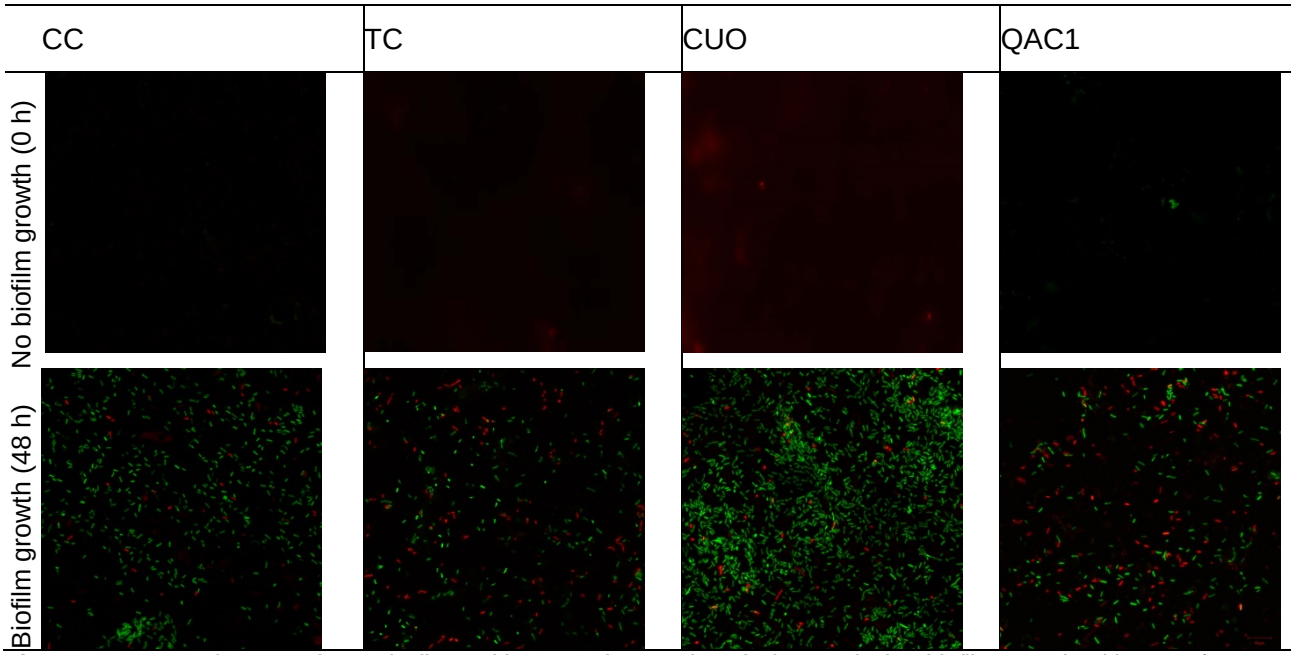

Figure 3.9: CLSM images of growth discs with respective coatings before and after biofilm growth with *Pseudomonas* sp. CT07::*gfp* stained with PI stain

Flow cytometry

The first image in Row 1 of Figure 3.10 is an illustration of the reported flow cytometry diagrams and demonstrates in which quadrant the microorganisms in their different metabolic states and the debris would lie in. The next three images in Row 1 display control samples that were run with *Pseudomonas* sp. CT07 indicating in which quadrant the unstained bacteria, viable bacteria stained with SYTO 9 and non-viable bacteria stained with PI stain respectively would lie in. Clear distinct populations of the controls could be observed (Figure 3.10). In Row 2, the images of samples CC, TC, CUO and QAC1 of the removed 48 h biofilm samples showed no distinct

populations in any quadrant. The populations present overlapped each other over all four quadrants. Thus, the separation of the populations to conduct enumeration analysis could not be done with accuracy. Paulse et al. (2007)[31] indicated that there is a possibility that non-microorganism biomass or debris in the samples subjected to flow cytometry may influence the cell. [31]These results are in correlation with the CLSM images from Figure 3.8 in which the metal and coatings showed bright green particles.

Controls	Unstained bacteria (Debris)	Viable bacteria stained with SYTO9 (Alive)	Non-viable bacteria stained with PI stain (Dead)
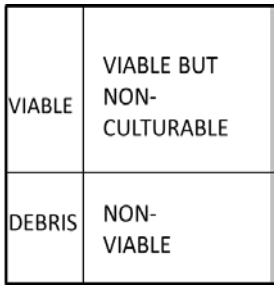	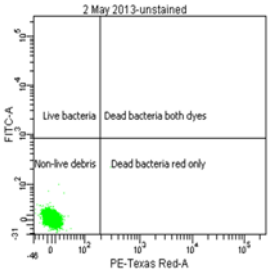	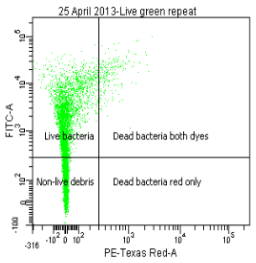	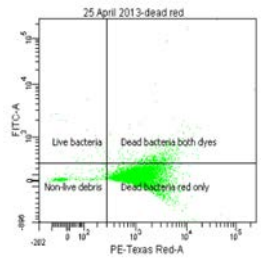
CC	TC	CUO	QAC 1
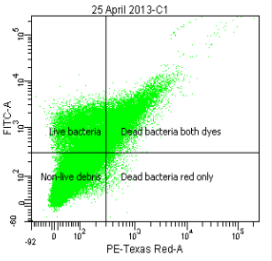	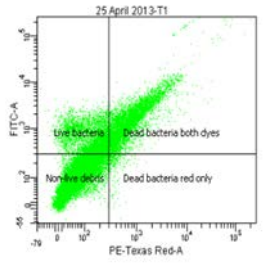	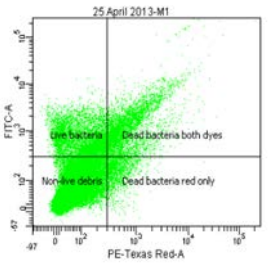	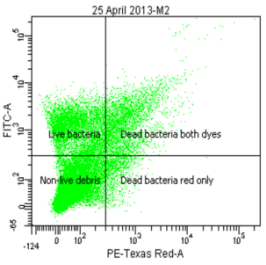

Figure 3.10 Diagrams of the data obtained from flow cytometry analysis of the removed biofilm grown from *Pseudomonas* sp. CT07

The experiment was repeated with *Pseudomonas* sp. CTO7::*gfp*. The first image in Row 1 of Figure 3.11 is an illustration of the reported flow cytometry diagrams and demonstrates in which quadrant the bacteria in their different metabolic states and the debris would lie in. The next two images in Row 1 display control samples that were run with *Pseudomonas* sp. CT07::*gfp* indicating in which quadrant the unstained bacteria and non-viable bacteria stained with PI stain respectively would lie in. Clear distinct populations of the controls could be observed (Figure 3.11). In Row 2 the images of samples CC, TC, CUO and QAC1 of the removed 48 h biofilm samples are displayed. A distinction could be made between the populations of viable and non-viable bacteria and debris in the four quadrants as it resembled the populations in the control images. Similar results were therefore observed both from CLSM and flow cytometry.

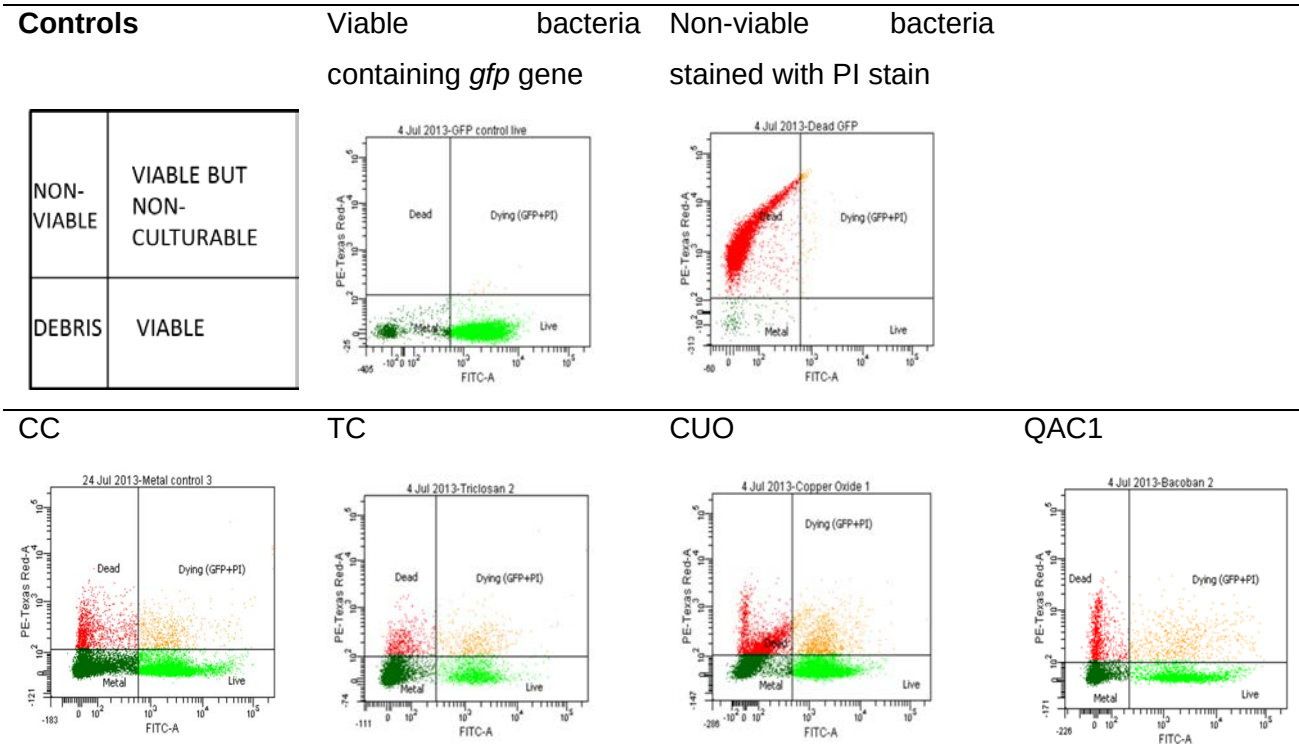

Figure 3.11: Diagrams of the data obtained from flow cytometry analysis of the removed biofilm grown from *Pseudomonas* sp. CT07::*gfp*

Williams et al. (1999)[30]and Ziglio et al. (2002)[38] also used flow cytometry in combination with CLSM with fluorescent dyes in their study of early attachment of *S. aureus*. The use of CLSM flow cytometry with GFP fluorescent bacterial cells have also shown to be successful by Unge et al. (1999).[37] *Pseudomonas* sp. CT07::*gfp* could therefore be used to distinguish between viable and non-viable cells in CLSM and flow cytometry analysis of *Pseudomonas* sp. biofilms.

3.3.4 Selection of coatings and biocides

Modified Kirby Bauer disc diffusion test

The antifouling activity of each industrial coating was different against the respective bacterial strains (Figure 3.12). One of the coatings, containing quaternary ammonium salt, showed clear zones against *E. coli* and *S. aureus* whilst the other indicated no zones. The coating containing triclosan showed the most prominent zones against both *E. coli* and *S. aureus.* The silver nano particle coating indicated no zones against either bacterium. The copper oxide showed no zone against *E. coli* and a slight zone against *S. aureus*. The three coatings selected for this study were QAC1, TC and CUO.

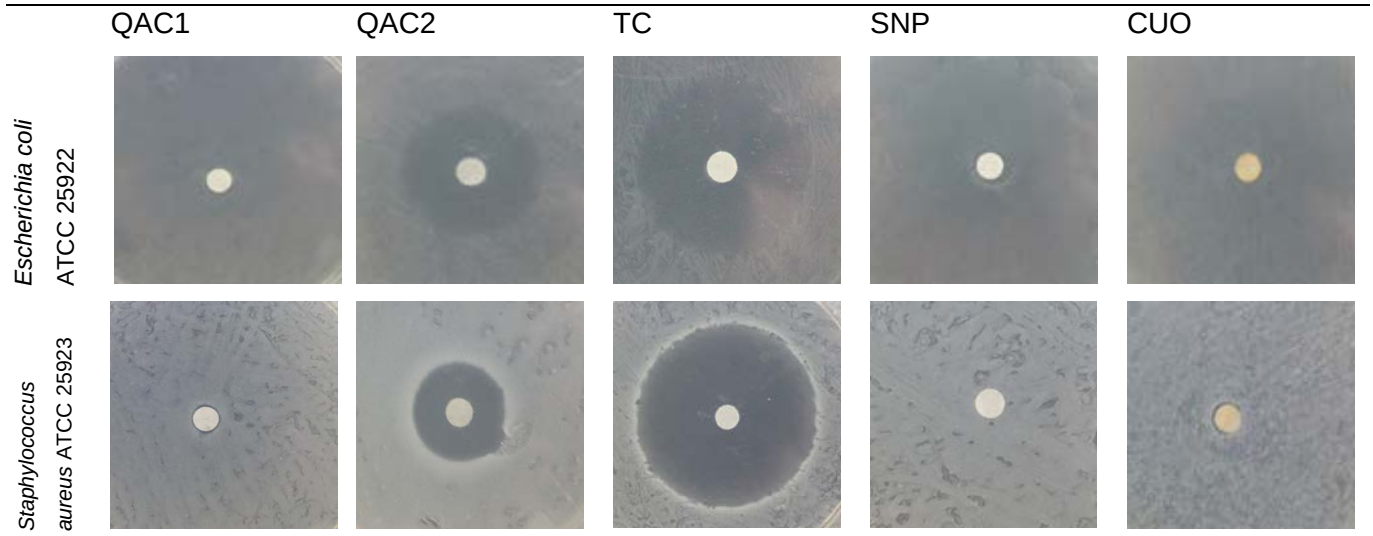

Figure 3.12: Kirby Bauer disc diffusion test results for commercially available antifouling coatings

The results of the disc diffusion test for biocides, outlined in Table 3.2, are indicated in Figure 3.13. All biocides showed clear zones against both *E. coli* and *S. aureus*. Copper sulphate showed the most prominent zones against both bacteria and furanone solution the least. A preliminary study showed that copper chloride did not dissolve in an epoxy based coating and was therefore not used in the rest of the study.

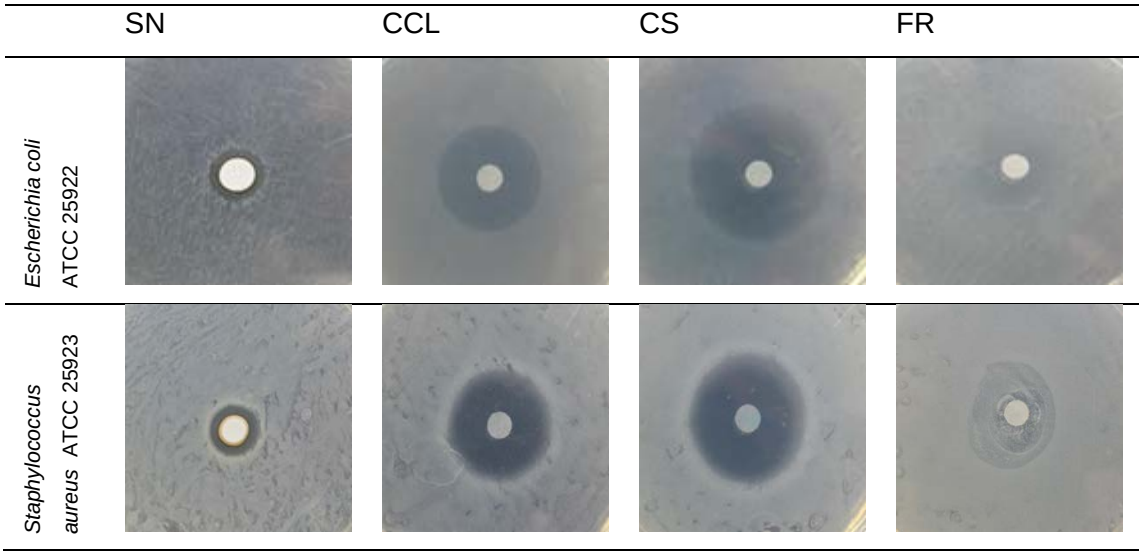

Figure 3.13: Kirby Bauer disc diffusion test results for biocide selection

Dilution susceptibility test

The highest dilution of each concentrated biocide solution where no bacterial growth was observed in test tubes was 0.02 % silver nitrate, 0.05 % copper sulphate and 6.25 % furanone solution. The calculated MIC of each biocide was therefore 432 ppm for silver nitrate, 160 ppm for copper sulphate and 6.25 % for furanone solution. These calculated biocide concentrations were incorporated into an epoxy base coating for further chemical and antifouling characterization studies.

3.4. Conclusions

To simulate biofilm growth in a cooling water system this study aimed to identify a metal substrate for growth discs, a microorganism for biofilm growth on metal discs, a biofilm removal method, quantitative and qualitative analysis of biofilms and selection of an appropriate coating. The following conclusions could be drawn:

- A metal alloy of stainless steel and mild steel (3CR12) was selected as metal substrate for the growth discs as mild steel used on its own corroded within 24 h.
- Sonification for 5 min was determined as the optimum biofilm removal method.
- To minimise fluorescence signals from metal discs during CLSM and flow cytometry analysis of biofilms, it was decided to use *Pseudomonas* sp. strain CT07::*gfp* to omit SYTO 9 stain from the LIVE/DEAD® Baclight™ Bacterial Viability kit.
- Quaternary ammonium salt 2, triclosan and copper oxide showed clear zones against *E. coli* ATCC 25922 and *S. aureus* ATCC 25923 and were selected as antifouling coatings for further experiments.
- Silver nitrate, copper sulphate and furanone showed zones against *E. coli* ATCC 25922 and *S. aureus* ATCC 25923 and were selected as biocides to be incorporated in an epoxy base coating.
- From the dilution susceptibility test the MIC values for silver nitrate, copper sulphate and furanone solution was determined as 432 ppm, 160 ppm and 6.25 %, respectively.

3.5. References

1. Bott, T. R. Techniques for reducing the amount of biocide necessary to counteract the effects of biofilm growth in cooling water systems. *Appl. Therm. Eng.* **18,** 1059–1066 (1998).

2. Flynn, D. *Nalco Water Handbook*. McGraw-Hill: Global education Holdings, LCC: Penn Plaza, 10th Floor, New York

3. Cloete, T. E., Jacobs, L. & Brözel, V. S. The chemical control of biofouling in industrial water systems. *Biodegradation* **9,** 23–37 (1998).

4. Flemming, H.-C. Biofouling in water systems--cases, causes and countermeasures. *Appl. Microbiol. Biotechnol.* **59,** 629–40 (2002).

5. Bott, T. R. Potential Physical Methods for the Control of Biofouling in Water Systems. *Chem. Eng. Res. Des.* **79,** 484–490 (2001).

6. Meesters, K. P. H., Van Groenestijn, J. W. & Gerritse, J. Biofouling reduction in recirculating cooling systems through biofiltration of process water. *Water Res.* **37,** 525–32 (2003).

7. Lee, S. B. *et al.* Permanent, nonleaching antibacterial surfaces. 1. Synthesis by atom transfer radical polymerization. *Biomacromolecules* **5,** 877–82 (2004).

8. Yebra, D. M., Kiil, S. & Dam-Johansen, K. Antifouling technology—past, present and future steps towards efficient and environmentally friendly antifouling coatings. *Prog. Org. Coatings* **50,** 75–104 (2004).

9. Dafforn, K. a, Lewis, J. a & Johnston, E. L. Antifouling strategies: history and regulation, ecological impacts and mitigation. *Mar. Pollut. Bull.* **62,** 453–65 (2011).

10. Macdonald, R. Reporter Systems for Microscopic Analysis of Microbial Biofilms. *Methods in enzymology*. **310**, 3-20 (1999).

11. Stoodley, P. *et al.* Growth and Detachment of Cell Clusters from Mature Mixed-Species Biofilms. *Appl. Environ. Microbiol.* **67 ,** 5608–5613 (2001).

12. Zbigniew Lewandowski, H. B. *Fundamentals of Biofilm research*. 452 Taylor and Francis Group, LLC, (2007).

13. Hunt, S. & Werner, E. Hypothesis for the role of nutrient starvation in biofilm detachment. *Appl. Environ. Microbiol.* **70,** 7418–7425 (2004).

14. Huang, C.-T., Peretti, S. & Bryers, J. Use of flow cell reactors to quantify biofilm formation kinetics. *Biotechnol. Tech.* **6,** 193–198 (1992).

15. Neu, T. R. & Lawrence, J. R. Development and structure of microbial biofilms in river water studied by confocal laser scanning microscopy. *FEMS Microbiol. Ecol.* **24,** 11–25 (1997).

16. Cloete, T. E., Brözel, V. S. & Von Holy, A. Practical aspects of biofouling control in industrial water systems. *Int. Biodeterior. Biodegradation* **29,** 299–341 (1992).

17. Gagnon, G. a & Slawson, R. M. An efficient biofilm removal method for bacterial cells exposed to drinking water. *J. Microbiol. Methods* **34,** 203–214 (1999).

18. Ig, A., Pantanella, F., Valenti, P., Natalizi, T. & Passeri, D. Analytical techniques to study microbial biofilm on abiotic surfaces: pros and cons of the main techniques currently in use. **30**, 31–42 (2013).

19. Jepras, R. I., Carter, J., Pearson, S. C., Paul, F. E. & Wilkinson, M. J. Development of a robust flow cytometric assay for determining numbers of viable bacteria . *Appl. Environ. Microbiol.* **61,** 2696–2701 (1995).

20. Dunne, W. M. Bacterial Adhesion: Seen Any Good Biofilms Lately? *Clin. Microbiol. Rev.* **15 ,** 155–166 (2002).

21. Kinner, N., Balkwill, D. & Bishop, P. Light and electron microscopic studies of microorganisms growing in rotating biological contactor biofilms. *Appl. Environ. Microbiol.* **45**, 1659–1669 (1983).

22. Lawrence, J. R., Korber, D. R., Hoyle, B. D., Costerton, J. W. & Caldwell, D. E. Optical sectioning of microbial biofilms. *J. Bacteriol.* **173,** 6558–67 (1991).

23. Bester, E., Edwards, E. A. & Wolfaardt, G. M. Planktonic cell yield is linked to biofilm development. *Can. J. Microbiol.* **55,** 1195–1206 (2009).

24. Bester, E., Wolfaardt, G., Joubert, L., Garny, K. & Saftic, S. Planktonic-Cell Yield of a Pseudomonad Biofilm. *Appl. Environ. Microbiol.* **71 ,** 7792–7798 (2005).

25. Lindsay, D. & von Holy, a. Evaluation of dislodging methods for laboratory-grown bacterial biofilms. *Food Microbiol.* **14,** 383–390 (1997).

26. Chambers, L. D., Stokes, K. R., Walsh, F. C. & Wood, R. J. K. Modern approaches to marine antifouling coatings. *Surf. Coatings Technol.* **201,** 3642–3652 (2006).

27. Mandy, F. F., Bergeron, M. & Minkus, T. Principles of flow cytometry. *Transfus. Sci.* **16,** 303–314 (1995).

28. Rieseberg, M., Kasper, C., Reardon, K. F. & Scheper, T. Flow cytometry in biotechnology. *Appl. Microbiol. Biotechnol.* **56,** 350–360 (2001).

29. Berney, M., Hammes, F., Bosshard, F., Weilenmann, H.-U. & Egli, T. Assessment and interpretation of bacterial viability by using the LIVE/DEAD BacLight Kit in combination with flow cytometry. *Appl. Environ. Microbiol.* **73,** 3283–90 (2007).

30. Williams, I. *et al.* Flow cytometry and other techniques show that Staphylococcus aureus undergoes significant physiological changes in the early stages of surface-attached culture. *Microbiology* **145,** 1325–33 (1999).

31. Paulse, A. N., Jackson, V. A. & Khan, W. Comparison of enumeration techniques for the investigation of bacterial pollution in the Berg River , Western Cape , South Africa. **33,** 165–174 (2007).

32. Wheat, P. F. History and development of antimicrobial susceptibility testing methodology. *J. Antimicrob. Chemother.* **48 ,** 1–4 (2001).

33. Lambert, R. J. W. & Pearson, J. Susceptibility testing: accurate and reproducible minimum inhibitory concentration (MIC) and non-inhibitory concentration (NIC) values. *J. Appl. Microbiol.* **88,** 784–790 (2000).

34. Costerton, J. Microbial biofilms. *Annu. Rev. Microbiol.* **49,** 711–745 (1995).

35. Percival, S. ., Knapp, J. ., Edyvean, R. G. . & Wales, D. . Biofilms, mains water and stainless steel. *Water Res.* **32,** 2187–2201 (1998).

36. Kobayashi, H., Oethinger, M., Tuohy, M. J., Procop, G. W. & Bauer, T. W. Improved detection of biofilm-formative bacteria by vortexing and sonication: a pilot study. *Clin. Orthop. Relat. Res.* **467,** 1360–4 (2009).

37. Unge, A., Tombolini, R., Mølbak, L., Janet, K. & Jansson, J. K. Simultaneous Monitoring of Cell Number and Metabolic Activity of Specific Bacterial Populations with a Dual gfp-luxAB Marker System. *Appl. Environ. Microbiol.* **62,** 813–821 (1999).

38. Ziglio, G. *et al.* Assessment of activated sludge viability with flow cytometry. *Water Res.* **36,** 460–8 (2002).

CHAPTER 4

Evaluation of chemical and antifouling characteristics of industrial and biocide-enriched epoxy coatings for application in cooling water systems

4.1. Introduction

Surfaces continuously exposed to water are at a high risk for biofilm formation. Although biofilm formation may be beneficial to certain environments (e.g. biological wastewater treatment systems), it is detrimental to most industrial aqueous environments, especially in cooling water systems.[1–3]

Biofouling can be defined as the build-up of biofilms on surfaces that leads to disadvantageous consequences.[2,4] In cooling water systems biofouling primarily occurs through micro-organisms and can lead to the following complications:

- Bio corrosion on metal surfaces in the system.[1–3,5]
- Physical blockages in the pipes and tubes inside the water flow system can occur and prevent water flow.[1–3,5]
- Reduced heat transfer effectiveness through heat exchanging surfaces.[1–3,5]
- Reduced efficiency of the entire cooling water system.[1]

The above-mentioned complications have serious financial consequences through increased maintenance costs and the loss of revenue. Thus it is beneficial for industries to employ biofouling prevention strategies for cooling water systems.[1] Currently the use of biocides in cooling water systems is a commonly accepted method for the control of biofouling.[6,7] This method is effective in controlling biofilm formation however it has significant disadvantages.[8,9] Most biocides are toxic antimicrobial compounds which are often hazardous to humans and the environment.[6,10] The use of biocides also leads to development of antimicrobial resistance in microorganisms and increased operating costs.[5,10] Another biofouling prevention method is the physical cleaning of the equipment in the system. This option has practical limitations since cooling towers usually have areas that are difficult to reach. It is also an expensive method due to labour, cleaning chemical costs as well and downtime.[2,11]

A possible alternative for biofilm control in cooling water systems is the use of antifouling coatings.[12,13] Antifouling coatings have been developed and tested for decades, but none have shown durable and environmentally friendly properties.[14,15] The first antifouling coatings contained heavy metal biocides such as copper, lead, mercury, arsenic and cadmium.[15] Most of these heavy metals leached out of the polymer matrix of the coatings which led to inefficient coatings and metal contamination of the environment.[16] In the 1960's antifouling paints containing organotin were produced.[12] The most effective antifouling coating contained tributyltin (TBT) which was in later years completely banned from use, due to its high environmental toxicity.[15,17] The use of

nanobiocides, in particular nano silver particles, became popular in the 90's. Nano biocides particles have an extremely large surface to area ratio which results in higher reactivity.[18] The higher reactivity unfortunately also results in higher toxicity levels to both the environment and mammalian cells. [19] The use of nanoparticles in polymer matrixes from which it could leach out, is therefore not an ideal alternative.[20] An ideal antifouling coating would be durable, cost-effective, easy to apply and contain environmentally-benign antimicrobial compounds which do not leach out. The cooling water system environment consists of metal heat exchange surfaces, continuously exposed to water containing organic and inorganic substances, that support heterogeneous bacterial populations that manifest in biofilms, resulting in biofouling [21,22]

In this chapter, commercial antifouling coatings for metal surfaces for aqueous environments were sourced from manufacturers globally. An anticorrosive epoxy resin coating was also sourced and different biocides identified and added to the base coating. These coatings were then characterized according to their chemical and antifouling properties on metal surfaces used in cooling water systems. Section A of this study includes all coatings sourced internationally and Section B the epoxy resin coatings with different incorporated biocides.

The commercial coatings contained one of three biocides; i.e. triclosan, copper oxide and a quaternary ammonium salt. Additionally, an anticorrosive epoxy resin coating was sourced and biocides, including silver nitrate, copper sulphate and furanone were dissolved and incorporated into the resin.

The aim of this study was to evaluate the chemical and antifouling characteristics of all coatings, in order to determine whether the coatings comply with the properties desired for use in cooling water systems.

4.2. Materials and Methods

4.2.1 Materials

Chemicals

Copper sulphate, silver nitrate, and furanone compound 2, 5-dimethyl-4-hydroxy-3(2H)-furanone were purchased from Sigma Aldrich, South Africa, and used as is. Propidium iodide (PI) and counting beads were purchased from Invitrogen life technologies.

Media

Tryptic Soy Broth (TSB) (Sigma-Aldrich South-Africa) and Bacterial agar (BioLab, BioLab Diagnostics, Midrand, SA) were used for culturing of micro-organisms.

Bacterial strains

Bester and co-workers (2005)[23] isolated a bacterial strain from an industrial cooling tower and subsequently identified it as closely related to a known *Pseudomonas* species by 16S rDNA

sequencing. This isolate was later designated as *Pseudomonas* sp. strain CT07 (GenBank Accession No.DQ 777633). For the purpose of confocal laser microscopy and flow cytometry analysis, a green-fluorescent protein gene (*gfp*) was inserted into the chromosome by Bester (2009).[24] *Pseudomonas* sp. strain CT07::*gfp* was kindly provided by the Biofilm Ecology Group (Ryerson University, Canada) for use in this study. Cultures were stored at -80°C in 40 % glycerol.[24]

Growth discs

The metal used as growth discs for coatings throughout this study was 3CR12, 1.2 mm grade stainless steel. The chemical composition of the metal used contains Carbon (C), Manganese (Mn), Silicon (Si), Phosphor (P), Sulphur (S), Chromium (Cr), Nickel (Ni) and Nitrogen (N). The metal was laser cut into 2 x 5 cm discs and sandblasted with particles sized between 80 and 160 µm, to improve the adherence of coatings to the metal surface.

Coatings

Section A – Industrial coatings

Three commercially available antimicrobial coatings were sourced from different manufactures. All information regarding the coating is propriety information except for the active biocide. Coatings were applied to metal surfaces according to the instructions from the manufacturer, which involved wetting of a non-woven cloth, wiping the cloth over the metal surface and leaving the coating to dry for 24 h at ambient temperatures. For the purpose of this study the respective coatings, containing various biocides, were labelled as indicated in Table 4.1.

Table 4.1: Industrial coatings containing three different biocides

Biocide incorporated in coating	Abbreviation
Metal control	CC
Triclosan	TC
Copper oxide	CUO
Quaternary ammonium salt	QAC

Section B – Biocide enriched epoxy coatings

Three commercially available biocides were added to an industrial anticorrosive epoxy resin manufactured by Kansai Plascon, South-Africa. All information regarding the epoxy resin coating is propriety information. According to the manufacturers the epoxy used in this study is a two-package system consisting of the epoxy resin component and curing agent, at a volume ratio of 4:1. The calculated MIC (chapter 3) of each biocide in solution was added to the epoxy resin which were silver nitrate (0.02 % (w/v)), copper sulphate (0.06 % (w/v)) and furanone (2.5 % (w/v)). After

addition the mixture were vortexed for 10 min. The curing agent was then added and mixed thoroughly. Coatings (0.2 mL per disc) were spread evenly over discs with a surgical scalpel blade and cross linked at 40 °C for 2 h after which it was analysed. For the purpose of this study the respective coatings containing incorporated biocides were labelled as indicated in Table 4.2.

Table 4.2: Industrial anticorrosive epoxy with incorporated biocides

Biocide incorporated in epoxy coating	Abbreviation
Epoxy control	EC
Epoxy silver nitrate	SN
Epoxy copper sulphate	CS
Epoxy furanone	FR

4.2.2 Methods

Coatings were chemically analysed, applied to metal growth discs, and subjected to biofilm growth in a controlled environment. Biofilms were qualitatively and quantitatively characterized (Figure 4.1).

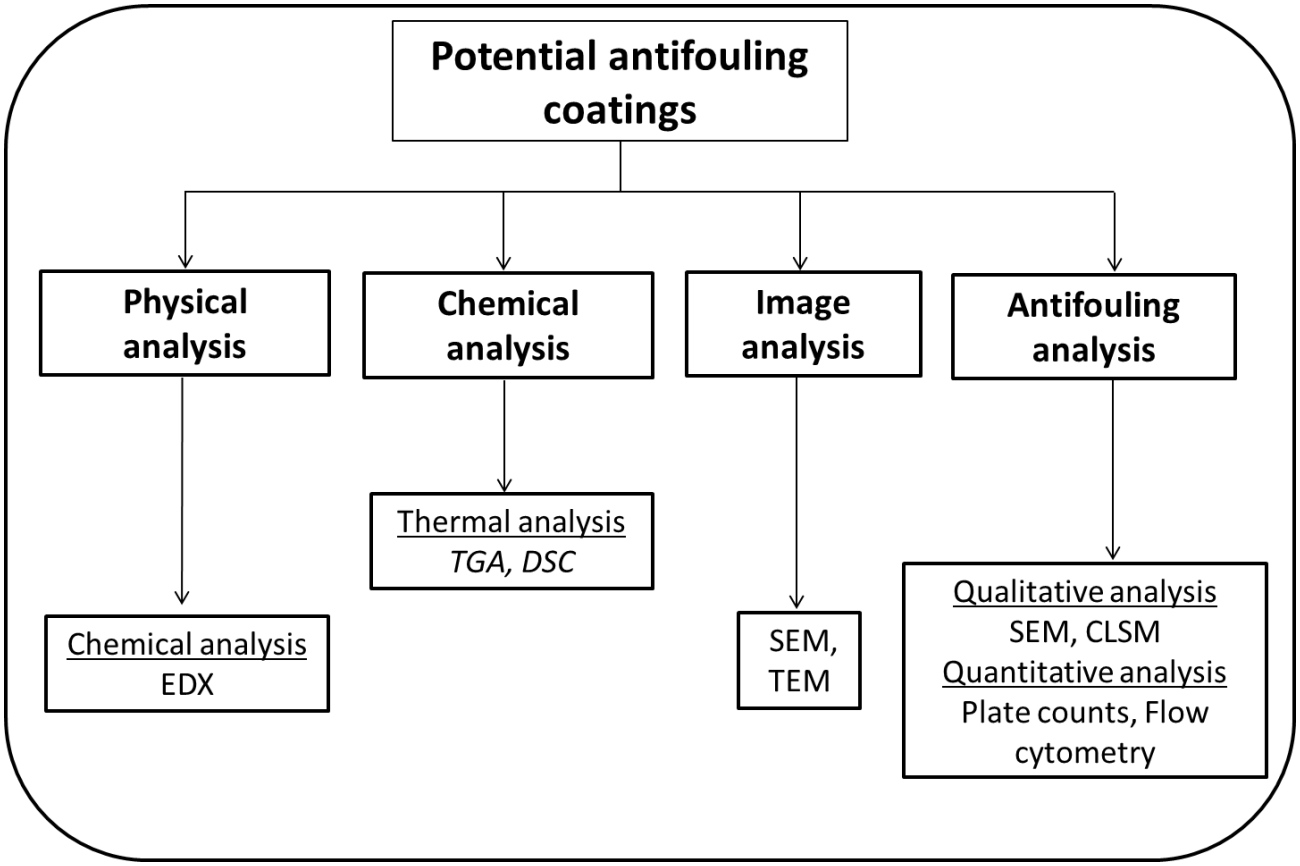

Figure 4.1: Schematic diagram of experimental methods

4.2.2.1 Evaluation of chemical characteristics of industrial coatings and biocide enriched epoxy coatings

Physical analysis

Thermogravimetric analysis

Thermogravimetric analysis (TGA) was performed with a Q500 Thermogravimetric analyser under continuous nitrogen flow. The samples were heated from 0 °C to 900 °C at a heating rate of 10 °C/min. All coatings from section A and B were subjected to TGA analysis before biofilm growth.

Differential scanning calorimetry

Differential scanning calorimetry (DSC) thermograms were recorded with a Q100 V9.9 calorimeter under continuous nitrogen flow. The samples of a mass weight of ± 3 mg were placed in aluminium pans with pierced lids which were heated at a heating rate of 10°C/min in the temperature range of -40 °C to 300 °C. All coatings from section A and B were subjected to DSC analysis.

Chemical analysis

Energy dispersive X-ray spectroscopy

Energy dispersive X-ray spectroscopy (EDX) analysis was performed on coated discs before biofilm growth and after 48 h biofilm. Analysis was done using a Zeiss EVO® MA15 Scanning Electron Microscope at the Stellenbosch University. Qualitative analysis and backscatter images required 15 µm thicknesses (peacock blue colour) of carbon coating, and a flat and polished surface. Samples were identified with backscattered electron (BSE) images, and phase compositions were quantified by EDX analysis using an Oxford Instruments® X-Max 20 mm^2 detector and Oxford INCA software. Beam conditions during the qualitative analysis were 20 KV, with a working distance of 8.5 mm and approximate beam current of -20 nA. The counting time was 10 sec. Internal Astimex Scientific mineral standards were used for standardization and verification of the analysis. Pure CO_2 was used periodically to correct for detector drift. Energy dispersive spectroscopy is only suitable for determining major elements at concentrations over 0.1 wt. %. The beam interaction volume extends between 100 nm and 5 µm into the surface, depending on the density of the sample. The spatial resolution with respect to analysis is 1 micron by beam spreading.

Image analysis

Scanning electron microscopy

Scanning electron microscopy was used to analyse the surfaces of coatings on the metal discs before and after biofilm growth. After growth the biofilm was removed from the metal growth discs through sonification for 5 min with a Branson 5510 sonicator (Chapter 3). Gold sputter coating was applied to discs and SEM image analyses were done at the Stellenbosch University Microscopy Unit on LEO® 1430VP and Cambridge S200 scanning electron microscopes. An accelerating voltage of 7 kV and a probe current of 150 pico amperes (pA) were used. Images were taken at 4000x magnification.

Transmission electron microscopy

For transmission electron microscopy (TEM) sample preparation, 3 µL of each coating (TC, CUO and QAC) was applied to a carbon film on a copper grid and allowed to dry for 24 h. The contrast of the samples was enhanced by negative staining. After the samples were attached to the carbon film on grids, 3 µL of ammonium molybdate stain was applied, blotted with filter paper and allowed to dry. Samples were viewed with a FEI Tecnai 20 transmission electron microscope operating at 200 kV (Lab6 emitter) fitted with a Tridiem energy filter. Images were photographed using a Gatan CCD camera and converted to Digital Micrograph (DM3) format and then to JPEG format for analysis.

4.2.2.2 Evaluation of antifouling characteristics of industrial coatings and biocide enriched epoxy coatings analysis

Biofilm growth assay

Modified flow cells fabricated from Nylon 6, 6 were used for biofilm growth in an enclosed flow system (Figure 4.2). Each flow cell contained ten recessed flow chambers sized at 5 x 2 x 0,001 cm. Ten metal discs were inserted into the flow cells and sealed. Flow chambers were sterilized by flushing with 70 % ethanol for 30 min followed by rinsing with 1 L sterile Reverse Osmosis (RO) water. A 1 L reservoir containing sterile 3 g/L Tryptic Soy Broth (TSB) was connected to a Watson Marlow 205S multichannel peristaltic pump. The broth was pumped through the system for 20 min at a flow rate of 13 mL h^{-1}. *Pseudomonas* sp. strain CT07:: *gfp* was aerobically cultured for 16 h in 10 mL 3 g/L TSB at 26°C and diluted with TSB to an optical density (OD) of 1 (±2 %) before 1 mL of the bacterial suspension was inoculated into the TSB reservoir. The reservoir was magnetically stirred throughout the experiment in order to improve aeration and to ensure optimal growth conditions for *Pseudomonas* sp. *strain* CT07::*gfp*. The system was kept under flow conditions at 26 ˚C (±2 °C) for 48 h. Metal discs were then removed from the flow cells and dipped five times in 30 mL SSS to remove planktonic cells. The biofilm growth assay was conducted in triplicate for every coating. Different techniques were used to analyse biofilm growth on metal surfaces. Three metal plates per biofilm growth assay were subjected to chemical and antifouling analysis techniques.

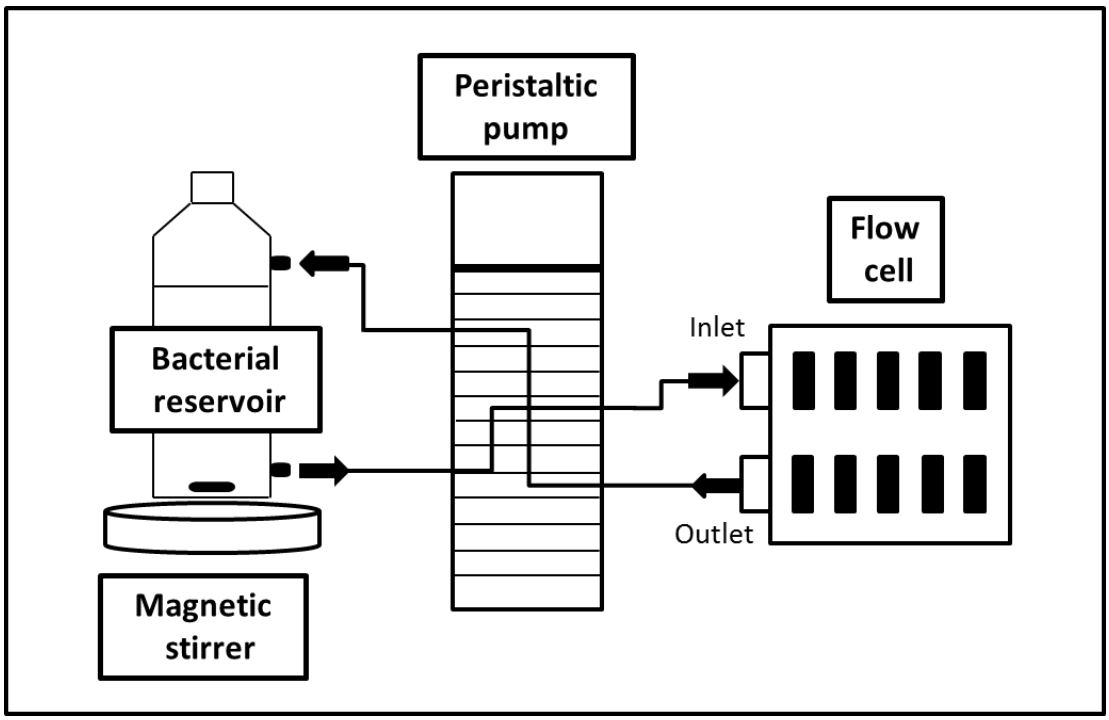

Figure 4.2: Schematic illustration of the biofilm growth flow cell system

Qualitative analysis

Scanning electron microscopy

Qualitative analysis of biofilms on all coatings was done using SEM imaging. Cells were fixated on metal growth discs with 1 mL 2.5 % gluteraldehyde (kept in dark for 2 h) and dehydrated with an ethanol dilution series of 50 %, 70 %, 90 % and 100 %. Image analyses was done at the Stellenbosch University Microscopy Unit on a LEO® 1430VP and a Cambridge S200 scanning electron microscope after gold sputter coating was applied. The conditions for image acquisition were an accelerating voltage of 7 kV and a probe current of 150 pico amperes (pA). Images were taken at 2000X magnification.

Confocal Laser Scanning Microscopy analysis of biofilms

The degree of viable and non-viable bacterial cells in the biofilms on all coatings was determined qualitatively through CLSM. This was achieved through appropriate staining methods without destructing the biofilm. Bacterial viability was determined *via* the incorporated green fluorescence gene of *Pseudomonas* sp. strain CT07::*gfp* and bacterial non-viability was determined by using a propidium iodide stain. Propidium iodide (PI) is a red fluorescent counterstain that stains bacteria with impaired membranes. PI was used in solution with anhydrous dimethylsulfoxide (DMSO) (LTC Tech, South Africa). Bacterial cells in the biofilm were stained through a single staining step with PI stain. The stock solution of the PI stain was diluted to a concentration of 0.3 % (v/v) in sterile saline. The PI solution (100 µL) was pipetted onto each metal plate, covered with a 2, 2 x 5 cm coverslip and kept in dark conditions for 15 min after which images were acquired at the Central Analytical Facility (CAF), Stellenbosch University. Three images were taken of every sample and analysed on a Carl Zeiss LSM780 confocal microscope (Carl Zeiss, Germany). Using an Argon

multiline laser as light source, images were excited at 488 nm or 514 nm. Emission was collected using a Spectral detection LSM780 GaAsP detector at 490-560 nm (eGFP) and 646-709 nm (PI). For image frame acquisition, a Plan-Apochromat 63x/1.40 Oil DIC M27 objective was used. The ZEN 2011 imaging software (Carl Zeiss, Germany) was used to acquire Z-stacks at 1 µm step width and images were processed by applying maximum intensity projection.

Quantitative analysis

For quantitative analysis biofilms were removed (as discussed in Chapter 3) and subjected to plate count and flow cytometry.

Plate counts (Pour plate method)

Serial dilutions of the biofilm solutions were prepared with sterile saline and the pour plate technique was used for enumeration of bacteria. One millilitre of each dilution was added to 3 g/L TSB soft agar (1 %) plates and incubated at 26 °C. Plate counts were performed after 72 h of incubation.

Flow cytometry

Viable and non-viable cell counts from the removed biofilms were done using flow cytometry in combination with PI staining, *Pseudomonas* sp. CTO7*::gfp*, and liquid counting beads (BD™ Liquid Counting Beads, LTC Tech, South Africa). According to the manufacturer's instructions, stock solution of the stain was diluted to a concentration of 0.4% (v/v) in sterile saline. The stain solution (200 µL) was pipetted onto 1 mL of the biofilm sample and kept in dark conditions for 15 min. After 15 min, 50 µL of liquid counting beads was added. Samples were analysed at the Central Analytical Facility (CAF), Stellenbosch University.

Each sample was analysed by a Becton Dickinson FACS Aria flow cytometer with a 13 mw, 488 nm Coherent® SapphireTM Solid State laser. *Pseudomonas* sp. CT07::*gfp* and PI stain were used to differentiate between bacterial cells and debris. For this study, the bacterial population was identified and gated on a forward scatter (FSC) vs. a side scatter (SSC) dotplot and a SSC vs. PerCP at 695/40 nm dotplot. The bead count was identified and gated on SSC vs. PerCP dotplot. The parameters were all measured using a logarithmic amplification scale. The threshold was set to 1000 FSC channels to remove debris from the sample.

To calculate fluorescence overlap between the two fluorochromes, compensation was measured. The *gfp* green fluorescent emission and PI red fluorescent emission were separately measured in the PE-Texas Red channel (610/20 nm) and the FITC channel (530/30 nm). For this purpose the following controls of *Pseudomonas* sp. CT07*::gfp* bacterial samples were included: i) non-stained, ii) stained with PI and iii) dead bacteria stained with PI. The compensation values were calculated by using the software BD FACSDiva (version 6.1.3).

By comparing cellular events to bead events, both determined by the flow cytometer, the absolute number of positive cells (cells/mL) could be calculated through the following equation according to the manufacturer's manual.

Equation 4.1: Total cell count equation

$$\frac{\text{Number of cell events}}{\text{Number of bead events}} \times \frac{\text{Assigned bead count (beads/50µL)}}{\text{Volume of sample}} \times 1000$$

NOTE: Bead concentration was recorded at 5.5×10^4 beads/50µL

Statistical analysis

Results obtained from flow cytometry and plate counts were statistically analysed using Statistica version 11 (Statsoft Inc., USA). Normality and homogeneity of variance was assessed in the data using the respective Shapiro-Wilks W test, normal probability plots and Levene's test. The Boxcox transformation was applied to data that was not normally distributed. Variation between viable and non-viable populations for different coatings was analysed using one-way or Kruskal-Wallis ANOVA for parametric and non-parametric data respectively. Pairwise differences were assessed with Tukey HSD test or multiple comparisons of mean ranks. Probability (p) values of less than 0.05 were considered as significant.

4.3. Results and discussion

4.3.1 Section A

4.3.1.1 Evaluation of chemical characteristics of industrial coatings

Physical analysis

Thermogravimetric analysis and Differential scanning calorimetry

Thermogravimetric analysis (TGA) was done to evaluate thermal stability of coatings in terms of weight loss over increasing temperature (Figure 4.3). Thermal decomposition of coatings TC and CUO occurred via two steps. The initial weight loss at 100 °C for coatings TC and CUO can be attributed to moisture or surfactant loss. At 400 °C coating TC lost its bulk weight up to 20 wt. %. Coating CUO showed a gradual weight loss between 250 °C and 600 °C and then stabilized at ± 50 wt. %. Coating QAC lost its bulk weight in one step between 25 °C and 225 °C up to 20 wt. %. Coatings TC and CUO were thermally stable to at least 200 °C. Water transported through a cooling water system would never exceed 100 °C, therefore coatings TC and CUO would be thermally stable in the cooling water tower as well as the transporting pipeline. However in a heat exchanger the temperature can exceed 260 °C, only coating CUO would be stable for use in the heat exchanger. Coating QAC is not thermally stable for any use in any section of a cooling water system.

The DSC thermogram shows no T_g, crystallization exotherm or melting endotherm for any of the three coatings (Figure 4.3). The DSC instrument used for the analysis was restricted to measurements down to – 40 °C, as it might be expected that all three coatings might have a lower T_g. As mentioned previously the chemical composition of all three coatings was unknown. In the case of surface coatings the T_g of the polymers that the coating is synthesized from should be below the ambient temperature range otherwise it will from brittle films (surface coatings). It is therefore favourable that the T_g of all three coatings are below ambient temperatures.

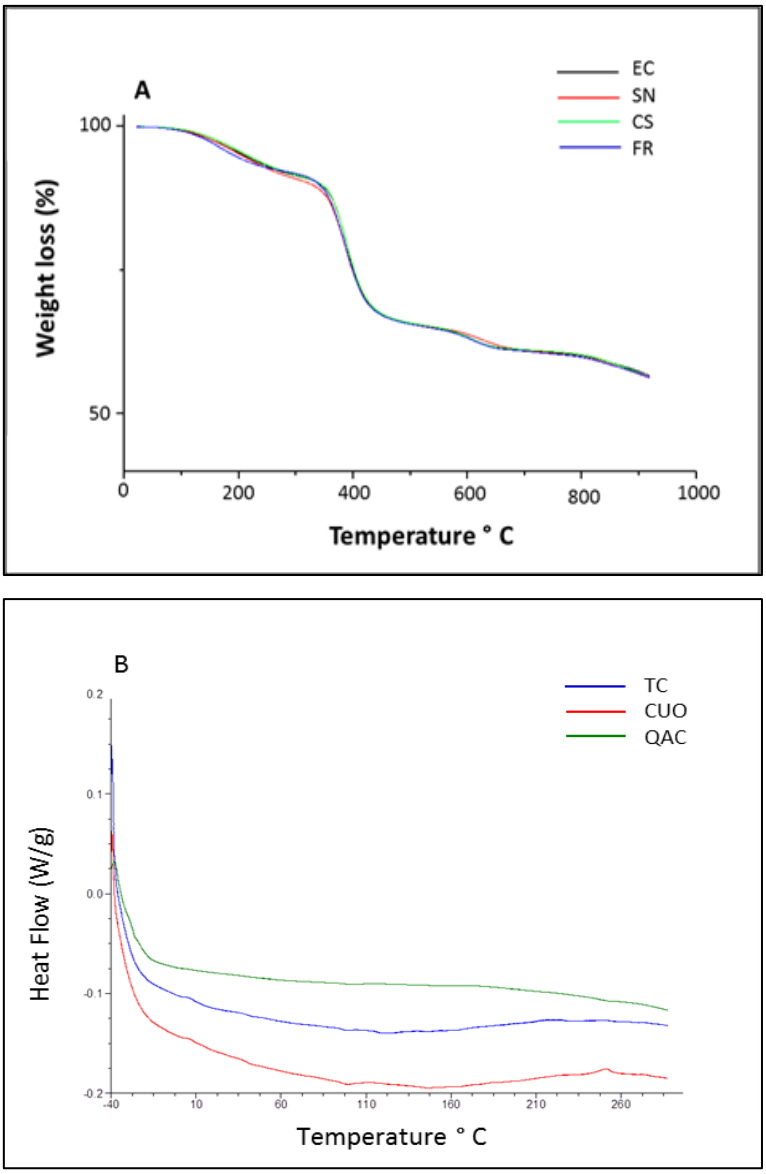

Figure 4.3: TGA (A) and DSC (B) thermograms comparing the thermal stability of coatings TC, CUO and QAC

Chemical analysis

Energy dispersive X-ray spectroscopy

The presence of Carbon (C) atoms was observed on all four discs, which was in compliance with the composition of the metal 3CR12 (Table 4.3). The C wt. % for coated metal discs (TC, CUO and QAC) was higher than for CC, which is a confirmation of the presence of the respective coatings on the surface. After biofilm growth the C wt. % decreased for all four discs. The weight percentage loss for CC, TC, and QAC were almost similar; indicating that coatings TC and QAC washed off and were therefore not durable after it was in contact with water for 48 h. Although C wt. % decreased for CUO it was still higher, indicating the presence of the coating even after biofilm growth. These results were confirmed by SEM analysis (Figure 4.4).

Oxygen (O) wt. % for CC before and after biofilm growth was in the same region (Table 4.3). For all three coatings O wt. % was higher than CC before biofilm growth and decreased after. This

might suggest that O atoms were present in the respective coatings. The O content for CUO was much higher than TC and QAC before and after growth. Copper (Cu) was only detected in CUO and this confirmed the presence of the biocide copper oxide (CuO) in the coating. However, the analysis of CUO after biofilm growth did not indicate the presence of Cu, which could indicate that the copper leached out of the polymer matrix.

Before biofilm growth higher silicon (Si) content was observed in all three coatings compared to the control CC (Table 4.3). This suggests that Si is present in all three coatings.

The presence of aluminium (Al), titanium (Ti), chrome (Cr), manganese (Mn) and iron (Fe) in all four discs was in compliance with the metal used in this study (Table 4.3). For all three coated discs the wt. % of elements mentioned above was lower before biofilm growth than after, because the respective coatings protected the metal surfaces. Weight percentages of elements after subjection to water were in the same range as the metal control.

Table 4.3: EDX results for control CC and coatings TC-QAC on metal discs before and after biofilm growth

	CC		TC		CUO		QAC	
Elements	**Before weight %**	**After weight %**	**Before weight %**	**After weight %**	**Before weight %**	**After weight %**	**Before weight %**	**After weight %**
C	6.58	7.82	15.6	8.39	31.22	9.21	12.86	5.90
O	6.52	6.24	8.76	5.73	13.40	7.54	8.17	4.01
Al	0.66	0.63	0.48	0.54	0.39	0.53	0.41	0.38
Si	0.31	0.28	1.32	0.34	3.80	1.28	1.01	0.41
Ti	0.29	0.28	0.2	0.26	0.24	0.27	0.19	0.17
Cr	10.15	10.13	8.87	10.14	6.18	9.85	9.52	10.64
Mn	0.72	0.68	0.57	0.64	0.40	0.64	0.64	0.66
Fe	73.78	72.94	64.09	72.98	44.08	70.79	69.10	77.22
Cu	0.00	0.00	0.00	0.00	0.28	0.00	0.00	0.00

Scanning electron microscopy

SEM images of control CC showed deterioration signs of metal surface after exposure to an aqueous biofilm growth environment for 48 h (Figure 4.4 CC (a)). Before biofilm growth, the presence of a coated film could be visualized on the metal surface for coatings TC, CUO and QAC, when compared to CC (Figure 4.4 (a)). After biofilm growth the presence of the film coating for coatings TC and QAC were no longer present (Figure 4.4 (b)). Coating CUO could still be visualized on the surface, but not as distinctively as before biofilm growth (Figure 4.4 CUO (b)). Metal growth discs of all three coatings showed signs of deterioration. It was concluded that coatings TC and QAC washed off completely from the metal g and coating CUO only partially.

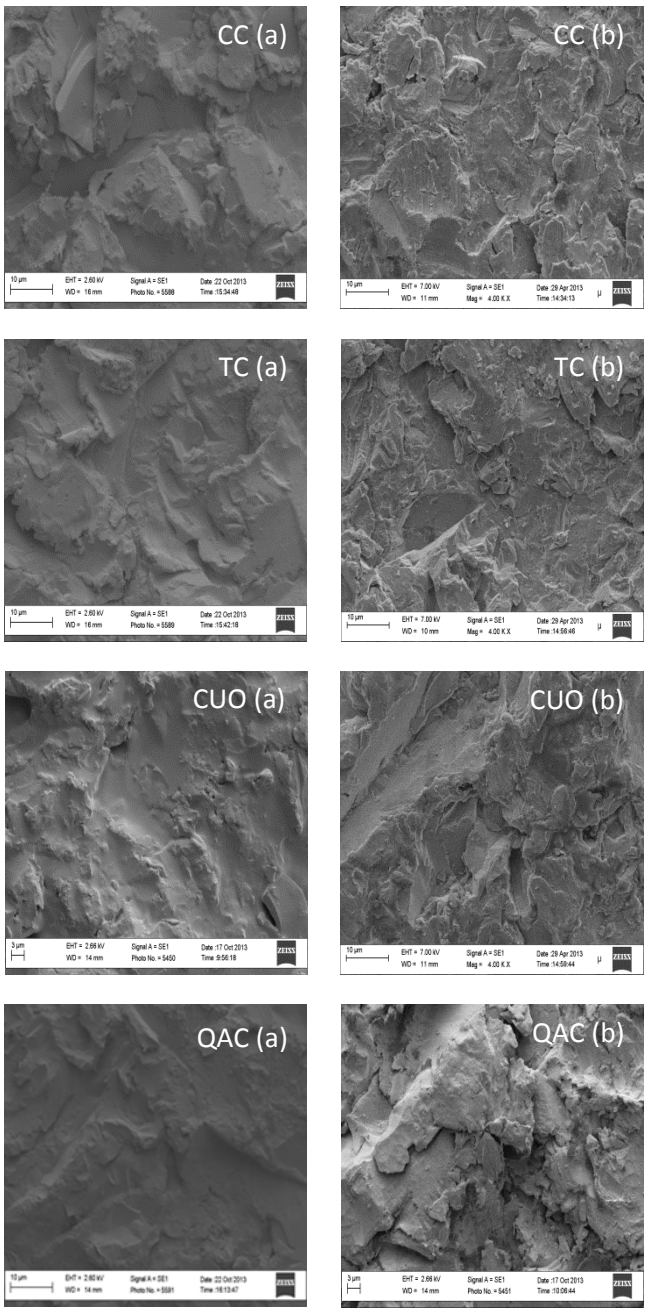

Figure 4.4: SEM images of control CC and coatings TC, COU and QAC before (a) and after (b) biofilm growth. The scale bar in the images corresponds to a length of 20 µm except for image CUO (a) and QAC (b) that corresponds to 10 µm.

Transmission electron microscopy

Particle morphology of the polymer matrixes of coatings TC, CUO and QAC were examined by TEM. TEM images of coatings TC, CUO and QAC showed well defined particles that were fairly homogeneously distributed throughout the coatings (Figure 4.5). Darker regions observed were attributed to the stain that was used to improve the contrast of the images and were trapped between the particles. No phase separation was visible here, which was confirmed by DSC results (Figure 4.3 B) for all three coatings. Coating QAC showed uniform distribution of particles but the presence of bigger darker flocculated particles is visible. The particles could be bigger molecules that were not linked to the polymer chain, but as the exact composition of the coating was not known, the particles could not be identified.

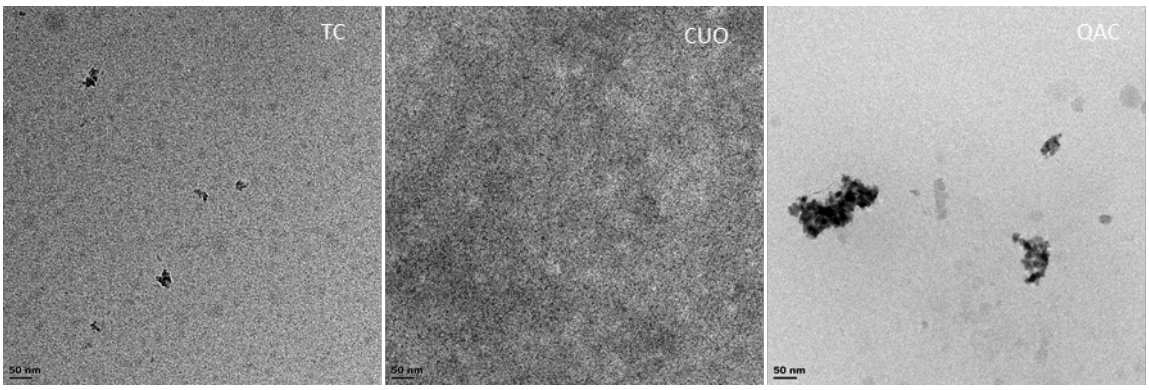

Figure 4.5: TEM images for coatings TC, CUO and QAC. The scale bars in the images correspond to a length of 50 nm.

Image analysis

4.3.1.2 Evaluation of antifouling characteristics of industrial coatings

Qualitative analysis

Scanning electron microscopy

Bacterial growth was observed on the surfaces of all four discs (Figure 4.6). On the surface of CUO a higher amount of growth was clearly visible. This was also confirmed through fluorescence microscopy (Figure 4.8). It was however difficult to qualitatively ascertain the quantity of bacteria attached to the respective surfaces due to extreme irregularities in the metal itself.

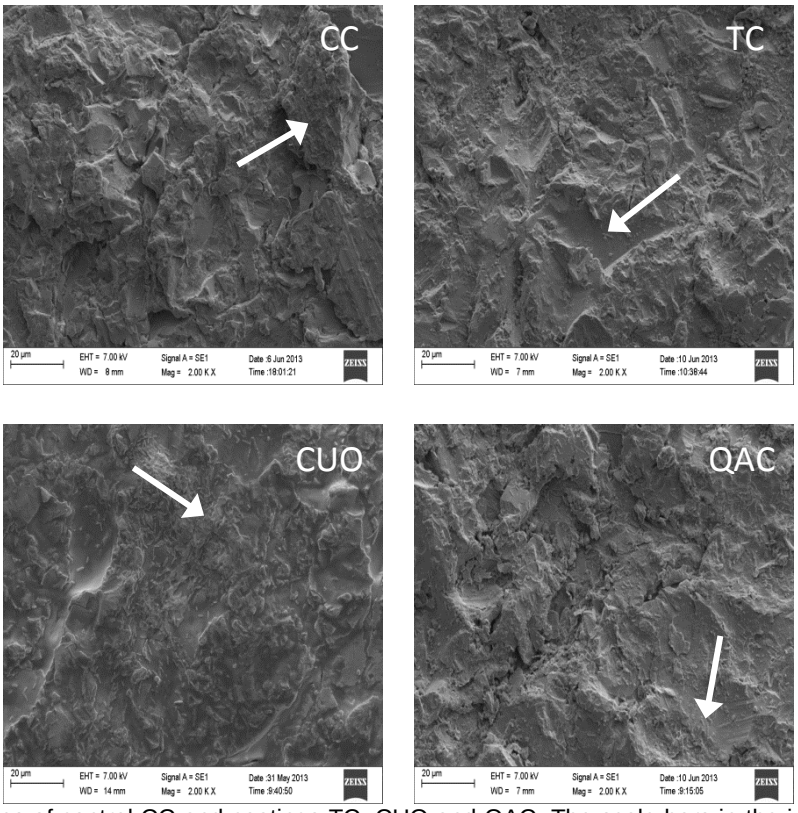

Figure 4.6: SEM images of control CC and coatings TC, CUO and QAC. The scale bars in the images correspond to a length of 20 µm. Arrows indicates attached bacteria to the surface.

Confocal laser scanning microscopy

Bacterial colonies were visualized and distinguished through fluorescent green (viable) and fluorescent red (non-viable) staining (Figure 4.7).

On the surface of the control CC, image (a) and (b), dense biofilm colonies were visible. In image (c), the bacterial cells were more evenly spread out, confirming the fact that biofilm growth is not uniform on metal surfaces. The number of viable cells was more than non-viable cells in all three images.

No dense biofilm populations could be observed on any of the images TC (a), (b) and (c). However, individual bacterial cells were spread over the surface. From images (a) and (b) it is clear that more non-viable cells than viable cells were present.

Dense biofilm growth occurred on all three images of the surface of coating CUO. This was also confirmed through the SEM images (Figure 4.6). The majority of cells were viable.

On the surface of coating QAC, images (b) and (c), and individual bacterial cells were relatively evenly spread over the surface. In image (a) a denser biofilm could be seen. There were slightly more viable cells in all three images.

In descending order the qualitative amount of bacteria visible on the respective surfaces was CUO>CC>QAC>TC. The attachment of bacteria and the formation of a biofilm are dependent on the roughness, polarization, oxide coverage and chemical composition of the metal surface[26]. Homogenous growth on a metal surface is therefore not possible, since the above-mentioned properties are not homogenous throughout the surface of the metal. This is also evident in the images of the control CC and coatings TC and QAC. Additionally, it was previously established that these coatings wash off from the disc surface (Table 3.3). It was evident that coating CUO promoted bacterial growth as more bacterial growth was observed on the surface, than on the control CC. The surface of CUO remained covered with the coating after 48 h, thus creating a homogenous surface for bacterial attachment (Figure 4.6). The influences that metal surfaces, as mentioned above, have on bacterial attachment were eliminated by the coated surface. This created more favourable conditions for biofilm formation. It was therefore concluded that the biocide in coating CUO was not efficient.

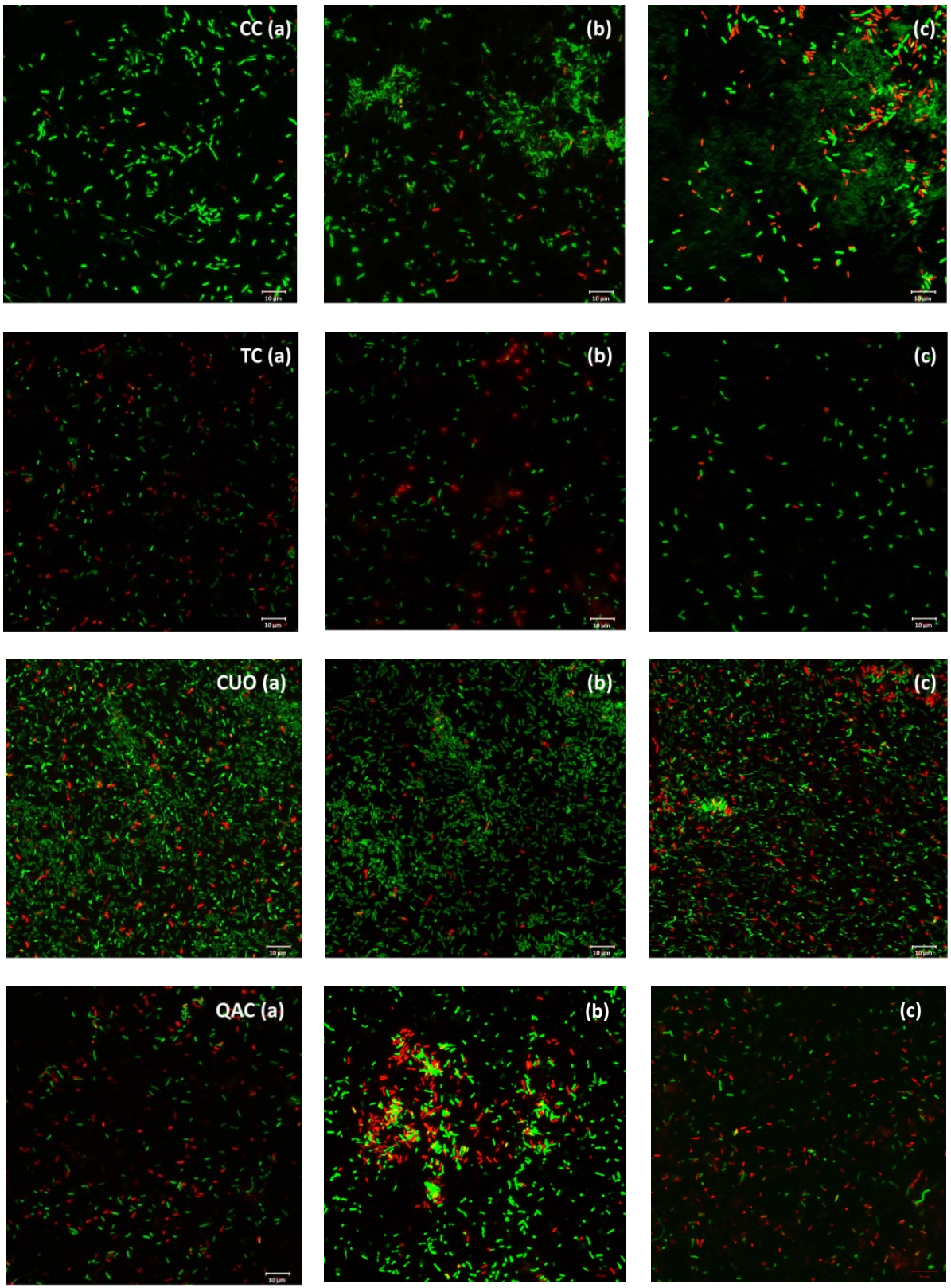

Figure 4.7: CLSM images after biofilm growth for the control CC and coatings TC, CUO and QAC. The scale bars in the images correspond to a length of 10 µm. Three images of each respective coating is shown (a – c)

Quantitative analysis

Plate counts (pour plate method) and flow cytometry

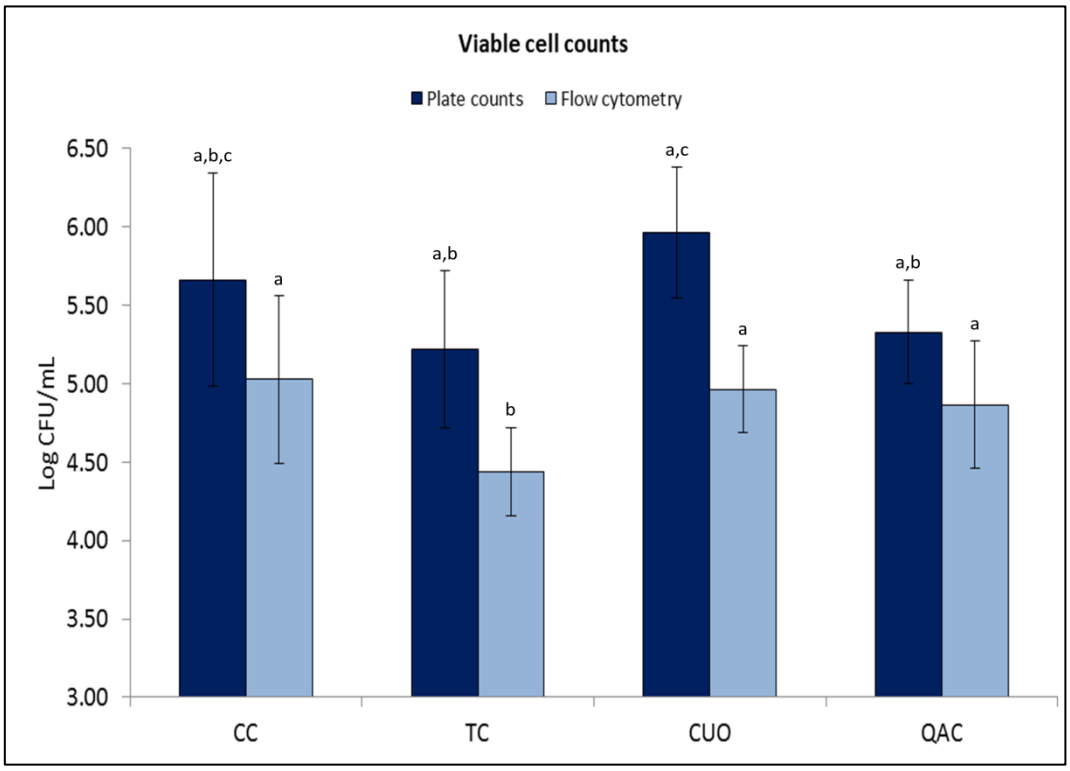

Figure 4.8: Enumeration of total viable and culturable bacteria (log CFU/mL) as determined by the pour plate technique and viable cell count through flow cytometry for the control CC and coatings TC, CUO and QAC. Values are indicated as mean ± standard deviation (STDEV) and values without common letters (a-c) differ significantly ($p<0.05$).

Average viable cell numbers determined using the pour plate method for coatings CC and CUO was between 5.5 and 6.0 log CFU / mL and for TC and QAC between 5.0 and 5.4 log CFU/mL (Figure 4.8). There was a significant difference between viable cell numbers for all four coatings (F_3, 36 = 4.12, $p=0.013$). There was no significant difference between coatings CC, TC and QAC or between CC and CUO. However, a significant difference could be observed between coating CUO and coatings TC ($p = 0.015$) and QAC ($p = 0.05$). Coating CUO showed the highest viable cell count, which was confirmed by CLSM (Figure 4.7) and SEM images (Figure 4.4).

All three coated surfaces and the uncoated control surface showed a higher viable than non-viable cell count. Results obtained through CLSM and plate counts indicated the highest viable cell count for coating CUO, while flow cytometry data indicated that control CC had a higher viable cell count than coatings CUO, TC and QAC. A reason for this could be that the cells on coating CUO clumped together and multiple cells were counted as one cell. There was a significant difference between the viable cell counts of three coatings compared to coating TC.

Flow cytometry

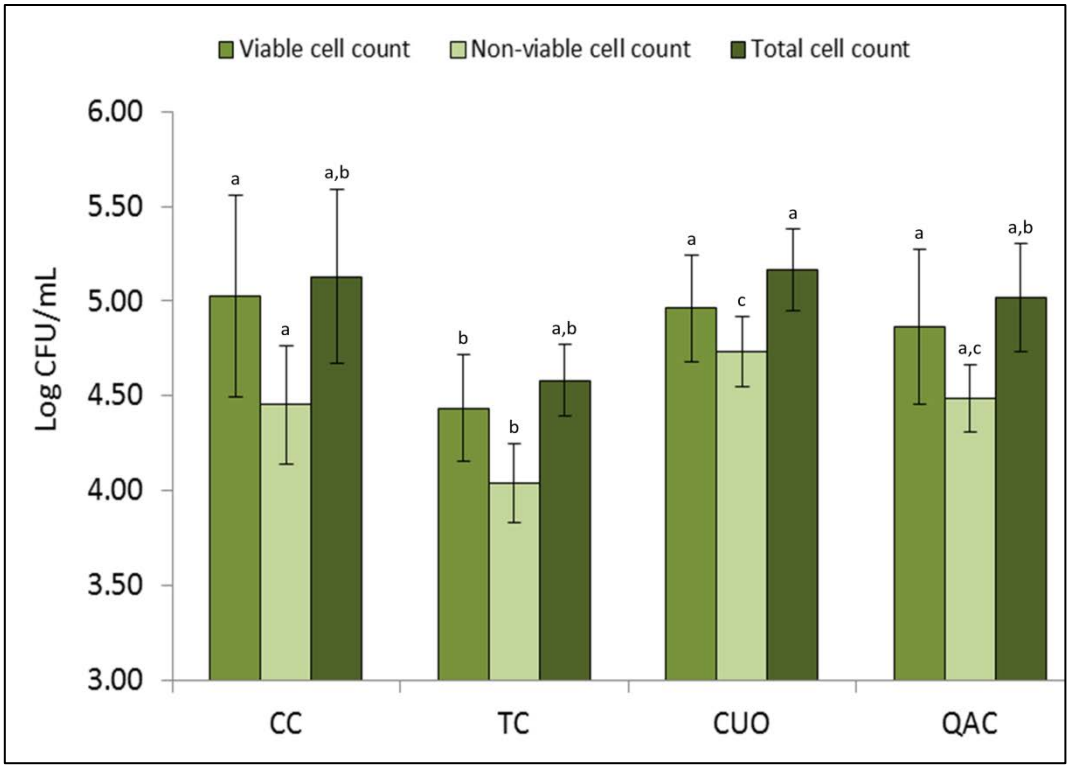

Figure 4.9: Enumeration of viable, non-viable and total bacterial cell count for control CC and coatings TC, CUO and QAC by means of flow cytometry analysis. Values are indicated as mean ± standard deviation (STDEV). Statistical analyses were performed on each parameter (viable, non-viable and total counts) respectively. Values without common letters (a-c) differ significantly ($p<0.05$).

There was a significant difference between viable cell numbers between all four coatings ($H_{3,}$ 40 = 9.71, p = 0.2). The average viable cell counts for coatings CC, CUO and QAC ranged between 4.8 and 5 log CFU/mL with no significant difference between them. Coating TC revealed a 4.4 log CFU/mL viable cell count. A significant difference between coating TC and coatings CUO (p = 0.018) was observed. The viable cell count in descending order was CC> CUO> QAC> TC.

There was a significant difference between non-viable cell numbers between all four coatings ($F_{3,}$ 36 = 14.32,p= 0.000003).The average non-viable cell count for coating CC was 4.46 log CFU/mL, indicating a significant difference between control CC and coatings TC (p = 0.013) and CUO (p = 0.013). TC and CUO showed non-viable cell counts of 4.04 and 4.73 CFU/mL, respectively. A significant difference between coatings QAC and TC (p =0.001) was also shown. QAC had a non-viable count of 4.49 CFU/mL. The non-viable cell count in descending order was CUO>CC>QAC>TC.

There was a significant difference between average total cell count between all four coatings ($H_{3,}$ 40 = 13.16, p = 0.043).The average total cell count for coatings CUO and QAC and metal control CC ranged between 5.02 and 5.16 CFU/mL. A significant difference was only observed between coatings CUO and TC (p = 0.002). The total cell count for TC was 4.58 CFU/mL. The total cell count in descending range was CUO>CC>QAC>TC.

All CFU counts were 0.5 – 1 log higher than determined by flow cytometry, due to the formation of cell clusters, as also found by Jepras et al (1995)[27]. They suggested that bacterial cells form clusters of cells during biofilm formation. The CLSM images also confirmed this cluster formation (Figure 4.7). These cell clusters are disintegrated during the dilution series for the plate count analysis. With flow cytometry, samples are not diluted and vortexed therefore remaining clumped together and these clumps are counted as single cells using the flow cytometer unit and hence the plate counts yielded higher numbers. The possibility however also exists that contamination could have taken place using the plate count method yielding higher numbers than with flow cytometry. Through flow cytometry only the *P.fluoresence* CT07 bacteria would be counted as viable cells as they are incorporated with the fluorescence *gfp* gene.

4.3.2 Section B

4.3.2.1 Evaluation of chemical characteristics of biocide enriched epoxy coatings

Physical analysis

Thermogravimetric analysis and Differential scanning calorimetry

Thermogravimetric analysis was done for coatings EC, SN, CS and FR to determine their thermal stability. The effect that different incorporated biocides had on the thermal stability of the respective coatings was also determined. Thermal decomposition of the coatings was almost exactly the same, and took place through two steps (Figure 4.10). Initial weight loss took place between 90 – 100 °C, which is probably due to moisture loss. All coatings started to lose their bulk weight between 300 and 400 °C. At 375 °C, coating SN showed a slightly greater weight loss than the other three coatings. All four coatings showed a very high thermal stability and the incorporation of biocides into the epoxy resin had a negligible influence. All four coatings would be thermally stable to be applied throughout an entire cooling water system.

All four coatings exhibited a single glass transition temperature (T_g) of between 115 °C and 135 °C, confirming the presence of an inter-cross-linked structure (Figure 4.10). Minor T_g differences were observed among coatings. Coating CS had the lowest T_g followed by coating SN, FR and EC. The biocides most likely acted as plasticisers which slightly decreased the packing efficiency of the epoxy resin, which explains the lower T_g's for coatings SN, CS and FR. The molecular structure of a cured epoxy resin is amorphous and therefore no crystalline exotherm or melting endotherm was observed.

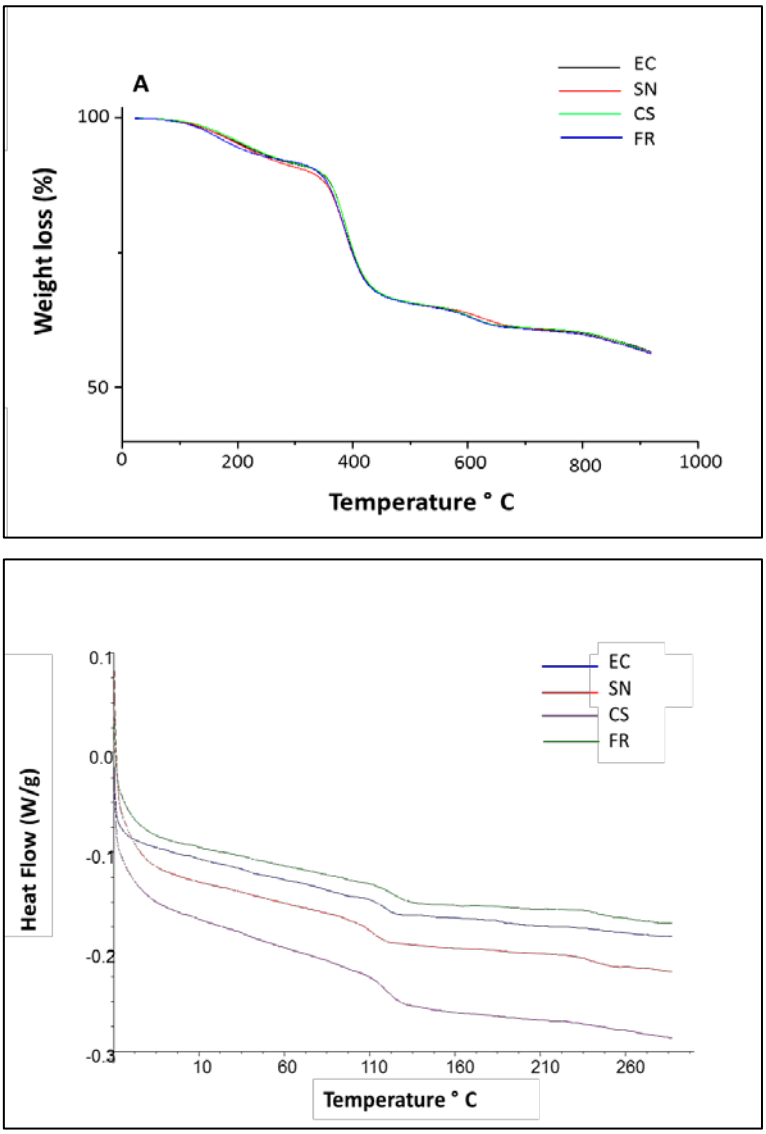

Figure 4.10: TGA (A) and DSC (B) thermograms comparing the thermal stability of control coating EC and coatings SN, CS and FR.

Chemical analysis

Energy dispersive X-ray spectroscopy

The presence of Carbon (C) atoms in all four discs was observed in the same weight percentage (60 -78 wt. %), confirming the presence of the base coating (Table 4.1). After biofilm growth the C wt. % decreased for all four discs. This might indicate that the coatings degraded slightly.

The Oxygen (O) concentration for coatings EC - FR before and after biofilm growth was in the same weight percentage (16 - 25 wt. %) (Table 4.4). The O wt. % increased slightly after biofilm growth for all four coatings.

It was expected that Ag and Cu would be present in coatings SN and CS, respectively, since silver nitrate was added to SN and copper sulphate to CS. However, there was no wt. % recorded for Ag and Cu. Possible explanations for this could be that the incorporated percentage of the respective biocides was too low for the sensitivity of EDX analysis and that it should rather be analysed through ICP-AES, or that the incorporated biocide was not present at the surface of the coatings.

Aluminium (Al), titanium (Ti), barium (Ba) and silicon (Si) was present in all four coated discs. For all four coated discs the wt. % of elements mentioned above increased after biofilm growth. This phenomenon might be attributed to the outer surface of the coating (the C backbone) that shields the other elements and once the outer surface of the coating is slightly degraded (as confirmed with the C wt. % decrease), the wt. % of other elements increased.

The presence of coatings after biofilm formation was confirmed by EDX and SEM (Table 4.4, Figure 12). The base coating was thus durable for 48 h.

Table 4.4: EDX analysis for coatings EC-FR on metal discs, before and after biofilm growth.

	EC		SN		CS		FR	
Elements	**Before weight %**	**After weight %**	**Before weight %**	**After weight %**	**Before weight %**	**After weight %**	**Before weight %**	**After weight %**
C	77.01	72.01	76.43	66.33	77.81	60.37	73.78	68.27
O	16.35	18.90	16.42	21.24	16.11	24.59	17.45	20.80
Al	0.64	0.92	0.70	1.28	0.61	1.72	0.90	1.06
Si	0.88	1.17	0.97	1.57	0.84	2.06	1.15	1.30
Ti	1.86	2.23	1.94	2.89	1.70	3.37	2.28	2.75
Fe	0.00	0.00	0.00	0.00	0.00	0.00	0.00	0.00
Cu	0.00	0.00	0.00	0.00	0.00	0.00	0.00	0.00
Ag	0.00	0.00	0.00	0.00	0.00	0.00	0.00	0.00
Ba	2.56	3.75	2.80	5.33	2.29	6.31	3.5	4.61

Image analysis

Scanning electron microscopy

Before biofilm formation on EC (a) no small dark regions were visible as in images for SN, CS and FR (Figure 12). This confirmed the absence of any biocide in the control coating EC, and the presence of biocides in coatings SN, CS and FR (Figure 4.11). The absence of the darker regions in the images taken after biofilm formation and removal for SN, CS and FR might indicate that the biocides leached out of the coatings (Figure 4.11). The texture of the surfaces of control coating EC and coatings SN, CS and FR before biofilm growth was even while roughness of coating surfaces increased after biofilm growth. Dents and bubbles were observed on the surface of control coating EC and coatings SN, CS and FR. It was concluded that the durability of the base coating decreased after being submerged in an aqueous environment for 48 h (Figure 4.11).

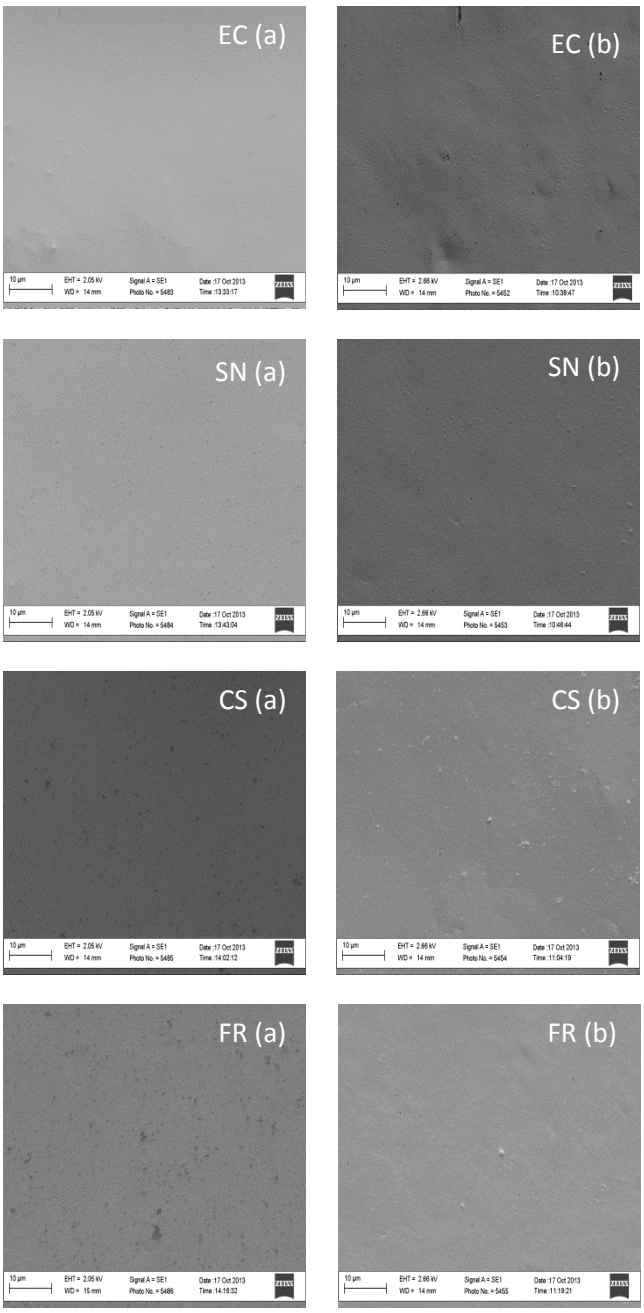

Figure 4.11: SEM images of coatings EC-FR before (a) and after (b) biofilm growth. Scale bars in images correspond to a length of 20 µm.

4.3.2.2 Evaluation of antifouling characteristics of biocide enriched epoxy coatings

Qualitative analysis

Scanning electron microscopy

Attachment of bacterial cells was observed on all four coatings after 48 h. (Figure 4.12). In image EC a more dense population of bacteria was observed, than on SN, CS and FR indicative of a more matured biofilm. Coatings SN and CS and FR qualitatively had less bacteria on the surface, which is in agreement with fluorescence microscopy results (Figure 4.12). More bacterial cells were detected on coating CS than coating SN and more cells on SN than on FR.

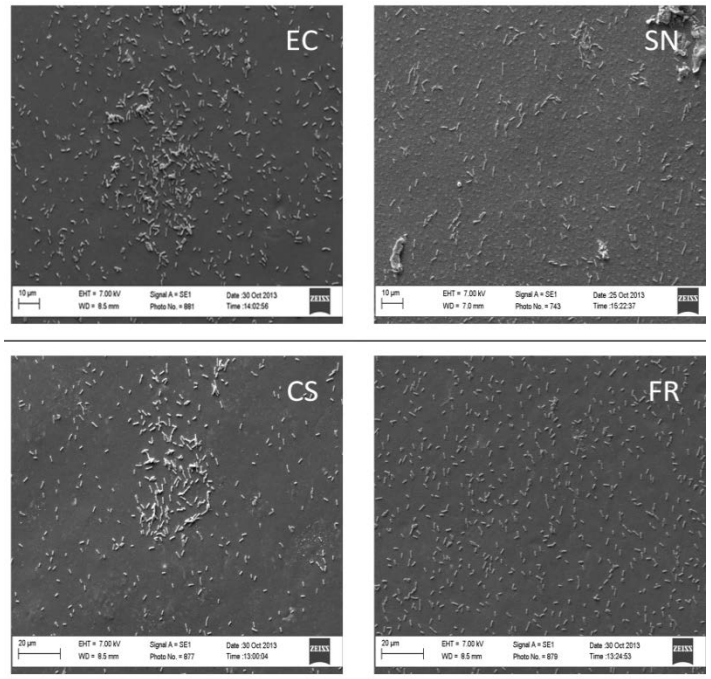

Figure 4.12: SEM images of control coating EC and coatings SN, CS and FR. Scale bars in the images CS and FR correspond to a length of 20 µm and for EC and SN to a length of 10µm.

Confocal laser scanning microscopy

On the surface of EC individual viable bacterial cells were almost uniformly spread with a few areas showing more bacterial cell clusters (Figure 4.13). In image (c) larger dense viable bacterial clusters were observed in contrast to the SEM image (Figure 4.13). The number of viable cells for all three images was also higher than the number of non-viable cells.

No dense bacterial cell clusters were observed on any of the images of coating SN. More non-viable bacterial cells were attached to the surface of treatment SN, compared to the other three coatings. Bacterial growth was the least visible on coating SN, which was confirmed through qualitative SEM analysis (Figure 4.13).

On the surface of coating CS, image (a) and (c), viable bacterial cells were spread evenly over the surface with a few denser cell clusters. The number of non-viable cells was also minimal. However, a larger dense bacterial cell cluster was observed in the centre of image (b). The number of viable and non-viable cells is almost similar for this treatment (Figure 4.13).

All three images of FR indicate individual viable bacterial cells that are uniformly spread over the coating. Denser bacterial cell clusters were observed and the majority of the bacterial cells were viable in all three images.

It was concluded that coating EC had the most viable bacterial cells on the surface, followed by coating FR, CS and SN. This was expected since the EC coating did not contain any biocide. The coating with the most non-viable cells was CS followed by EC, FR and SN in descending order. Bacterial density as well as viable and non-viable differences could be seen between the three images of each coating respectively.

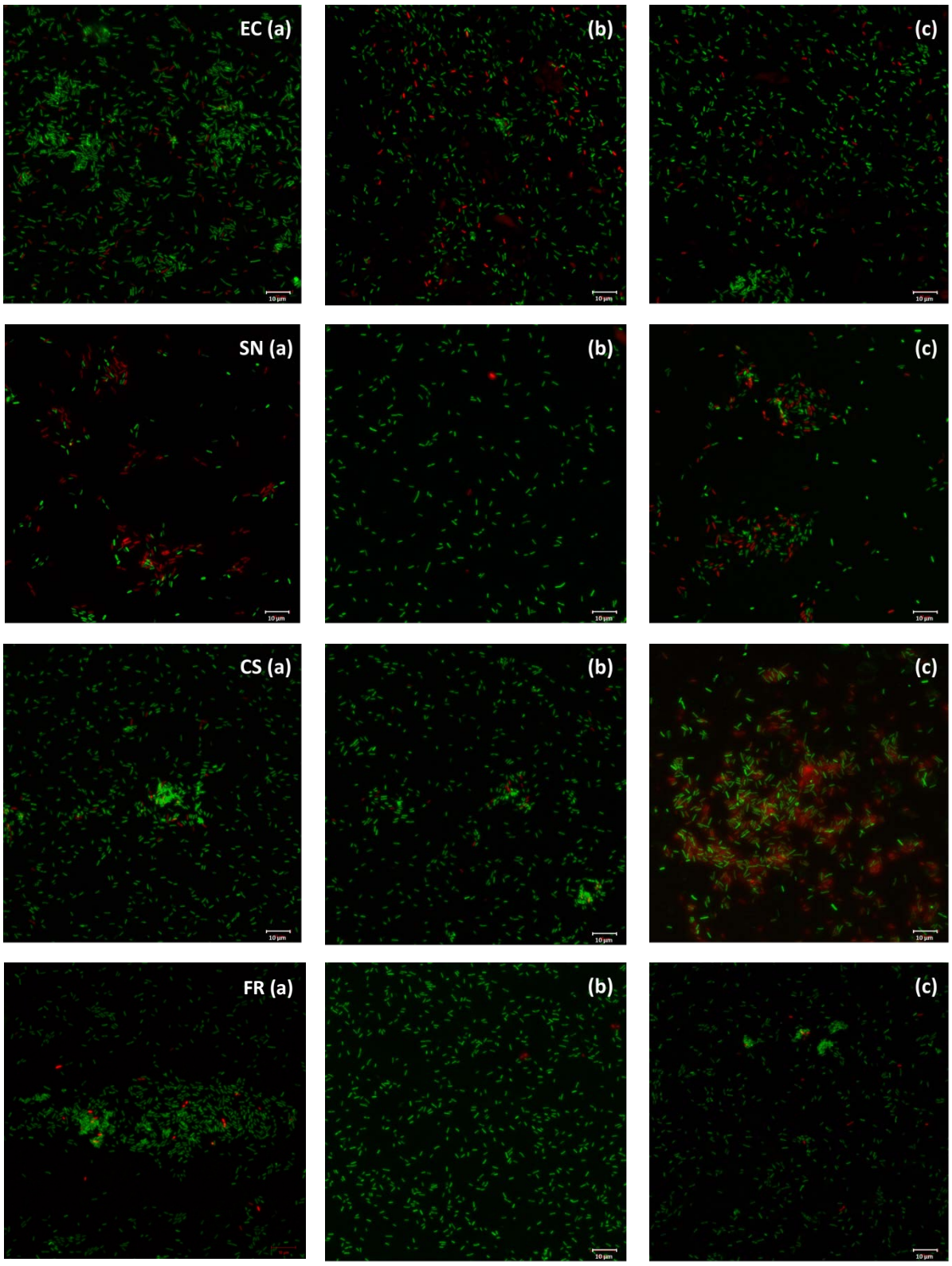

Figure 4.13: CLSM images after biofilm growth for the control coating EC and coatings SN, CS and FR. Scale bars in the images correspond to a length of 10 µm. Three images of each respective coating are shown (a – c).

Quantitative analysis

Plate counts (Pour plate method)

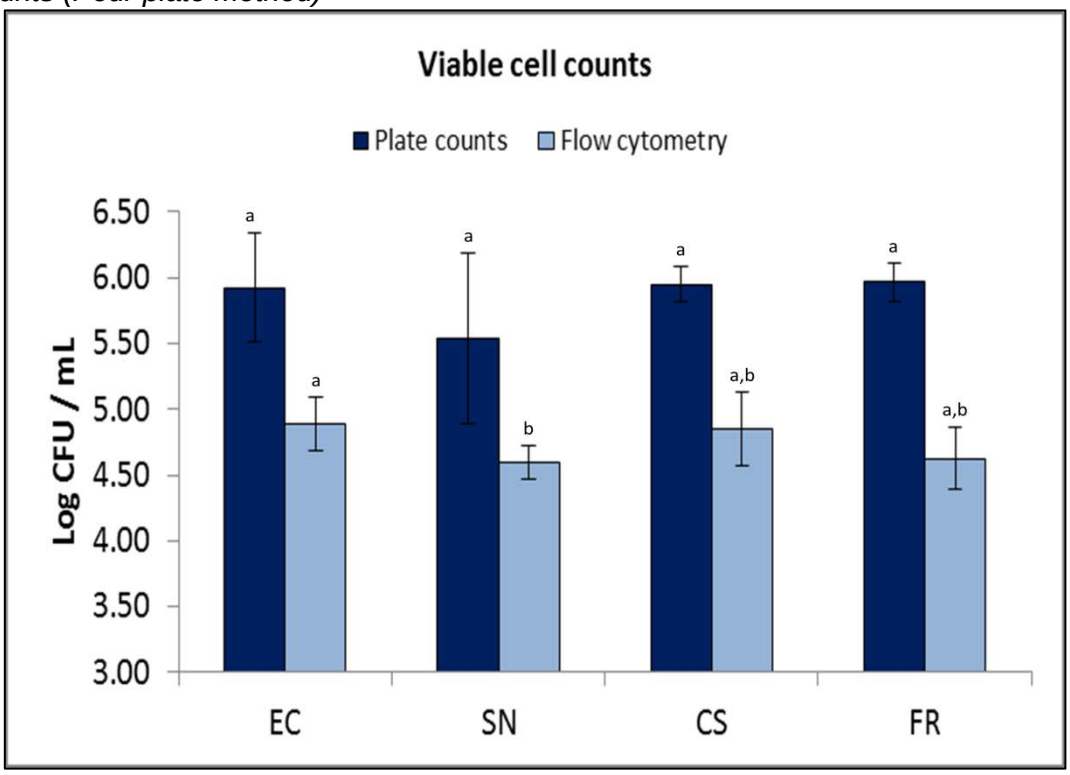

Figure 4.14: Enumeration of total viable and culturable bacteria (CFU/mL) using the pour plate technique and viable cell count through flow cytometry for control coating EC and coatings SN, CS and FR Values are indicated as mean ± standard deviation (STDEV) and values without common letters (a-c) differ significantly ($p<0.05$).

The average viable cell counts obtained through the pour plate method for coatings EC, SN, CS and FR ranged between 5.5 and 6.0 log CFU/mL. There was no difference between coatings EC, CS and FR, but coating SN did indicate a slight decrease in viable cell count that was also confirmed by CLSM (Figure 4.13) and SEM images (Figure 4.12). Additionally, no significant difference existed amongst coatings EC, SN, CS, and FR as indicted in Figure 4.14.

Flow cytometry

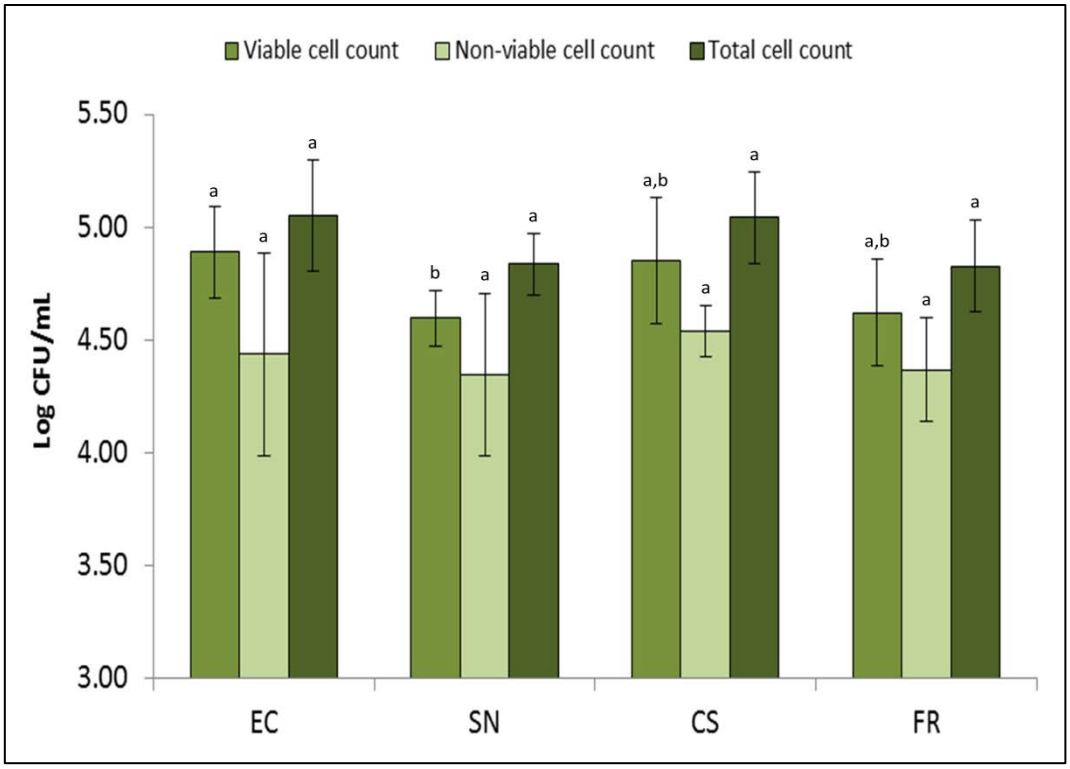

Figure 4.15: Enumeration of viable, non - viable and total bacterial cell count for control coating EC and coatings SN, CS and FR by means of flow cytometry analysis. Values are indicated as mean ± standard deviation (STDEV) and values without common letters (a-c) differ significantly ($p<0.05$).

Total viable and non-viable cell counts were calculated from the data obtained from flow cytometry analysis in combination with the total cell count equation (Equation 4.1). The data obtained from the calculation were further analysed using statistical ANOVA analysis.

The average viable cell counts for control coating EC and coatings SN, CS and FR ranged between 4.5 and 5.0 log CFU/mL. There was no significant difference in the viable cell count amongst coatings EC, CS, FR or between CS, FR and SN (Figure 4.15). The only significant difference was between coatings EC and SN ($H_{3,40} = 2.49$, $p = 0.036$). The viable cell count in descending order was EC>CS>FR>SN.

The average non-viable cell count for control coating EC and coatings SN, CS and FR was between 4.0 and 4.5 log CFU/mL. No significant difference existed amongst any of the respective coatings. The total non-viable cells for all coatings were between 0, 5 and 1.0 log CFU less than the viable cell count. This is in line with CLSM results, but it is still higher than expected when compared with CLSM images (Figure 4.13). A reason for this could be that the bacterial samples had to be stored for longer periods of time before it was subjected to flow cytometry in which time viable cells could have entered a non-viable state. The non-viable cell count in descending order was CS>EC>FR>SN.

The average total cell count for control coating EC and coatings SN, CS and FR ranged between 4.7 and 5.2 CFU/mL. No significant difference existed amongst any of the coatings. The total cell count in descending order was EC>CS>FR>SN.

The CFU counts for all four coatings were between 1 – 1, 5 log higher than determined by flow cytometry (Figure 4.14, Figure 4.15). Possible reasons for this are previously discussed in section A 4.1.2.

4.4. Conclusions

It was determined that none of the industrial coatings or the biocide incorporated epoxy coatings that were used in this study would be efficient for the use on metal surfaces in cooling water systems.

Section A

- Industrial coatings TC and CUO are thermally stable for the utilization in cooling water towers and pipeline but not in heat exchangers. QAC is not thermally stable for use in any section of cooling water system.
- Through SEM imaging and EDX analysis it was confirmed that the metal surface showed signs of deterioration, and coatings TC and QAC washed off from the metal growth discs. Hence it was concluded that the adhesion properties of these coatings to a metal growth discs for the application in aqueous environments were insufficient.
- Coating CUO was observed on the surface of the metal however the biocide element, Cu could no longer be detected after the coating was exposed to an aqueous environment for 48 h.
- The attachment of bacteria on the surfaces of coatings TC, CUO and QAC and control CC was difficult to observe using SEM imaging as the metal has a rough surface. Attachment of bacteria on coated surfaces was however confirmed using CLSM. The results from CLSM correlated with the results from plate counts and flow cytometry.
- A significant difference in viable cell count was observed between coating TC and coatings CUO, QAC and the control CC. It was also established that coating CUO promoted biofilm growth.

Section B

- Biocide enriched epoxy coatings are thermally stable to be utilized throughout cooling water systems.
- The presence of coatings before and after biofilm formation was confirmed through SEM imaging and EDX analysis.

- Before biofilm growth the presence of silver and copper ions in coatings SN and CS was confirmed through EDX. After biofilm formation no silver or copper ions could be confirmed in SN or CS coatings.
- The presence of biocides was confirmed through SEM imaging for coatings SN, CS and FR before biofilm growth. After biofilm growth the presence of respective biocides could not be confirmed.
- Silver nitrate biocide incorporated into epoxy coating showed slight antifouling properties, but over time the biocide would leach out of the coating.
- The attachment of bacteria on the surfaces of coatings SN, CS, FR and control EC could easily be observed through SEM and CLSM imaging. The results from SEM and CLSM correlated with the results from plate counts and flow cytometry.
- No significant difference in viable cell count was observed between the control coating EC and coatings SN, CS and FR.

4.5. References

1. Flynn, D. *Nalco Water Handbook*. McGraw-Hill: Global education Holdings, LCC: Penn Plaza, 10th Floor, New York.

2. Bott TR, *Industrial biofouling. Elsevier:* The boulevard, Langford Lane, Kidlington, Oxford, UK (2011).

3. Cloete, T. E., Jacobs, L. & Brözel, V. S. The chemical control of biofouling in industrial water systems. *Biodegradation* **9,** 23–37 (1998).

4. Coetser, S. E. & Cloete, T. E. Biofouling and biocorrosion in industrial water systems. *Crit. Rev. Microbiol.* **31,** 213–32 (2005).

5. Melo, L. F. & Bott, T. R. Biofouling in water systems. *Exp. Therm. Fluid Sci.* **14,** 375–381 (1997).

6. Bott, T. R. & Tianqing, L. Ultrasound enhancement of biocide efficiency. *Ultrason. Sonochem.* **11,** 323–6 (2004).

7. Cloete, T. E., Brözel, V. S. & Von Holy, A. Practical aspects of biofouling control in industrial water systems. *Int. Biodeterior. Biodegradation* **29,** 299–341 (1992).

8. Silkina, A., Bazes, A., Mouget, J.-L. & Bourgougnon, N. Comparative efficiency of macroalgal extracts and booster biocides as antifouling agents to control growth of three diatom species. *Mar. Pollut. Bull.* **64,** 2039–46 (2012).

9. Cloete, T. E. Resistance mechanisms of bacteria to antimicrobial compounds. *Int. Biodeterior. Biodegradation* **51,** 277–282 (2003).

10. White, D. G. & McDermott, P. F. Biocides, drug resistance and microbial evolution. *Curr. Opin. Microbiol.* **4,** 313–7 (2001).

11. Touir, R. *et al.* Corrosion and scale processes and their inhibition in simulated cooling water systems by monosaccharides derivatives. *Desalination* **249,** 922–928 (2009).

12. Dafforn, K. a, Lewis, J. a & Johnston, E. L. Antifouling strategies: history and regulation, ecological impacts and mitigation. *Mar. Pollut. Bull.* **62,** 453–65 (2011).

13. Cloete, T. E. Biofouling control in industrial water systems: What we know and what we need to know. *Mater. Corros.* **54,** 520–526 (2003).

14. Murata, H., Koepsel, R. R., Matyjaszewski, K. & Russell, A. J. Permanent, non-leaching antibacterial surface--2: how high density cationic surfaces kill bacterial cells. *Biomaterials* **28,** 4870–9 (2007).

15. Qian, P.-Y., Chen, L. & Xu, Y. Mini-review: Molecular mechanisms of antifouling compounds. *Biofouling* **29,** 381–400 (2013).

16. Konstantinou, I. K. & Albanis, T. A. Worldwide occurrence and effects of antifouling paint booster biocides in the aquatic environment: a review. *Environ. Int.* **30,** 235–48 (2004).

17. Thomas, K. V., Fileman, T. W., Readman, J. W. & Waldock, M. J. Antifouling Paint Booster Biocides in the UK Coastal Environment and Potential Risks of Biological Effects. *Mar. Pollut. Bull.* **42,** 677–688 (2001).

18. Garnett, M. C. & Kallinteri, P. Nanomedicines and nanotoxicology: some physiological principles. *Occup. Med. (Lond).* **56,** 307–11 (2006).

19. Hoet, P. H., Brüske-Hohlfeld, I. & Salata, O. V. Nanoparticles - known and unknown health risks. *J. Nanobiotechnology* **2,** 12 (2004).

20. Le, Y., Hou, P., Wang, J. & Chen, J.-F. Controlled release active antimicrobial corrosion coatings with Ag/SiO2 core–shell nanoparticles. *Mater. Chem. Phys.* **120,** 351–355 (2010).

21. Meesters, K. P. H., Van Groenestijn, J. W. & Gerritse, J. Biofouling reduction in recirculating cooling systems through biofiltration of process water. *Water Res.* **37,** 525–32 (2003).

22. Flemming, H.-C. Biofouling in water systems--cases, causes and countermeasures. *Appl. Microbiol. Biotechnol.* **59,** 629–40 (2002).

23. Bester, E., Wolfaardt, G., Joubert, L., Garny, K. & Saftic, S. Planktonic-Cell Yield of a Pseudomonad Biofilm. *Appl. Environ. Microbiol.* **71 ,** 7792–7798 (2005).

24. Bester, E., Edwards, E. A. & Wolfaardt, G. M. Planktonic cell yield is linked to biofilm development. *Can. J. Microbiol.* **55,** 1195–1206 (2009).

25. Keranov, I., Vladkova, T., Minchev, M., Kostadinova, A. & Altankov, G. Preparation, characterization, and cellular interactions of collagen-immobilized PDMS surfaces. *J. Appl. Polym. Sci.* **110,** 321–330 (2008).

26. Faisal M AlAbbas, John R Spear, Anthony Kakpovbia, Nasser M Balhareth, David L Olson, and B. M. Bacterial attachment to metal substrate and its effects on microbiologically-influenced corrosion in transportin hydrocarbon pipelines. *J. pipeline Eng.* **11,** 63–72 (2012).

27. Jepras, R. I., Carter, J., Pearson, S. C., Paul, F. E. & Wilkinson, M. J. Development of a robust flow cytometric assay for determining numbers of viable bacteria . *Appl. Environ. Microbiol.* **61,** 2696–2701 (1995).

CHAPTER 5

Synthesis of an environmentally friendly antifouling coating

5.1. Introduction

Biofouling control in recirculating cooling water systems, in the energy sector, is of great financial concern.[1] Biofouling causes acceleration of metallic corrosion commonly referred to as bio corrosion, heat exchanger inefficiency, physical blockages of pipes and an increased frictional resistance of the flow water, leading to additional maintenance and ultimately high operation costs.[2,3] Chemical and physical biofouling control methods have been developed and tested over decades. Currently, the most implemented and successful method for biofouling control in cooling water systems is the addition of biocides to recirculating cooling water, however this approach has disadvantages.[2,3] Biocides are introduced into the environment through the deposition of the coolant water into rivers, sea or through blow down water. Apart from being very expensive, these biocides are environmentally hazardous and enhance the development of antimicrobial resistance.[4] An alternative to biocides is the use of antifouling coatings. However in the early 70's, the most successful antifouling coating was banned from production and use due to the high toxicity level of the incorporated biocide.[5]

The antifouling properties of furanones were first observed within the marine red algae *Delisea pulchra.* The absence of fouling was observed on the surface of the red alga. Researchers discovered that the algae produces and excretes more than 30 different furanone derivatives through gland cells that are captured in vesicles beneath the surface of the algae.[4,6] Today natural and synthetic furanones are widely used for different applications.

Biofouling in cooling water systems entails the growth of a wide variety of bacteria in a biofilm community on surfaces exposed to water. One of the factors that are essential for biofilm formation is cell to cell communication amongst the bacteria in the biofilm, termed quorum sensing. Furanones act as quorum sensing inhibitors by disrupting the cell-cell communication between the bacteria which in turn prevents the biofilm from developing or expanding.[7] Antifouling coatings with incorporated furanone derivatives, as active biocides, have already been developed and used since 1998.[6]

The development of environmentally friendly biocides which are permanently bonded to a polymer backbone has since received much attention. It was attempted to synthesize such a coating. A furanone derivative was selected for this study as an environmentally friendly biocide to be chemically bonded onto a poly-(styrene-*alt*-maleic) anhydride (SMA) coating. Scheme 5.1 schematically illustrates the synthesis of such SMA-Furanone coating, the immobilization of the furanone derivative onto the SMA backbone through a nucleophilic substitution reaction on the maleic anhydride repeat units.

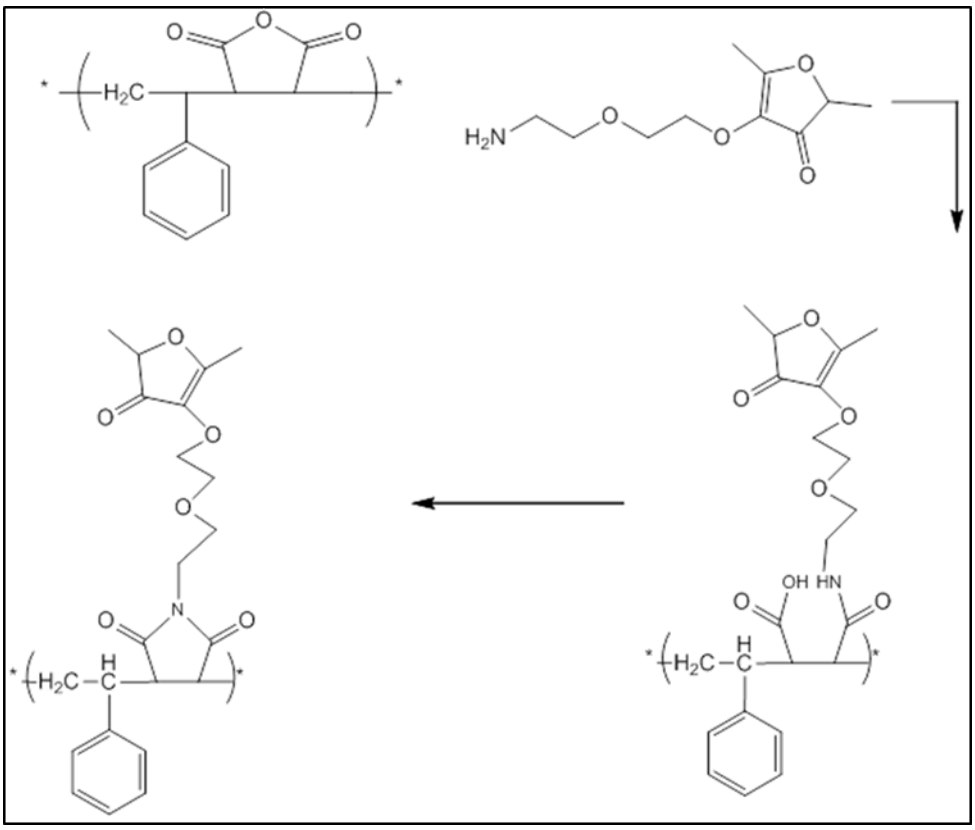

Scheme 5.1: Schematic illustration for the synthesis of SMA-Furanone

The synthesis of the furanone derivative was carried out as described by Buttery and Ling (1999)[8] and Gule et al (2012)[9] as summarised in Scheme 5.4. Primary amine functionality was introduced onto the furanone through an alcohol, alcohol reaction.

Strong alternating SMA, of 1:1 Styrene: maleic anhydride, was synthesised through radical polymerization, carried out as described by Cloete *et al* (2011).[10] Radical polymerization is a popular chain growth polymerization technique, which can take place quite easily under undemanding conditions.[11] Today this technique is widely used for industrial as well as laboratory polymer synthesis.[12] Relatively high molar mass polymer chains can be produced from a wide variety of monomers through this technique. Radical polymerization takes place through four kinetic events which are; 1) radical formation, 2) initiation, 3) propagation and 4) termination. A limitation of this technique is that there is poor control over elements that would ensure the synthesis of a polymer with controlled molecular weight, polydispersity, composition and chain architecture.[11]

SMA is a copolymer that is regarded as a very functional or reactive polymer. Its functionality and reactivity is brought about the maleic anhydride in the backbone of the polymer which is reactive to numerous nucleophilic reagents.[13] For this study a nucleophilic substitution reaction with a primary amine through a ring opening reaction of the maleic anhydride unit was attempted. The significance of SMA copolymer can also be attributed to its numerous utilization areas including

binder application, microcapsules, pharmaceutical applications and for our application as a coating.[14]

In this chapter the objective was to synthesise an antifouling coating for the application on metal surfaces. SMA was used as the coating and a furanone derivative as biocide. The biocide would be chemically bound to the polymer back bone of the coating. The concept is illustrated in Figure 5.1.

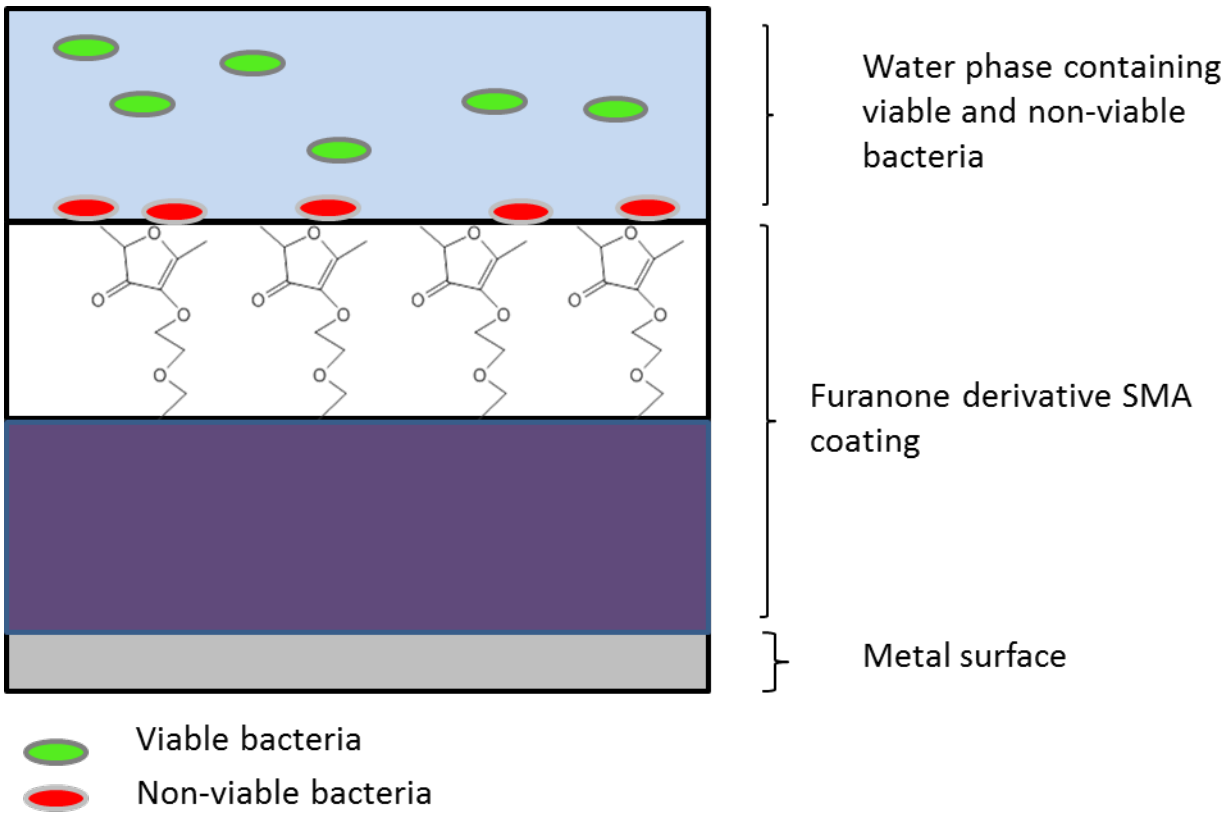

Figure 5.1: Illustration of metal surface coated with Furanone derivative SMA coating with antifouling properties

5.2 Experimental setup

5.2.1 Chemicals

All chemicals and solvents used were purchased from commercial sources and used without further purification, unless stated otherwise. Styrene monomer was obtained from Kansai Plascon Research Centre at Stellenbosch and purified by distillation under reduced pressure after removal of inhibitors by washing with $KOH_{(aq)}$ and $NaOH_{(aq)}$ respectively and drying over $MgSO_4$-anhydrous. Maleic anhydride (Merck 99%), methyl ethyl ketone (MEK) (Sasol), azobisisobutronitrile (AIBN) (Riedel-DeHaën; SIGMA-ALDRICH; recrystallized from methanol), iso-propanol (Sasol), di-tert butyl dicarbonate (Boc_2O) (Merck), iodine (Merck), 2,2-(aminoethoxy)ethanol (Aldrich), sodium hydrogen carbonate (Merck), sodium thiosulfate (Merck), sodium sulfate (Merck), diethyl ether (Sasol), hexane (Sasol), 2,5-dimethyl-4-hydroxy-3(2H)-furanone (Aldrich 15%), 2,5-dimethyl-4-hydroxy-3(2H)-furanone (Aldrich 98%), p-toluene sulfonic acid (Merck), anhydrous ethanol (Merck), anhydrous benzene (Merck), succinic anhydride (Aldrich), anhydrous p-toluene sulfonic chloride (Fluka), anhydrous tolune (Aldrich), sodium chloride (Sasol), magnesium sulfate (Merck),

anhydrous tetrahydrofuran (THF) (Merck), *N*,*N*'-dicyclohexylcarbodiimide (DCC) (Jansson chemicals),4-dimethylaminopyridine (DMAP) (Fluka).

5.2.2 Analytical Methods

5.2.2.1 Nuclear Magnetic Resonance

One dimensional ^{1}H spectra were acquired with a Varian Unity Inova 600MHz, 400MHz or 300MHz Nuclear Magnetic Resonance (NMR) spectrometer with 5 mm Dual Broad Band PFG Probe at 25°C in deuterated chloroform ($CDCl_3$). Relaxation delays of 1 second were used and the spectra were internally referenced to TMS at 0 ppm. All peaks are reported downfield of TMS.

5.2.2.2 Size exclusion chromatography

Size exclusion chromatography (SEC) analysis was done on an instrument that included a Waters 1515 isocatic pump, a Waters inline degasser AF, a Waters 717 plus auto sampler with a 100 µL sample loop, a Waters 2487 dual wavelength absorbance UV detector, a Waters 2414 refractive index detector at 30 °C. SEC measurements were performed on a set of two PLgel columns (Polymer laboratories). A 5 µm Mixed-C column (300x7.5mm) connected in series with a PLgel guard column (50x7.5 mm). THF (stabilized by 0.125 % BHT) was used as mobile phase at a flow-rate of 1 mL/min. Sample concentrations were 1 g/L and injection volumes were 100 µL. The columns were calibrated with polystyrene standards (Polymer laboratories, Church Stretton, Shropshire, UK). Data processing was performed using Breeze version 3.30 SPA (Waters) software.

5.*2.2.3 Electron Spray Mass spectroscopy (ES-MS)*

Electron spray mass spectrometry was carried out using a Waters API Q-TOF Synapt G2 equipped with a Waters UPLC. The sample (1 µL) was injected into a stream of acetonitrile and 0.1% formic acid at a capillary voltage of 2.5 kV and a cone voltage of 15 V. The source temperature was maintained at 120 °C and the desolvation temperature at 275 °C. The desolvation gas was set at 650 L/h and the cone gas at 50 L/h. Scans between m/z 100 and m/z 2000 were taken per sample.

5.3 Synthetic procedures

5.3.1 Synthesis of SMA

A strongly alternating copolymer of styrene and maleic anhydride was synthesized via radical polymerization in a 1:1 molar ratio of styrene: maleic anhydride (Scheme 5.2).

Styrene monomer (15 g, 0.14 mol) and maleic anhydride (14.12 g, 0.14 mol) were dissolved in MEK (200 mL) along with AIBN (0.1182 g, 7.1 $x10^{4}$ mol). The mixture was degassed by purging with Nitrogen for 30 min, and then heated overnight at 60 °C. The polymer product was cooled to room temperature and isolated by precipitation from iso-propanol (500 mL), after which it was dried at 90 °C in a vacuum oven for 8 h to in order to remove unreacted monomer and residual solvent. The polymer was analysed using ^{1}H NMR and SEC.

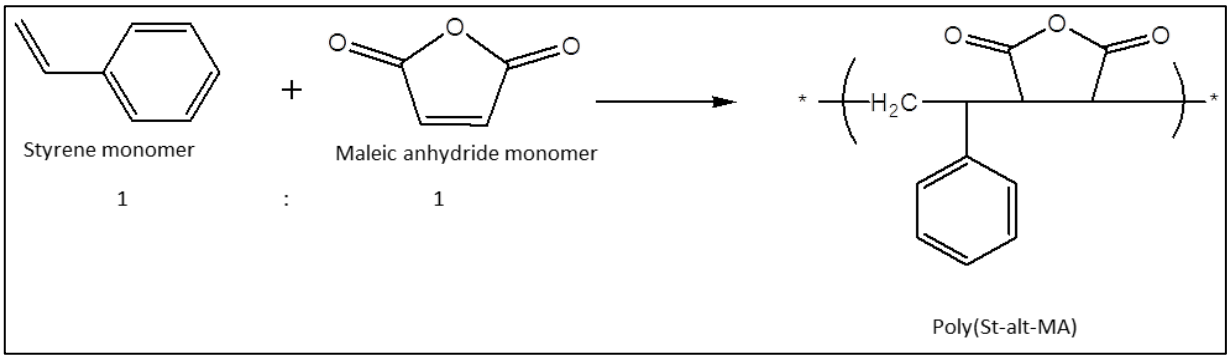

Scheme 5.2: Reaction scheme for the synthesis of alternating SMA through conventional radical polymerization

5.3.2 Synthesis of tert-butyl 2-(2-hydroxyethoxy) ethylcarbamate

$(Boc)_2O$ (10.51 g, 0.5 mol), and a catalytic amount of iodine (2.5 g), were added to a round bottom flask containing a magnetic stirrer. The mixture was stirred in an ice bath and then 2(2-aminoethoxy) ethanol (20.7 mL, 0.2 mol) was added drop wise (Scheme 5.3). The mixture was then allowed to warm up to room temperature and was stirred for 7 h, during which the mixture changed to a dark brown viscous liquid. Afterwards diethyl ether (15 ml) was added, and the mixture stirred until a homogeneous solution was obtained. The mixture was then washed with aqueous $Na_2S_2O_3$ (25 mL) and saturated $NaHCO_3$ (25 mL), dried over anhydrous Na_2SO_4 followed by removing the solvent under reduced pressure. The crude product was purified by column chromatography using diethyl ether and hexane (1:1 v/v) as the mobile phase, to give a pale yellow product.

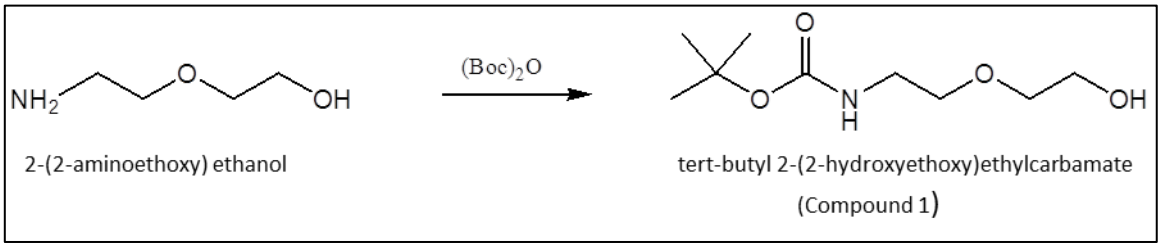

Scheme 5.3: Synthesis of tert-butyl 2-(2-hydroxyethoxy)ethylcarbamate.

5.3.3 Synthesis of 3(2H) furanone derivative

Three approaches towards the synthesis of 4-(2-(2-aminoethoxy)ethoxy)-2,5-dimethylfuran-3(2H)-one, (Compound 4) Scheme 5.4 were attempted.

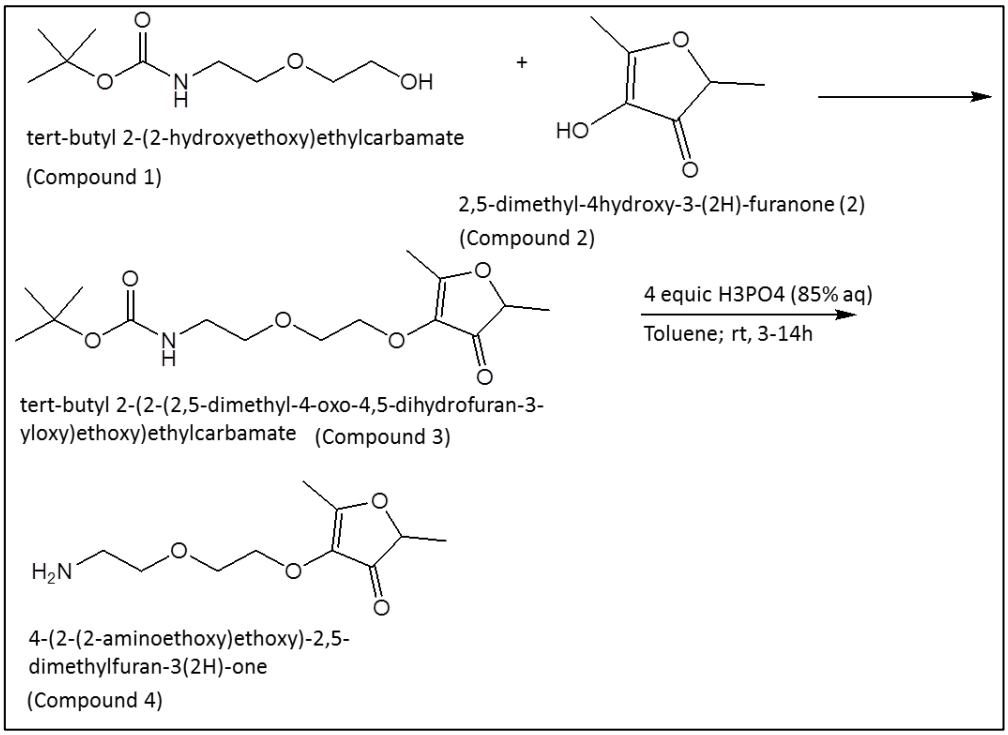

Scheme 5.4: Schematic illustration of two approaches followed for the synthesis of compound 3

Approach 1

Compound 1 was reacted with compound 2 (15 wt. % in propylene glycol) according to literature (Gule 2012). Two different procedures were followed.

Procedure 1: Compound 1 (8 g, 0.04 mol), compound 2 (15% in propylene glycol) (2.5 g, 2.9 x 10^{-3} mol), and *p*-toluenesulfonic acid (100 mg, 5.8 x 10^{-4} mol) were added to a round bottom flask. The mixture was heated up to 90 °C and stirred for 8 h after which the mixture was cooled down to room temperature. The acid catalyst was removed by stirring the reaction mixture for 2 h over $NaHCO_3$ followed by filtering to remove the $NaHCO_3$. The remaining product was light orange oil. ^{1}H NMR analysis was used to investigate the structure of the product. NMR analysis indicated that this procedure was not successful; hence, Procedure 2 was investigated.

Procedure 2: A similar procedure as described in the procedure above (Procedure 1) was repeated with the addition of anhydrous ethanol (10 mL) as a solvent. The product was a dark yellow oily substance with a caramel-like flavour smell; however, ^{1}H NMR analysis showed that it was not the targeted product. To determine the possible reasons for the unsuccessful synthesis of the furanone derivative, the ^{1}H NMR spectrum of Gule (2012)[15] was re-evaluated. It was found that propylene glycol peaks and furanone peaks occur at the same wavenumbers and was interpreted as furanone peaks (see discussion in paragraph 5.4.3). Therefore the presence of the propylene glycol in the furanone solution might have prevented or limited the proceeding and the selectivity of the reaction. In the second approach, therefore, 98 % pure 2,5-dimethyl-4hydroxy-3-(2H)-furanone (compound 2) was used in attempt to synthesise the targeted product (i.e. compound 4) as outlined below.

Approach 2

As outlined in Approach 1, the use of ≥ 98 % pure 2,5-dimethyl-4hydroxy-3-(2H)-furanone was attempted. Two different procedures were followed as described below.

Procedure 1: Compound 1 (5 g, 0.02 mol), compound 2 (≥98 % pure) (3 g, 0.02 mol) and *p*-toleunesulfonic acid (100 mg, 5.8 $x10^{-4}$ mol) were added to a round bottom flask equipped with a reflux condenser, in the presence of anhydrous ethanol (10 mL) as a solvent. The mixture was refluxed for 8 h. The mixture was then allowed to cool down to room temperature before a saturated solution of $NaHCO_3$ was added, the mixture was allowed to stir for 2 h to remove the acid catalyst. The excess $NaHCO_3$ was filtered and the solvent was removed under reduced pressure. The remaining crude product was purified by silica-gel chromatography using pentane and ethylacetate (2:1 v/v) as the solvent, and was analysed by ^{1}H NMR spectroscopy.

Procedure 2: In this procedure, an attempted synthesis was done as reported by Buttery and Ling (1996). Compound 1 (5 g, 0.02 mol), compound 2 (≥98 % pure) (3 g, 0.02 mol) was added to a round bottom flask in the presence of *p*-toleunesulfonic chloride (100 mg, 5.8 $x10^{-4}$ mol). Anhydrous benzene (10 mL) was added to the mixture as solvent. The flask was equipped with a reflux condenser with a drying tube on top as well as a Dean-Stark trap. The mixture was refluxed at 85 °C for 16 h. The mixture was cooled down to room temperature. The acid catalyst was removed by stirring the mixture over $NaHCO_3$ for 2 h. The excess $NaHCO_3$ was filtered and the solvent was removed under reduced pressure to produce light yellow crystals, was analysed by ^{1}H NMR spectroscopy.

Approach 3

Since Approach 1 and 2 was not successful a new synthetic approach was attempted. In this approach a more reactive esterification reaction was used in an attempt to synthesise the targeted compound 4 as indicated in Scheme 5.5.

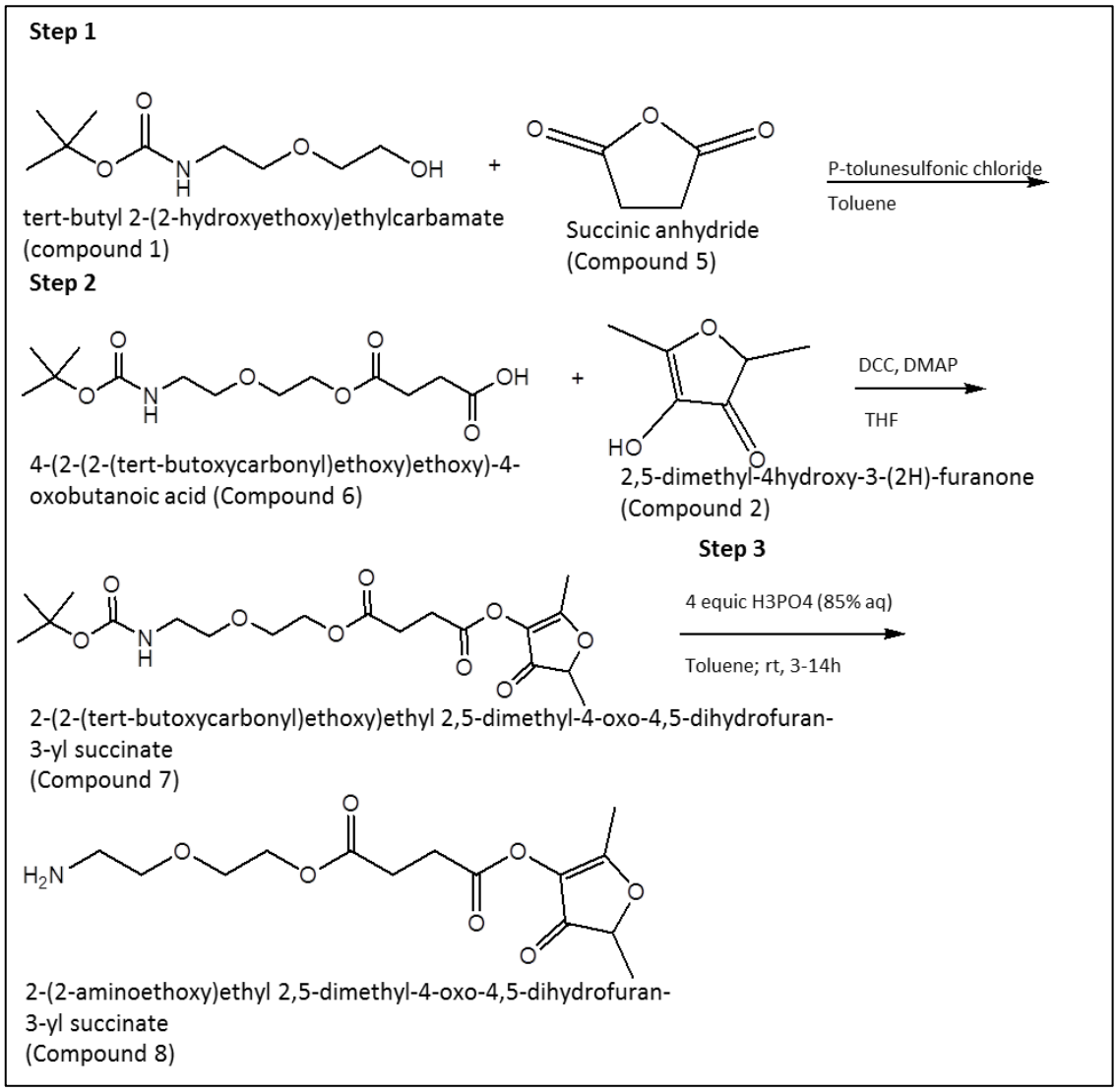

Scheme 5.5: Reaction scheme for Approach 3 for the synthesis of 2-(2-aminoethoxy)ethyl 2,5-dimethyl-4-oxo-4,5-dihydrofuran-3-yl succinate

Step 1: Compound 1 (4 g, 0.02 mol), compound 5 (2 g, 0.02 mol), anhydrous *p*-toluenesulfonyl chloride acid (0.02 g, 1.04 x10^4 mol) and anhydrous toluene (20 mL) were added to a round bottom flask equipped with a Dean-Stark trap and a reflux condenser. The mixture was then heated for 14 h at 80 °C. Once the mixture cooled to room temperature, a saturated $NaHCO_3$ solution (15 mL) was added. The water layer was extracted with hexane (3 x 25 mL) after which the organic layer was washed with aqueous solution of saturated NaCl (10 mL) and water followed by drying over anhydrous $MgSO_4$. The excess solvent was removed under reduced pressure, and the product was analysed by ^{1}H NMR spectroscopy and MS.

Step 2: Compound 6 (0.4 g, 1 mol), compound 2 (≥98 % pure) (0.18 g, 1.1 mol) and anhydrous THF (20 mL) were added to a round bottom flask. The mixture was cooled down to 0 °C in an ice bath and DCC (0.32 g, 1.2 mol) was added and stirred for 2 min, there after DMAP (0.032g, 2 x 10^4 mol) was slowly added. The mixture was allowed to warm up to room temperature and stirred for 8 h. Afterwards the solvent was removed under reduced pressure and the remaining crude

product was purified by column chromatography using ethyl acetate and pentane (2:1) as mobile solvent system. The obtained fractions was analysed by ^{1}H NMR analysis.

5.4 Results and discussion

5.4.1 Synthesis of SMA

The synthesis of alternating SMA, by radical polymerization, was successful. Its structure and molecular weight was confirmed through ^{1}H NMR and SEC analysis respectively (Figure 5.2, Figure 5.3).

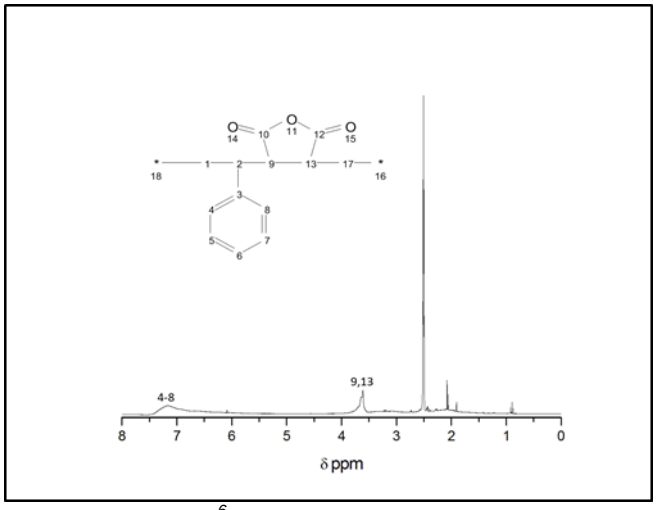

Figure 5.2: ^{1}H NMR spectrum of SMA in DMSO-d^{6}

^{1}H NMR (DMSO-d^{6}) Spectral peak assignments of alternating SMA

- δ 2.2 ppm (singlet, 2H on carbons 17)
- δ 3.61 ppm (singlet, 2H on carbons 9,13)
- δ 7.3 ppm (singlet, 5H on carbons 4-8)

The broad peak at shift 7.3 ppm corresponds to the presence of the protons on the aromatic ring of the styrene unit and peaks at 2.2 ppm and 3.61 ppm to the styrene polymer backbone and the protons of the maleic anhydride.

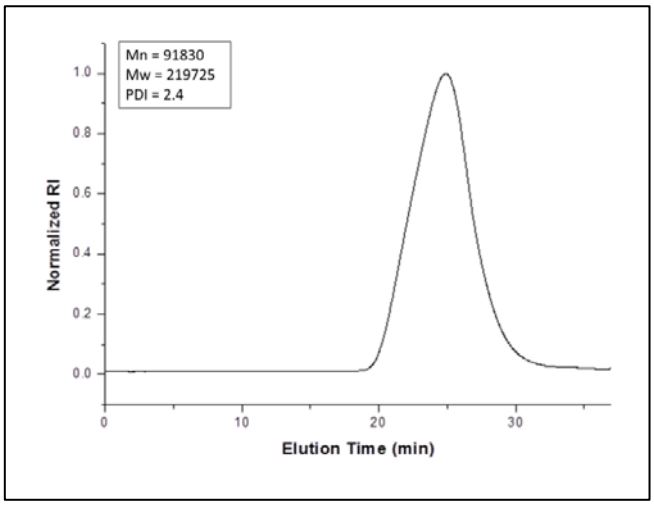

Figure 5.3: SEC chromatogram indicating the Molecular weight (Mw) distribution of SMA

SEC was used to determine the molecular weight and molecular weight distribution of the SMA. A monomodal SEC trace of the polymer was observed between the elution times of 20 – 30 min (Figure 5.3). A high molecular weight polymer with a weight average molecular weight (Mw) of 219725 g/mol with dispersity (Đ) of 2.4 were obtained. From literature it is known that the synthesis of SMA through radical polymerization are characterized by broad molecular weight distributions with polydispersities of approximately 2.[16]

5.4.2 Synthesis of tert-butyl 2-(2-hydroxyethoxy) ethylcarbamate

The synthesis of compound 2 was successful. Its structure and molar mass was confirmed through ^{1}H NMR and ES-MS+.

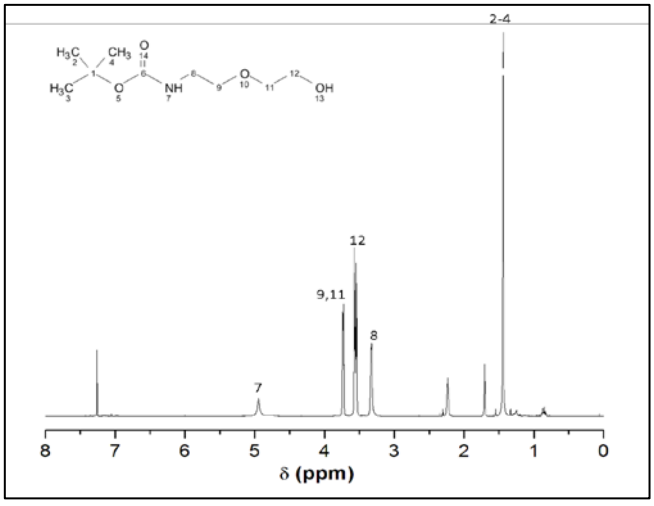

Figure 5.4: ^{1}H NMR spectrum of compound 1 in $CDCl_3$

^{1}H NMR ($CDCl_3$) spectral peak assignments of compound 1

- δ 1.4 ppm (singlet, 9H on carbons 2,3 and 4)
- δ 3.3 ppm (doublet, 2H on carbon 8)
- δ 3.5 ppm (multiplet, 4H on carbons 9 and 11)
- δ 3.7 ppm (quartet, 2H on carbon 12)
- δ 4.9 ppm (singlet, 1H on nitrogen 7)

All the protons of compound 1 could be accounted for through ^{1}H NMR (Figure 5.4). It appears as if the compound is present. For confirmation ES–MS+ analysis were done.

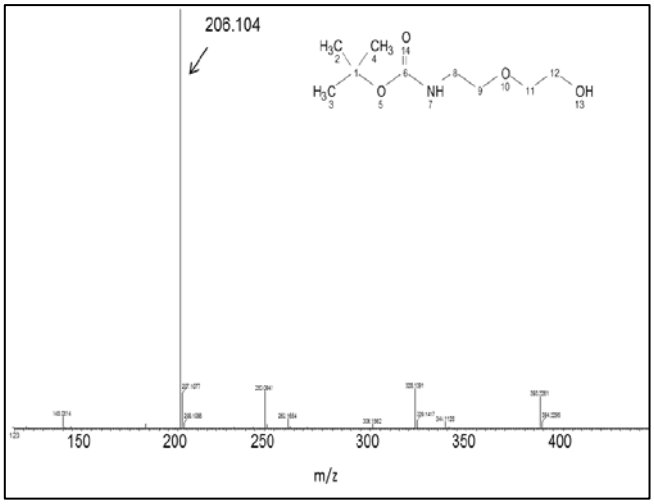

Figure 5.5: Mass spectrum of compound 1

From the ES-MS+ spectra there is a strong peak at 206 mz which is the M+1 peak. This peak can be attributed to compound 1, as compound 1 has a molar mass of 205 g/mol. The synthesis of compound 1 was successful confirmed through ^{1}H NMR and ES-MS+.

5.4.3 Synthesis of 3(2H) furanone derivative (compound 4 or compound 8).

Approach 1

Procedure 1 and 2

The spectrum for both procedures are relatively the same except for a few impurity peaks. The spectra are therefore discussed toghether.

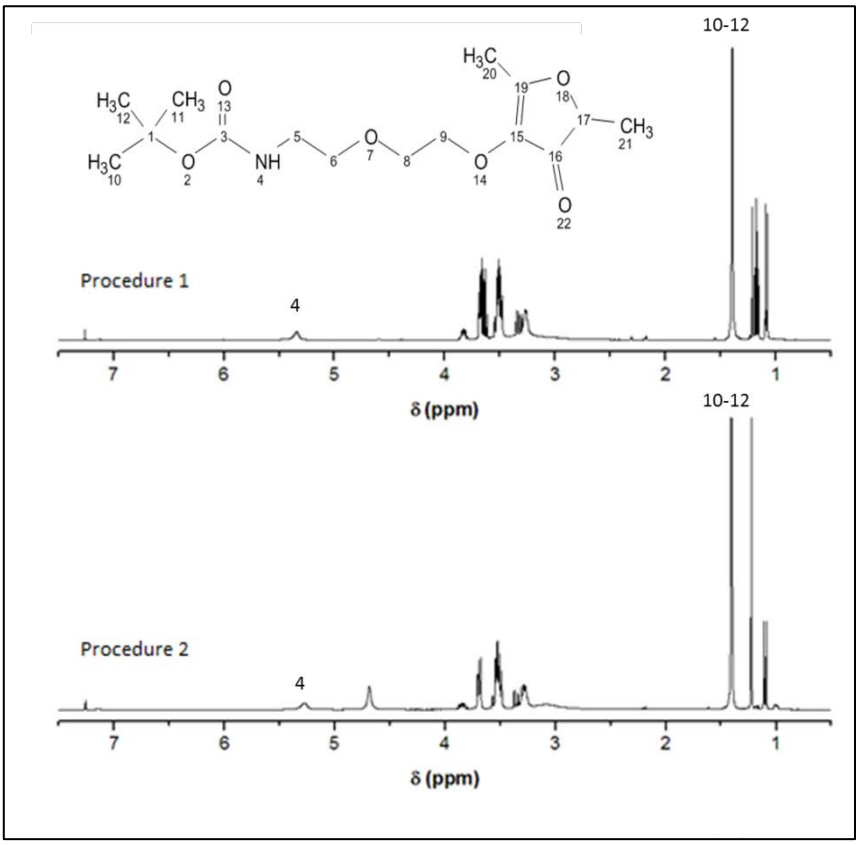

Figure 5.6: ^{1}H NMR spectrum of products obtained from Approach 1, Procedure 1 and 2

^{1}H NMR ($CDCl_3$) Spectral peak assignments of compound 3

- δ 1.4 ppm (singlet, 9H on carbons 10-12)
- δ 4.9 ppm (singlet, 1H on nitrogen 4)

In accordance with literature, the two peaks identified in Figure 5.6 could characteristically be assigned to the protons of the carbons of $(Boc)_2O$ and the one proton on the nitrogen of amino ethoxy ethanol. The identification of the peaks between 3 ppm and 4 ppm was not upfront as the peaks of compound 1 and propolene glycol overlap. The doublet peak around 1.17 ppm was assigned for the methyl groups of the propylene glycol. No distinct furanone protons (e.g. protons 17, 20 and 21, Figure 5.6) peaks were observed and hence unsuccesful reaction. The failure of this reaction could possibly be due to the low concentration of the furanone derivative in the reaction mixture (15 % wt) as well as the presence of propylene glycol that might have reduced the selectivity of the reaction between compound 1 and compound 2. As mentioned in section 5.3.3, it was also concluded that the reported product from Gule (2012)[15] was not obtained and the reasons are outlined in the spectrum A-D below.

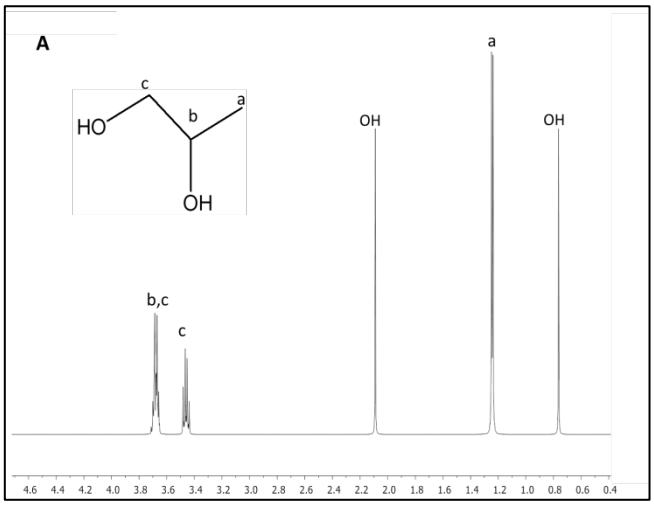

Figure 5. 7 Spectrum A – predicted ^{1}H NMR spectrum of propylene glycol

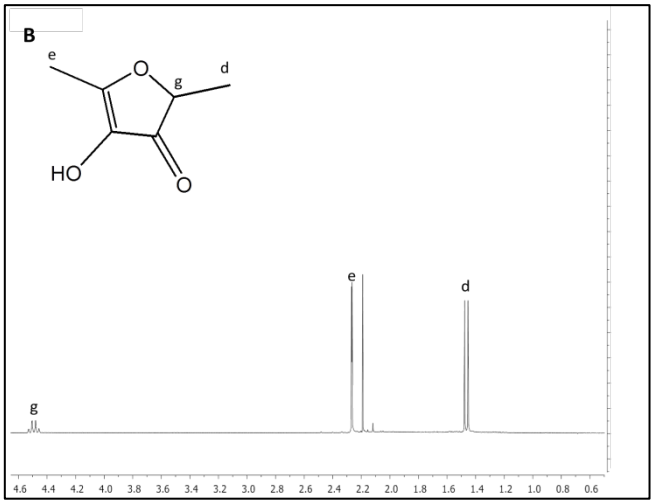

Figure 5.8 Spectrum B - ^{1}H NMR spectrum of 98 % pure 2,5-dimethyl-4-hydroxy-3-(2H)-furanone

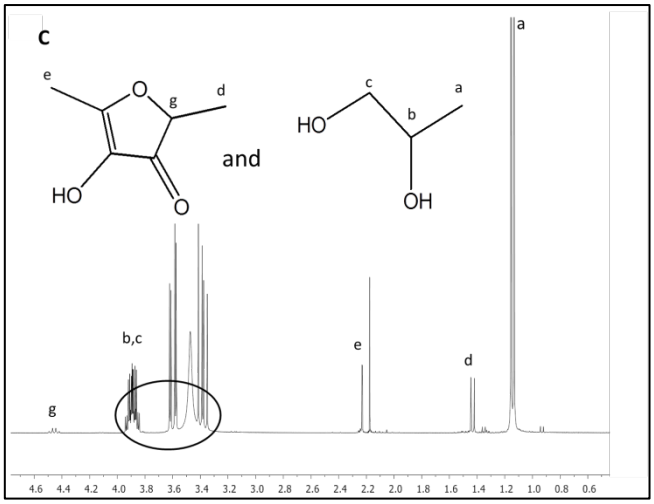

Figure 5.9 Spectrum C - ^{1}H NMR spectrum of 2,5-dimethyl-4-hydroxy-3-(2H)-furanone (15 % wt) in propylene glycol

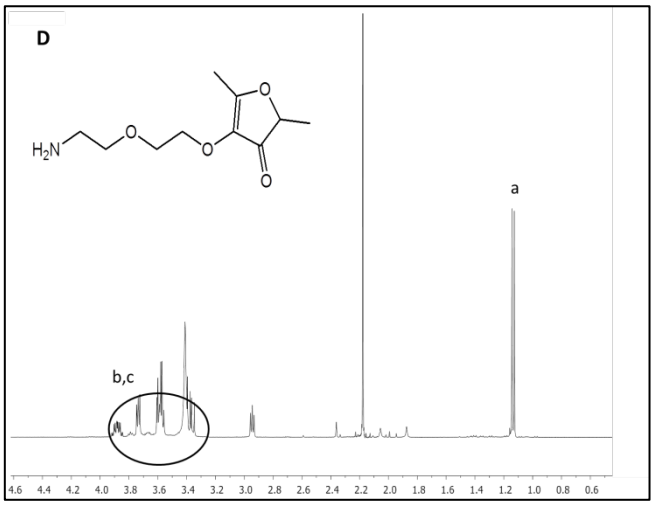

Figure 5.10 Spectrum D - ^{1}H NMR spectrum from Gule (2012)[15] used with permission from the author.

Spectrum A (**Figure 5. 7**) is the predicted spectrum of pure propylene glycol. The peaks were assigned accordingly. Spectrum B (**Figure 5.8**) represents the NMR of 98 % pure 2,5-dimethyl-4-hydroxy-3-(2H)-furanone and the peaks were assigned accordingly. Spectrum C (**Figure 5.9**) shows the NMR of 15 % 2,5-dimethyl-4-hydroxy-3-(2H)-furanone in propylene glycol. The peaks were assigned accordingly to 2,5-dimethyl-4-hydroxy-3-(2H)-furanone and propylene glycol (Figure 5.9) respectfully in accordance with Spectrum A and B. Spectrum D shows the product which was obtained by Gule (2012).[15] The peak at 2.2 ppm in Spectrum B, C and D was most likely acetone contamination as acetone appears at 2.17. Propylene glycol was not considered in the peak assignment of the spectra in Gule (2012).[15] After further investigation and comparison of Spectrum D with Spectrum C, it became evident that peaks a, b and c were distinct propylene glycol peaks.

Approach 2

Procedure 1

Compound 4 was not successfully synthesized through Approach 2, Procedure 1. Reasons for the unsuccessful synthesis of the expected product could be in the use of anhydrous ethanol as solvent. The furanone and the ethanol will compete in the reaction with the alcohol from compound 1.

Procedure 2

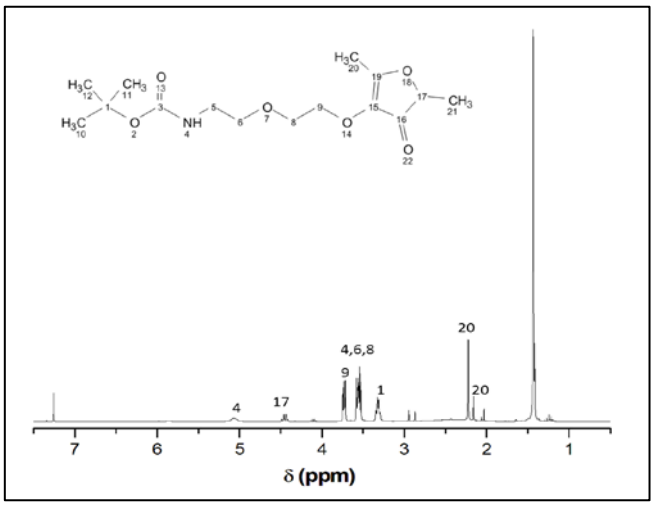

Figure 5.11: ^{1}H NMR spectrum from the product of Approach 2, Procedure 2.

^{1}H NMR ($CDCl_3$) Spectrum peak assignments of the product of approach 2, procedure 2

- δ 2.17 ppm (singlet,3H on carbon 20)
- δ 2.24 ppm (doublet, 3H on carbon 20)
- δ 3.33 ppm (quartet, 2H on carbon 1)
- δ 3.57 ppm (multiplet, 4H on carbons 6 and 8)
- δ 3.75 ppm (multiplet, 2H on carbon 9)
- δ 4.47 ppm (quartet, 1H on carbon 17)
- δ 5.09 ppm (singlet, 1H on nitrogen 4)

The only peaks that could not distinctively be reported for is for 3H on carbon 21 and the 9H on carbons 10,11,12. There is a peak at 1.43 ppm where it would be expected for both these peaks to be indicated so it was suggested that the peaks could be overlapping. The sample was analysed by ES-MS+ analysis to obtain further information.

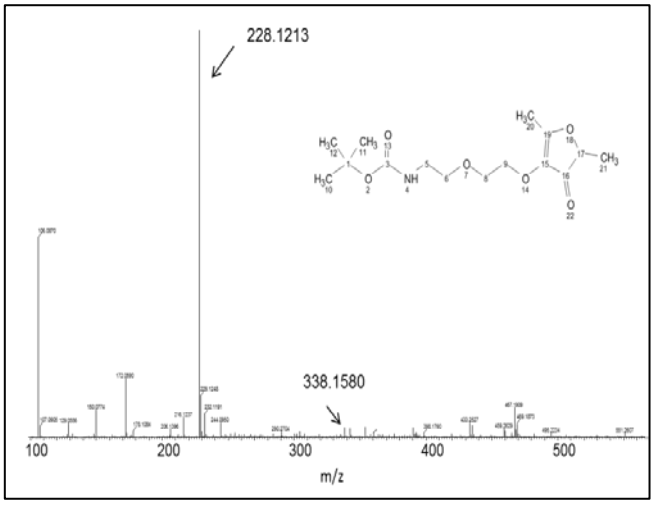

Figure 5.12: Mass spectrum of the product from Approach 2, Procedure 2

From the ES-MS+ spectra a strong peak was observed at 228 m/z. There is no product or starting material that could be accounted for with 227g/mol^{-1} mass. A small peak could be observed at 338 m/z. This could be the expected product with a sodium atom which is a typical phenomenon with electro spray positive (ES+) analysis. The calculated mass of the expected product is 315g/mol^{-1}.

A reason why the reaction might not have taken place is the choice of solvent which prevented the furanone to be in solution. Benzene is a non-polar solvent. The boc product is non-polar and the furanone is polar. Therefore the boc product could have been dissolved into the benzene solvent but not the furanone. Therefore they were not in the same solvent phase and could not react with each other.

Approach 3

Step 1

The synthesis of compound 6 was successful. Its structure and molar mass was confirmed through 1H NMR and ES-MS+ respectively.

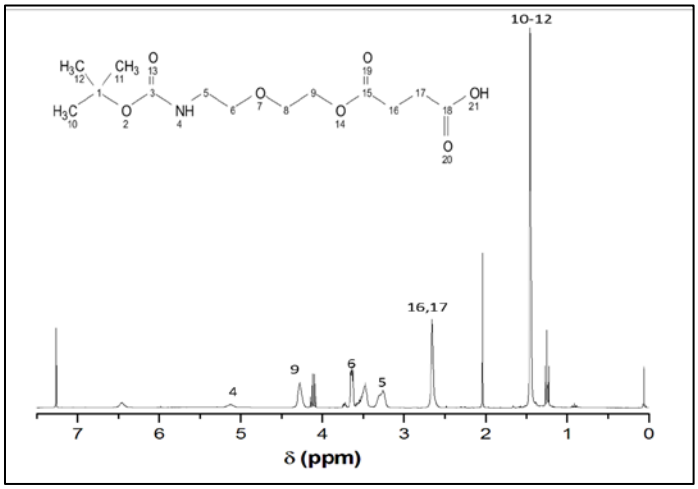

Figure 5.13: ^{1}H NMR spectrum for compound 6

^{1}H NMR ($CDCl_3$) Spectral peak assignments

- δ 1.46 ppm (singlet, 9H on carbons 10,11 and 12)
- δ 2.68 ppm (singlet, 4H on carbons 16 and 17)
- δ 3.29 ppm (singlet, 2H on carbon 5)
- δ 3.51 ppm (singlet, 2H on carbon 8)
- δ 3.66 ppm (multiplet, 2H on carbon 6)
- δ 4.30 ppm (singlet, 2H on carbon 9)
- δ 5.17 ppm (singlet, 1H on nitrogen 4)

All the protons of compound 6 could be accounted for through ^{1}H NMR (Figure 5.9). It appears as if the compound is present. For confirmation ES-MS- analysis was done.

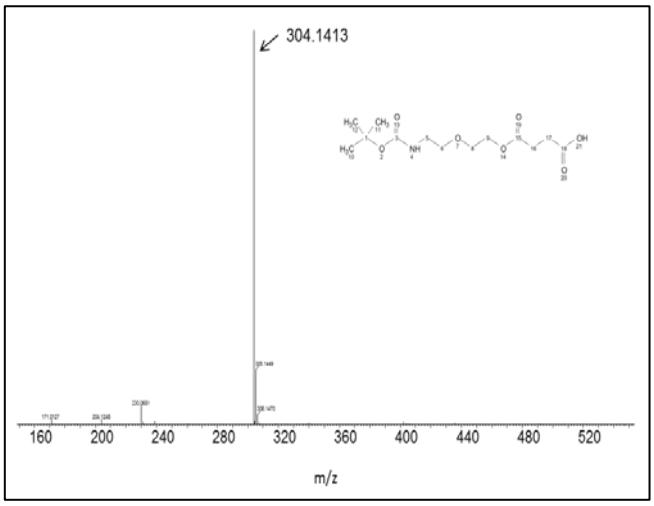

Figure 5.14: Mass spectrum of compound 6

From the ES-MS$^-$ spectra a strong peak was observed at 304 m/z. Compound 6 has a molar mass of 303 g/mol^{-1} which confirms the synthesis of compound 6.

Step 2

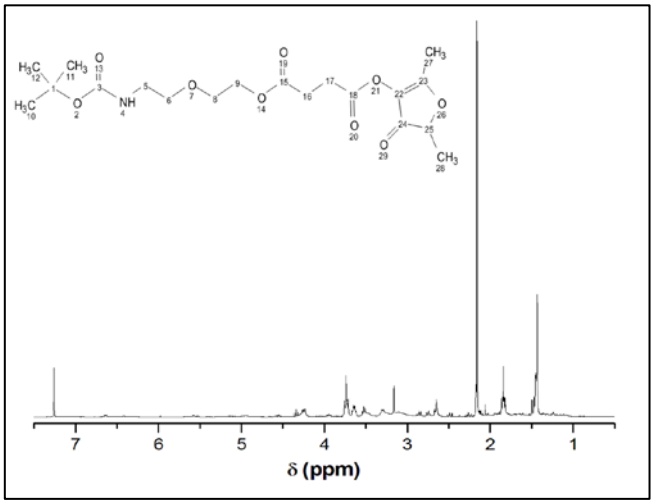

Figure 5.15: ^{1}H NMR spectrum for the product obtained from Approach 3, Step 2

The Steglich esterification reaction between compound 6 and compound 2 (Scheme 5) was unsuccessful as no peak assignments could be made. The reaction was done in combination with a carbodiimide and a catalytic amount of 4-dimethylaminopyridine (DMAP). The carbodiimide used was N,N'-dicyclohexylcarbodiimide (DCC). DCC is a reagent widely used for such reactions as it is readily commercially available, has low-cost and is stable, however it has a few drawbacks. The one that played a role in this reaction was the production of a by-product N,N'-dicyclohexylurea which trace elements after filtration is difficult to remove.

5.5 Conclusions

- The radical polymerization reaction for the synthesis of SMA was successful as confirmed through ^{1}H NMR and SEC.
- The synthesis of compound 1 was successful as confirmed through ^{1}H NMR and ES-MS^{+}.
- The synthesis of compound 6 was successful as confirmed through ^{1}H NMR and ES-MS^{-}.
- The synthesis of compound 4 could not be achieved through the attempted Approach1. This was due to the presence of propylene glycol in the furanone solution.
- The synthesis of compound 4 could not be achieved through the attempted Approach 2. This was likely due to the use of polar solvent. For future attempts phase transfer reagents might be added to the reaction.
- The synthesis of compound 8 could not be achieved. The coupling reaction with DCC in the second step was unsuccessful; however, this reaction should be further investigated using different catalyst system. In future a different coupling agent such as N,N'-diisopropylcarbodiimide (DIC) should be investigated.

5.6. References

1. Meesters, K. P. H., Van Groenestijn, J. W. & Gerritse, J. Biofouling reduction in recirculating cooling systems through biofiltration of process water. *Water Res.* **37,** 525–32 (2003).

2. Cloete, T. E., Jacobs, L. & Brözel, V. S. The chemical control of biofouling in industrial water systems. *Biodegradation* **9,** 23–37 (1998).

3. Bott, T. R. & Tianqing, L. Ultrasound enhancement of biocide efficiency. *Ultrason. Sonochem.* **11,** 323–6 (2004).

4. White, D. G. & McDermott, P. F. Biocides, drug resistance and microbial evolution. *Curr. Opin. Microbiol.* **4,** 313–7 (2001).

5. Silkina, A., Bazes, A., Mouget, J.-L. & Bourgougnon, N. Comparative efficiency of macroalgal extracts and booster biocides as antifouling agents to control growth of three diatom species. *Mar. Pollut. Bull.* **64,** 2039–46 (2012).

6. De Nys, R. & Steinberg, P. D. Linking marine biology and biotechnology. *Curr. Opin. Biotechnol.* **13,** 244–248 (2002).

7. Flynn, D. *Nalco Water Handbook*. McGraw-Hill: Global education Holdings, LCC: Penn Plaza, 10th Floor, New York.

8. Buttery, R. G. & Ling, L. C. Direct Formation of 4-Alkoxy Derivatives from 2 , 5-Dimethyl-4-hydroxy-3 (2 H) -furanone and Aliphatic Alcohols. *Agric. Food Chem.* **3,** 1512–1514 (1996).

9. Gule, N. P., Bshena, O., de Kwaadsteniet, M., Cloete, T. E. & Klumperman, B. Immobilized Furanone Derivatives as Inhibitors for Adhesion of Bacteria on Modified Poly (styrene-co-maleic anhydride). *Biomacromolecules* **13,** 3138–3150 (2012).

10. Cloete, W. J., Adriaanse, C., Swart, P. & Klumperman, B. Facile immobilization of enzymes on electrospun poly (styrene-alt-maleic anhydride) nanofibres. *Polym. Chem.* **2,** 1479–1481 (2011).

11. Braunecker, W. A. & Matyjaszewski, K. Controlled/living radical polymerization: Features, developments, and perspectives. *Prog. Polym. Sci.* **32,** 93–146 (2007).

12. Moad, G., Rizzardo, E. & Thang, S. H. Toward living radical polymerization. *Acc. Chem. Res.* **41,** 1133–42 (2008).

13. Saad, G. R., Morsi, R. E., Mohammady, S. Z. & Elsabee, M. Z. Dielectric relaxation of monoesters based poly(styrene-co-maleic anhydride) copolymer. *J. Polym. Res.* **15,** 115–123 (2008).

14. Tsavalas, J. G., Schork, F. J., de Brouwer, H. & Monteiro, M. J. Living radical polymerization by reversible addition-fragmentation chain transfer in ionically stabilized miniemulsions. *Macromolecules* **34,** 3938–3946 (2001).

15. Gule, N. P. Electrospun antimicrobial and antibiofouling nanofibres. 153 (2012).

16. Lessard, B. & Marić, M. One-Step Poly(styrene- alt -maleic anhydride)- block -poly(styrene) Copolymers with Highly Alternating Styrene/Maleic Anhydride Sequences Are Possible by Nitroxide-Mediated Polymerization. *Macromolecules* **43,** 879–885 (2010).

CHAPTER 6

Conclusions and recommendations for future research

6.1 Conclusions

The accumulation of bacteria on metal surfaces submerged in aqueous environments leads to the development of biofilms and subsequently biofouling.[1,2] Biofouling is a large financial liability for the food, maritime, manufacturing and petroleum industries. In recirculating cooling water systems and the petroleum industry biofouling on metal surfaces leads to reduced heat transfer, increased maintenance, equipment deterioration, water contamination and unscheduled shutdowns.

In industrial cooling water systems biofilm growth is controlled by physical or chemical treatments.[3] Currently the most common practice for biofouling control in cooling water systems is chemical treatment through the addition of biocides into the system. Unfortunately these biocides are hazardous to the environment and of great financial expense.

The use of antifouling coatings for metal surfaces in cooling water systems is a potential alternative. Successful methods for fabricating antifouling surfaces entail either applying antimicrobial compounds to surfaces or combining it with other materials to form a coating. The development of such coatings has been the goal of numerous researchers for decades.[4]

This study firstly aimed to evaluate the characteristics of industrial antifouling coatings and biocide enriched coatings according to their chemical and antifouling properties before and after biofilm growth. Secondly, to synthesise a SMA coating and a furanone derivative that could be chemically bound to the coating for the potential application on metal surfaces in recirculating cooling water systems.

To conduct chemical and microbial analysis on respective coatings the coatings had to be coated onto a metal surface exposed to biofilm growth and analysed with chemical and microbial methods. Biofilm growth systems and conditions and a few analytical methods had to be optimized for specific experimental conditions.

In Chapter 3 a flow cell system was designed to simulate biofilm growth in a cooling water system, a metal surface for growth discs was selected, *Pseudomonas* sp. strain CT07 was selected to grow biofilms on metal discs, a biofilm removal method was identified, fluorescence analytical methods were optimised and industrial coatings and biocides were selected for further analysis.

Results obtained in Chapter 3 indicated that a metal alloy of stainless steel and mild steel (3CR12) was the best option for the metal growth discs as mild steel on its own corroded within 24 h. For qualitative analysis of the biofilms, the biofilms had to be removed from the growth discs. Sonification for 5 min was determined as the optimum biofilm removal method over scraping and swabbing. Metal discs visualised by confocal laser scanning microscopy (CLSM) and flow cytometry after biofilms were removed revealed that the fluorescence dye SYTO 9 chemically

interacted with the metal surface as well as with the respective industrial coatings. To minimise the background fluorescence signals it was decided to replace *Pseudomonas* sp. strain CT07 with *Pseudomonas* sp. strain CT07::*gfp* for the cultivation of biofilms on the metal discs and only use the propidium iodide (PI) stain. Industrial coatings containing Quaternary ammonium salt 2 (QAC), Triclosan (TC) and Copper oxide (CUO) respectively showed clear zones against *E. coli* ATCC 25922 and *S. aureus* ATCC 25923 in the inhibition zone tests. Through the dilution susceptibility test the minimum inhibitory concentration of selected biocides namely silver nitrate (SN), Copper (II) sulphate pentahydrate (CS) and 2,5-dimethyl-4-hydroxy-3(2H)-furanone 15% (FR) was determined.

In Chapter 4 industrial and biocide enriched epoxy coatings were chemically and microbially evaluated to determine whether the coatings comply with the properties desired for use in cooling water systems. Commercial antifouling coatings for metal surfaces in aqueous environments were sourced from various manufacturers. An anticorrosive epoxy coating was also sourced from industry and enriched with biocides selected and tested in Chapter 3. All information regarding the coatings is propriety information. All coatings were evaluated according to their chemical characteristics before and after biofilm growth through thermogravimetric analysis (TGA), differential scanning calorimetry (DSC), energy dispersive X-ray spectroscopy (EDX), scanning electron microscopy (SEM) and transmission electron microscopy (TEM). The coatings were also qualitatively characterised according to fouling ability through SEM and CLSM and quantitatively through plate counts (pour plate method) and flow cytometry. Chemical evaluation confirmed that all coatings were thermally stable for utilization in cooling water systems except coating QAC. SEM images and EDX analysis confirmed that coatings TC and QAC washed off from the metal growth discs. Coating CUO remained on the surface of the metal, but the biocide metal, Cu, could no longer be detected after the coating was exposed to biofilm growth for 48 h. The presence of all biocide-enriched epoxy coatings was confirmed on metal discs as well as the presence of all biocides incorporated into coatings. After exposure to biofilm growth no signs of silver or copper ions could be confirmed in SN or CS coatings.

The attachment of bacteria on the surfaces of coatings TC, CUO and QAC and control CC was difficult to observe with SEM imaging as the metal had a rough surface. Attachment of bacteria could however be confirmed using CLSM. A significant difference in viable cell count was observed between coating TC and coatings CUO, QAC and the control CC. It was also established that coating CUO promoted biofilm growth.

Bacterial attachment on the surfaces of coatings SN, CS, FR and control EC could easily be observed through SEM and CLSM imaging. Results from SEM and CLSM correlated with those from plate counts and flow cytometry. No significant difference was observed in viable cell count between the control coating EC and coatings AN, CS and FR.

In Chapter 5 it was attempted to synthesise a poly(styrene-*alt*-maleic anhydride) (SMA) coating and to chemically bind a furanone derivative to the polymer back bone of SMA coating to be applied to a metal surface as an antifouling coating. Through radical polymerization SMA was successfully synthesised and confirmed with ^{1}H NMR and SEC. Synthesis of tert-butyl 2-(2-hydroxyethoxy) ethylcarbamate the starting material for synthesis of furanone derivative was successful as confirmed through ^{1}H NMR and ES-MS+. The synthesis of the 3(2H) furanone derivative was attempted through three different reaction approaches.

Approach 1 was not successful; this was due to the presence of propylene glycol in the furanone solution and consequently the incorrect interpretation of ^{1}H NMR spectra from Gule (2012).[5] Approach 2 was not successful, which was likely due to the use of polar solvent. The first step of approach 3 was successful, the synthesis of 4-(2-(2-(tert-butoxycarbonyl)ethoxy)ethoxy)-4-oxobutanoic acid as confirmed through ^{1}H NMR and ES-MS^{+}. The synthesis of product from step 2 was not successful, which was probably due to the use of DCC as a coupling agent.

The synthesis of the end furanone derivative product could not be achieved through any of the three attempted approaches.

6.2 Recommendations

Future studies should focus on how the biocides could be chemically linked to the epoxy base coating to ensure a more permanent attachment so that the biocide would be present for a longer period of time. Laboratory experiments are only confided to one bacterial species and cooling water system simulation. It would be beneficial if antifouling coatings could be tested in industrial settings. The synthesis of a furanone derivative through approach 3 should be further investigated using a different catalyst system as well as different coupling agents such as N,N'-diisopropylcarbodiimide (DIC).

6.3 References

1. Bott, T. R. Potential Physical Methods for the Control of Biofouling in Water Systems. *Chem. Eng. Res. Des.* **79,** 484–490 (2001).

2. Flemming, H.-C. Biofouling in water systems--cases, causes and countermeasures. *Appl. Microbiol. Biotechnol.* **59,** 629–40 (2002).

3. Cloete, T. E., Brözel, V. S. & Von Holy, A. Practical aspects of biofouling control in industrial water systems. *Int. Biodeterior. Biodegradation* **29,** 299–341 (1992).

4. Lee, S. B. *et al.* Permanent, nonleaching antibacterial surfaces. 1. Synthesis by atom transfer radical polymerization. *Biomacromolecules* **5,** 877–82 (2004).

5. Gule, N. P. Electrospun antimicrobial and antibiofouling nanofibres. 153 (2012).